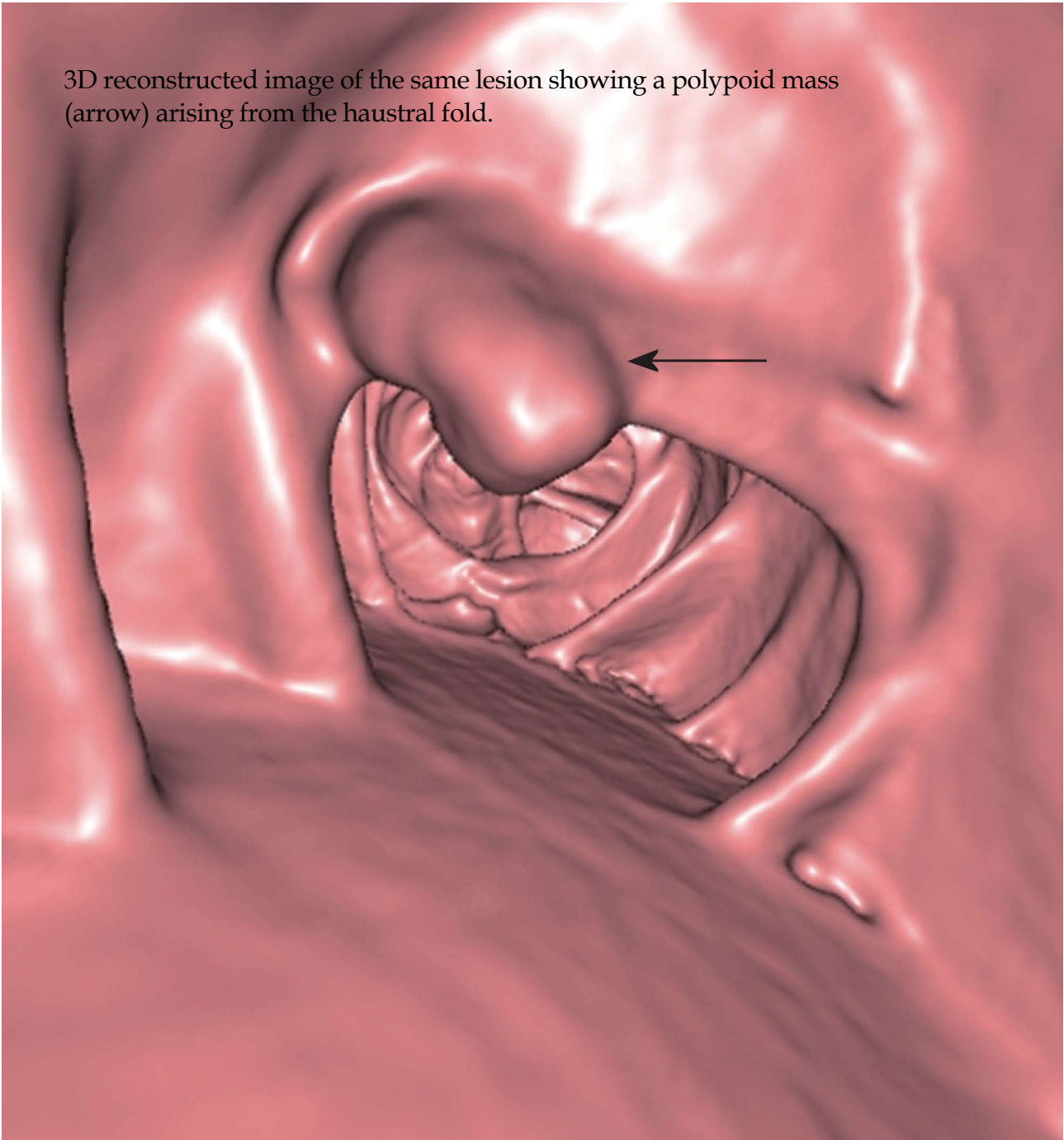


A peer-reviewed, online, open-access journal of Radiology

3D reconstructed image of the same lesion showing a polypoid mass (arrow) arising from the haustral fold.



Editorial Board

2009-2013

The *World Journal of Radiology* Editorial Board consists of 308 members, representing a team of worldwide experts in radiology. They are from 39 countries, including Australia (3), Austria (4), Belgium (4), Brazil (2), Canada (9), Chile (1), China (24), Denmark (1), Egypt (4), Estonia (1), Finland (1), France (6), Germany (17), Greece (8), Hungary (1), India (9), Iran (5), Ireland (1), Israel (4), Italy (28), Japan (14), Lebanon (1), Libya (1), Malaysia (2), Mexico (1), Netherlands (4), New Zealand (1), Norway (1), Saudi Arabia (3), Serbia (1), Singapore (2), Slovakia (1), South Korea (16), Spain (8), Switzerland (5), Thailand (1), Turkey (20), United Kingdom (15), and United States (76).

PRESIDENT AND EDITOR-IN-CHIEF

Lian-Sheng Ma, *Beijing*

STRATEGY ASSOCIATE EDITORS-IN-CHIEF

Ritesh Agarwal, *Chandigarh*
 Kenneth Coenegrachts, *Bruges*
 Meng Law, *Los Angeles*
 Ewald Moser, *Vienna*
 Aytakin Oto, *Chicago*
 AAK Abdel Razek, *Mansoura*
 Àlex Rovira, *Barcelona*
 Yi-Xiang Wang, *Hong Kong*
 Hui-Xiong Xu, *Guangzhou*

GUEST EDITORIAL BOARD MEMBERS

Wing P Chan, *Taipei*
 Wen-Chen Huang, *Taipei*
 Shi-Long Lian, *Kaohsiung*
 Chao-Bao Luo, *Taipei*
 Shu-Hang Ng, *Taoyuan*
 Pao-Sheng Yen, *Haulien*

MEMBERS OF THE EDITORIAL BOARD



Australia

Karol Miller, *Perth*
 Tomas Kron, *Melbourne*
 Zhonghua Sun, *Perth*



Austria

Herwig R Cerwenka, *Graz*

Daniela Prayer, *Vienna*
 Siegfried Trattnig, *Vienna*



Belgium

Piet R Dirix, *Leuven*
 Yicheng Ni, *Leuven*
 Piet Vanhoenacker, *Aalst*



Brazil

Emerson L Gasparetto, *Rio de Janeiro*
 Wellington P Martins, *São Paulo*



Canada

Sriharsha Athreya, *Hamilton*
 Mark Otto Baerlocher, *Toronto*
 Martin Charron, *Toronto*
 James Chow, *Toronto*
 John Martin Kirby, *Hamilton*
 Piyush Kumar, *Edmonton*
 Catherine Limperopoulos, *Quebec*
 Ernest K Osei, *Kitchener*
 Weiguang Yao, *Sudbury*



Chile

Masami Yamamoto, *Santiago*



China

Feng Chen, *Nanjing*
 Ying-Sheng Cheng, *Shanghai*
 Guo-Guang Fan, *Shenyang*

Shen Fu, *Shanghai*
 Gang Jin, *Beijing*
 Tak Yeung Leung, *Hong Kong*
 Wen-Bin Li, *Shanghai*
 Rico Liu, *Hong Kong*
 Yi-Yao Liu, *Chengdu*
 Wei Lu, *Guangdong*
 Fu-Hua Peng, *Guangzhou*
 Li-Jun Wu, *Hefei*
 Zhi-Gang Yang, *Chengdu*
 Xiao-Ming Zhang, *Nanchong*
 Chun-Jiu Zhong, *Shanghai*



Denmark

Poul Erik Andersen, *Odense*



Egypt

Mohamed Abou El-Ghar, *Mansoura*
 Mohamed Ragab Nouh, *Alexandria*
 Ahmed A Shokeir, *Mansoura*



Estonia

Tiina Talvik, *Tartu*



Finland

Tove J Grönroos, *Turku*



France

Alain Chapel, *Fontenay-Aux-Roses*

Nathalie Lassau, *Villejuif*
Youlia M Kirova, *Paris*
Géraldine Le Duc, *Grenoble Cedex*
Laurent Pierot, *Reims*
Frank Pilleul, *Lyon*
Pascal Pommier, *Lyon*



Germany

Ambros J Beer, *München*
Thomas Deserno, *Aachen*
Frederik L Giesel, *Heidelberg*
Ulf Jensen, *Kiel*
Markus Sebastian Juchems, *Ulm*
Kai U Juergens, *Bremen*
Melanie Kettering, *Jena*
Jennifer Linn, *Munich*
Christian Lohrmann, *Freiburg*
David Maintz, *Münster*
Henrik J Michaely, *Mannheim*
Oliver Micke, *Bielefeld*
Thoralf Niendorf, *Berlin-Buch*
Silvia Obenauer, *Duesseldorf*
Steffen Rickes, *Halberstadt*
Lars V Baron von Engelhardt, *Bochum*
Goetz H Welsch, *Erlangen*



Greece

Panagiotis Antoniou, *Alexandroupolis*
George C Kagadis, *Rion*
Dimitris Karacostas, *Thessaloniki*
George Panayiotakis, *Patras*
Alexander D Rapidis, *Athens*
C Triantopoulou, *Athens*
Ioannis Tsalafoutas, *Athens*
Virginia Tsapaki, *Anixi*
Ioannis Valais, *Athens*



Hungary

Peter Laszlo Lakatos, *Budapest*



India

Anil Kumar Anand, *New Delhi*
Surendra Babu, *Tamilnadu*
Sandip Basu, *Bombay*
Kundan Singh Chufal, *New Delhi*
Shivanand Gamanagatti, *New Delhi*
Vimoj J Nair, *Haryana*
R Prabhakar, *New Delhi*
Sanjeeb Kumar Sahoo, *Orissa*



Iran

Vahid Reza Dabbagh Kakhki, *Mashhad*
Mehran Karimi, *Shiraz*
Farideh Nejat, *Tehran*
Alireza Shirazi, *Tehran*
Hadi Rokni Yazdi, *Tehran*



Ireland

Joseph Simon Butler, *Dublin*



Israel

Amit Gefen, *Tel Aviv*
Eyal Sheiner, *Be'er-Sheva*
Jacob Sosna, *Jerusalem*
Simcha Yagel, *Jerusalem*



Italy

Mohssen Ansarin, *Milan*
Stefano Arcangeli, *Rome*
Tommaso Bartalena, *Imola*
Filippo Cademartiri, *Parma*
Sergio Casciaro, *Lecce*
Laura Crocetti, *Pisa*
Alberto Cuocolo, *Napoli*
Mirko D'Onofrio, *Verona*
Massimo Filippi, *Milan*
Claudio Fiorino, *Milano*
Alessandro Franchello, *Turin*
Roberto Grassi, *Naples*
Stefano Guerriero, *Cagliari*
Francesco Lassandro, *Napoli*
Nicola Limbucci, *L'Aquila*
Raffaele Lodi, *Bologna*
Francesca Maccioni, *Rome*
Laura Martincich, *Candiolo*
Mario Mascalchi, *Florence*
Roberto Miraglia, *Palermo*
Eugenio Picano, *Pisa*
Antonio Pinto, *Naples*
Stefania Romano, *Naples*
Luca Saba, *Cagliari*
Sergio Sartori, *Ferrara*
Mariano Scaglione, *Castel Volturno*
Lidia Strigari, *Rome*
Vincenzo Valentini, *Rome*



Japan

Shigeru Ehara, *Morioka*
Nobuyuki Hamada, *Chiba*
Takao Hiraki, *Okayama*
Akio Hiwatashi, *Fukuoka*
Masahiro Jinzaki, *Tokyo*
Hiroshi Matsuda, *Saitama*
Yasunori Minami, *Osaka*
Jun-Ichi Nishizawa, *Tokyo*
Tetsu Niwa, *Yokohama*
Kazushi Numata, *Kanagawa*
Kazuhiko Ogawa, *Okinawa*
Hitoshi Shibuya, *Tokyo*
Akira Uchino, *Saitama*
Haiquan Yang, *Kanagawa*



Lebanon

Aghiad Al-Kutoubi, *Beirut*



Libya

Anuj Mishra, *Tripoli*



Malaysia

R Logeswaran, *Cyberjaya*
Kwan-Hoong Ng, *Kuala Lumpur*



Mexico

Heriberto Medina-Franco, *Mexico City*



Netherlands

Jurgen J Fütterer, *Nijmegen*
Raffaella Rossin, *Eindhoven*
Paul E Sijens, *Groningen*
Willem Jan van Rooij, *Tilburg*



New Zealand

W Howell Round, *Hamilton*



Norway

Arne Sigmund Borthne, *Lørenskog*



Saudi Arabia

Mohammed Al-Omran, *Riyadh*
Ragab Hani Donkol, *Abha*
Volker Rudat, *Al Khobar*



Serbia

Djordjije Saranovic, *Belgrade*



Singapore

Uei Pua, *Singapore*
Lim CC Tchoyoson, *Singapore*



Slovakia

František Dubecký, *Bratislava*



South Korea

Bo-Young Choe, *Seoul*
Joon Koo Han, *Seoul*
Seung Jae Huh, *Seoul*
Chan Kyo Kim, *Seoul*
Myeong-Jin Kim, *Seoul*
Seung Hyup Kim, *Seoul*
Kyoung Ho Lee, *Gyeonggi-do*
Won-Jin Moon, *Seoul*
Wazir Muhammad, *Daegu*
Jai Sung Park, *Bucheon*
Noh Hyuck Park, *Kyunggi*
Sang-Hyun Park, *Daejeon*
Joon Beom Seo, *Seoul*
Ji-Hoon Shin, *Seoul*
Jin-Suck Suh, *Seoul*
Hong-Gyun Wu, *Seoul*



Spain

Eduardo J Aguilar, *Valencia*

Miguel Alcaraz, *Murcia*
Juan Luis Alcazar, *Pamplona*
Gorka Bastarrrika, *Pamplona*
Rafael Martínez-Monge, *Pamplona*
Alberto Muñoz, *Madrid*
Joan C Vilanova, *Girona*



Switzerland

Nicolau Beckmann, *Basel*
Silke Grabherr, *Lausanne*
Karl-Olof Lövblad, *Geneva*
Tilo Niemann, *Basel*
Martin A Walter, *Basel*



Thailand

Sudsriluk Sampatchalit, *Bangkok*



Turkey

Olus Api, *Istanbul*
Kubilay Aydın, *Istanbul*
İşıl Bilgen, *Izmir*
Zulkif Bozgeyik, *Elazig*
Barbaros E Çil, *Ankara*
Gulgun Engin, *Istanbul*
M Fatih Evcimik, *Malatya*
Ahmet Kaan Gündüz, *Ankara*
Tayfun Hakan, *Istanbul*
Adnan Kabaalioglu, *Antalya*
Fehmi Kaçmaz, *Ankara*
Musturay Karcaaltincaba, *Ankara*
Osman Kizilkilic, *Istanbul*
Zafer Koc, *Adana*
Cem Onal, *Adana*
Yahya Paksoy, *Konya*
Bunyamin Sahin, *Samsun*
Ercument Unlu, *Edirne*
Ahmet Tuncay Turgut, *Ankara*
Ender Uysal, *Istanbul*



United Kingdom

K Faulkner, *Wallsend*

Peter Gaines, *Sheffield*
Balaji Ganeshan, *Brighton*
Nagy Habib, *London*
Alan Jackson, *Manchester*
Pradesh Kumar, *Portsmouth*
Tarik F Massoud, *Cambridge*
Igor Meglinski, *Bedfordshire*
Ian Negus, *Bristol*
Georgios A Plataniotis, *Aberdeen*
N J Raine-Fenning, *Nottingham*
Manuchehr Soleimani, *Bath*
MY Tseng, *Nottingham*
Edwin JR van Beek, *Edinburgh*
Feng Wu, *Oxford*



United States

Athanassios Argiris, *Pittsburgh*
Stephen R Baker, *Newark*
Lia Bartella, *New York*
Charles Bellows, *New Orleans*
Walter L Biffl, *Denver*
Homer S Black, *Houston*
Wessam Bou-Assaly, *Ann Arbor*
Owen Carmichael, *Davis*
Shelton D Caruthers, *St Louis*
Yuhchayou Chen, *Rochester*
Melvin E Clouse, *Boston*
Ezra Eddy Wyssam Cohen, *Chicago*
Aaron Cohen-Gadol, *Indianapolis*
Patrick M Colletti, *Los Angeles*
Kassa Darge, *Philadelphia*
Abhijit P Dattir, *Miami*
Delia C DeBuc, *Miami*
Russell L Deter, *Houston*
Adam P Dicker, *Phil*
Khaled M Elsayes, *Ann Arbor*
Steven Feigenberg, *Baltimore*
Christopher G Filippi, *Burlington*
Victor Frenkel, *Bethesda*
Thomas J George Jr, *Gainesville*
Patrick K Ha, *Baltimore*
Robert I Haddad, *Boston*
Walter A Hall, *Syracuse*
Mary S Hammes, *Chicago*

John Hart Jr, *Dallas*
Randall T Higashida, *San Francisco*
Juebin Huang, *Jackson*
Andrei Iagaru, *Stanford*
Craig Johnson, *Milwaukee*
Ella F Jones, *San Francisco*
Csaba Juhasz, *Detroit*
Mannudeep K Kalra, *Boston*
Riyad Karmy-Jones, *Vancouver*
Daniel J Kelley, *Madison*
Amir Khan, *Longview*
Vikas Kundra, *Houston*
Kennith F Layton, *Dallas*
Rui Liao, *Princeton*
CM Charlie Ma, *Philadelphia*
Nina A Mayr, *Columbus*
Thomas J Meade, *Evanston*
Steven R Messé, *Philadelphia*
Feroze B Mohamed, *Philadelphia*
Koenraad J Morteale, *Boston*
Mohan Natarajan, *San Antonio*
John L Nosher, *New Brunswick*
Chong-Xian Pan, *Sacramento*
Dipanjan Pan, *St Louis*
Martin R Prince, *New York*
Reza Rahbar, *Boston*
Carlos S Restrepo, *San Antonio*
Veronica Rooks, *Honolulu*
Maythem Saeed, *San Francisco*
Edgar A Samaniego, *Palo Alto*
Jason P Sheehan, *Charlottesville*
William P Sheehan, *Willmar*
Charles Jeffrey Smith, *Columbia*
Dan Stoianovici, *Baltimore*
Dian Wang, *Milwaukee*
Jian Z Wang, *Columbus*
Liang Wang, *New York*
Shougang Wang, *Santa Clara*
Wenbao Wang, *New York*
Aaron H Wolfson, *Miami*
Ying Xiao, *Philadelphia*
Juan Xu, *Pittsburgh*
Benjamin M Yeh, *San Francisco*
Terry T Yoshizumi, *Durham*
Jinxing Yu, *Richmond*
Jianhui Zhong, *Rochester*

Contents

Monthly Volume 2 Number 5 May 28, 2010

- | | | |
|---|-----|---|
| EDITORIAL | 151 | Use of computed tomography in the management of colorectal cancer
<i>Tan CH, Iyer R</i> |
| | 159 | Magnetic resonance imaging staging of nasopharyngeal carcinoma in the head and neck
<i>King AD, Bhatia KSS</i> |
| OBSERVATION | 166 | Update on the natural history of intracranial atherosclerotic disease: A critical review
<i>Komotar RJ, Kellner CP, Raper DM, Strozyk D, Higashida RT, Meyers PM</i> |
| GUIDELINES FOR CLINICAL PRACTICE | 172 | Imaging in male-factor obstructive infertility
<i>Donkol RH</i> |
| REVIEW | 180 | Multi-parametric MR imaging of transition zone prostate cancer: Imaging features, detection and staging
<i>Kayhan A, Fan X, Oommen J, Oto A</i> |
| | 188 | A review on dural tail sign
<i>Sotoudeh H, Yazdi HR</i> |
| CASE REPORT | 193 | Systemic air embolism after transthoracic lung biopsy: A case report and review of literature
<i>Bou-Assaly W, Pernicano P, Hoeffner E</i> |

ACKNOWLEDGMENTS I Acknowledgments to reviewers of *World Journal of Radiology*

APPENDIX I Meetings
 I-V Instructions to authors

ABOUT COVER Tan CH, Iyer R.
 Use of computed tomography in the management of colorectal cancer.
World J Radiol 2010; 2(5): 151-158
<http://www.wjgnet.com/1949-8470/full/v2/i5/151.htm>

AIM AND SCOPE *World Journal of Radiology* (*World J Radiol*, *WJR*, online ISSN 1949-8470, DOI: 10.4329) is a monthly peer-reviewed, online, open-access, journal supported by an editorial board consisting of 308 experts in radiology from 39 countries.
 The major task of *WJR* is to rapidly report the most recent improvement in the research of medical imaging and radiation therapy by the radiologists. *WJR* accepts papers on the following aspects related to radiology: Abdominal radiology, women health radiology, cardiovascular radiology, chest radiology, genitourinary radiology, neuroradiology, head and neck radiology, interventional radiology, musculoskeletal radiology, molecular imaging, pediatric radiology, experimental radiology, radiological technology, nuclear medicine, PACS and radiology informatics, and ultrasound. We also encourage papers that cover all other areas of radiology as well as basic research.

FLYLEAF I-III Editorial Board

EDITORS FOR THIS ISSUE

Responsible Assistant Editor: *Na Liu*
 Responsible Electronic Editor: *Xiao-Mei Zheng*
 Proofing Editor-in-Chief: *Lian-Sheng Ma*

Responsible Science Editor: *Jian-Xia Cheng*

NAME OF JOURNAL
World Journal of Radiology

LAUNCH DATE
 December 31, 2009

SPONSOR
 Beijing Baishideng BioMed Scientific Co., Ltd.,
 Room 903, Building D, Ocean International Center,
 No. 62 Dongsihuan Zhonglu, Chaoyang District,
 Beijing 100025, China
 Telephone: 0086-10-8538-1892
 Fax: 0086-10-8538-1893
 E-mail: baishideng@wjgnet.com
<http://www.wjgnet.com>

EDITING
 Editorial Board of *World Journal of Radiology*,
 Room 903, Building D, Ocean International Center,
 No. 62 Dongsihuan Zhonglu, Chaoyang District,
 Beijing 100025, China
 Telephone: 0086-10-5908-0036
 Fax: 0086-10-8538-1893
 E-mail: wjr@wjgnet.com
<http://www.wjgnet.com>

PUBLISHING
 Beijing Baishideng BioMed Scientific Co., Ltd.,
 Room 903, Building D, Ocean International Center,
 No. 62 Dongsihuan Zhonglu, Chaoyang District,
 Beijing 100025, China
 Telephone: 0086-10-8538-1892
 Fax: 0086-10-8538-1893
 E-mail: baishideng@wjgnet.com
<http://www.wjgnet.com>

SUBSCRIPTION
 Beijing Baishideng BioMed Scientific Co., Ltd.,
 Room 903, Building D, Ocean International Center,
 No. 62 Dongsihuan Zhonglu, Chaoyang District,
 Beijing 100025, China
 Telephone: 0086-10-8538-1892
 Fax: 0086-10-8538-1893
 E-mail: baishideng@wjgnet.com
<http://www.wjgnet.com>

ONLINE SUBSCRIPTION
 One-Year Price 216.00 USD

PUBLICATION DATE
 May 28, 2010

CSSN
 ISSN 1949-8470 (online)

PRESIDENT AND EDITOR-IN-CHIEF
 Lian-Sheng Ma, *Beijing*

STRATEGY ASSOCIATE EDITORS-IN-CHIEF
 Ritesh Agarwal, *Chandigarh*
 Kenneth Coenegrachts, *Bruges*
 Adnan Kabaalioglu, *Antalya*
 Meng Law, *Los Angeles*
 Ewald Moser, *Vienna*
 Aytekin Oto, *Chicago*
 AAK Abdel Razek, *Mansoura*
 Àlex Rovira, *Barcelona*
 Yi-Xiang Wang, *Hong Kong*
 Hui-Xiong Xu, *Guangzhou*

EDITORIAL OFFICE
 Na Ma, Director
World Journal of Radiology
 Room 903, Building D, Ocean International Center,
 No. 62 Dongsihuan Zhonglu, Chaoyang District,
 Beijing 100025, China
 Telephone: 0086-10-5908-0036
 Fax: 0086-10-8538-1893
 E-mail: wjr@wjgnet.com
<http://www.wjgnet.com>

COPYRIGHT
 © 2010 Baishideng. All rights reserved; no part of this publication may be reproduced, stored in a retrieval system, or transmitted in any form or by any means, electronic, mechanical, photocopying, recording, or otherwise without the prior permission of Baishideng. Authors are required to grant *World Journal of Radiology* an exclusive license to publish.

SPECIAL STATEMENT
 All articles published in this journal represent the viewpoints of the authors except where indicated otherwise.

INSTRUCTIONS TO AUTHORS
 Full instructions are available online at http://www.wjgnet.com/1949-8470/g_info_20100316162358.htm. If you do not have web access please contact the editorial office.

ONLINE SUBMISSION
<http://www.wjgnet.com/1949-8470office>

Use of computed tomography in the management of colorectal cancer

Cher Heng Tan, Revathy Iyer

Cher Heng Tan, Department of Diagnostic Radiology, Tan Tock Seng Hospital, 11 Jalan Tan Tock Seng, Singapore 308433, Singapore

Revathy Iyer, Division of Diagnostic Imaging, MD Anderson Cancer Center, 1515 Holcombe Blvd, Houston, TX 77030, United States

Author contributions: Both authors contributed equally to this work.

Correspondence to: Dr. Cher Heng Tan, Department of Diagnostic Radiology, Tan Tock Seng Hospital, 11 Jalan Tan Tock Seng, Singapore 308433, Singapore. tchers1977@yahoo.com.sg
Telephone: +65-63578111 Fax: +65-63578112

Received: April 2, 2010 Revised: April 21, 2010

Accepted: April 28, 2010

Published online: May 28, 2010

© 2010 Baishideng. All rights reserved.

Key words: Computed tomography; Perfusion; Positron emission tomography; Rectal cancer

Peer reviewer: Herwig R Cerwenka, Professor, MD, Department of Surgery, Medical University of Graz, Auenbruggerplatz 29, A-8036 Graz, Austria

Tan CH, Iyer R. Use of computed tomography in the management of colorectal cancer. *World J Radiol* 2010; 2(5): 151-158
Available from: URL: <http://www.wjgnet.com/1949-8470/full/v2/i5/151.htm> DOI: <http://dx.doi.org/10.4329/wjr.v2.i5.151>

Abstract

Computed tomography (CT) plays an important role in the management of colorectal cancer (CRC). The use of CT (colonography) as a screening tool for CRC has been validated and is expected to rise over time. The results of prior studies suggest that CT is suboptimal for assessment of local T stage and moderate for N stage disease. Recent advances in CT technology are expected to lead to some improvement in staging accuracy. At present, the main role of CT in pre-treatment imaging assessment lies in its use for the detection of distant metastases, especially in the liver. In a select group of patients, routine post-treatment surveillance with CT confers survival benefits. The role of CT for post-treatment assessment has been radically altered and improved with the advent of fusion positron emission tomography/CT. Perfusion CT shows promise as another functional imaging modality but further experience with this technique is necessary before it can be applied to routine clinical practice.

INTRODUCTION

The majority of patients suffering from colorectal cancer (CRC) are over 50 years of age, with a relatively equal gender incidence^[1]. Recent declines in CRC incidence and mortality are attributable to reduced risk factor exposure, early detection and prevention through polypectomy, and improved treatment^[2]. Despite this, CRC remains the third commonest adult cancer with approximately 1 in 19 adults diagnosed with CRC during their lifetime^[1].

Imaging plays an important role in screening for CRC. According to the current American Cancer Society guidelines for CRC screening, 5-yearly computed tomography (CT) colonography (CTC) is recommended for asymptomatic patients with average risk^[3]. In patients with known CRC, CT plays an important role in both pretreatment staging of disease, as well as assessing for response to treatment. Traditionally, this has been done by anatomical imaging assessment on CT. Advances in technology have further increased the role of CT, by facilitating functional imaging with positron emission tomography (PET) and perfusion studies.

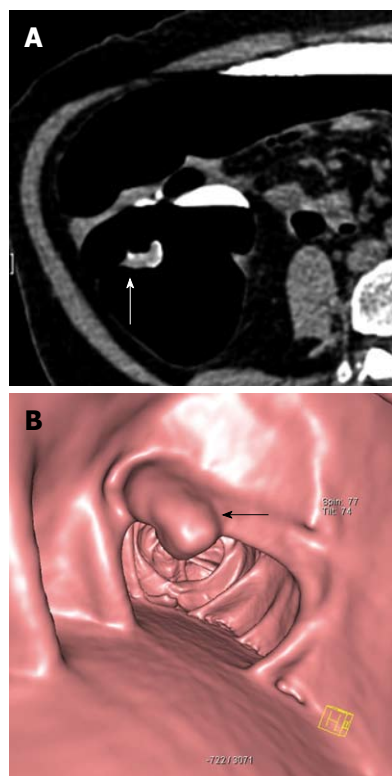


Figure 1 73-year-old female. Faecal occult blood positive. Sigmoidoscopy was normal. A: Source axial computed tomography (CT) image from CT colonography study in the prone position demonstrates focal thickening (arrow) along a haustral fold in the proximal colon. Note the presence of contrast tagged faecal material coating the lesion; B: 3D reconstructed image of the same lesion showing a polypoid mass (arrow) arising from the haustral fold. Biopsy was positive for adenocarcinoma and the patient underwent curative right hemicolectomy.

ANATOMICAL IMAGING BY CT

Screening

Although elevated serum carcinoembryonic antigen (CEA) levels are often present in CRC, they are neither sensitive nor specific enough to be used as a screening tool for asymptomatic patients^[4]. CTC (otherwise known as virtual colonoscopy) allows a minimally invasive imaging examination of the entire colon and rectum. Compared to optical colonoscopy, the risk for colonic perforation during screening is extremely low, being 0.005%^[5] for asymptomatic patients and up to 0.06% for symptomatic patients^[6]. Use of carbon dioxide with an insufflator that regulates pressure rather than room air for gas insufflation of the colon may further reduce the incidence of perforation^[5].

In CTC, high resolution image acquisition of the entire large intestine in a single breath hold is permitted by the use of multi-row detector CT. Integrated 3D and 2D analysis with specialised post-processing software allows for ease of polyp detection, characterization of lesions and location. For optimal assessment, adequate bowel preparation and gaseous distension of the colon are essential. Newer techniques such as faecal tagging reduce the need for vigorous bowel preparation^[7] and decreases

false positives from the presence of adherent faecal matter. In contrast with optical colonoscopy, extracolonic structures are also evaluated in the same examination. Hellström *et al*^[8] showed that potentially important extracolonic findings, such as lymphadenopathy, aortic aneurysms and solid hepatic and renal masses, were present in 23% of patients.

The American College of Radiology Imaging Network National CT Colonography Trial, which included 2500 patients across 15 institutions in the United States, has shown comparable accuracy between CTC and standard colonoscopy. Pickhardt *et al*^[9] reported a sensitivity of 89% for adenomas greater than 5 mm. For invasive CRC, the pooled CTC sensitivity was higher at 96%. As with other screening techniques, CTC accuracy improves with lesion size. All patients with one or more polyps larger than 10 mm or 3 or more polyps larger than 6 mm should be referred for colonoscopy^[10]. However, the management of patients with fewer polyps (fewer than three) in which the largest polyp is 6 to 9 mm or smaller remains controversial at present^[11,12].

For patients with suspected CRC, the diagnostic accuracies of contrast-enhanced CTC were even better. Using the tumour, node, and metastasis system, rates of 95%, 85%, and 100% were achieved. The sensitivity of both CTC and optical colonoscopy for cancer detection were both 100%, while the overall sensitivity of CT colonography was even higher than initial colonoscopy for polyp detection (90% *vs* 78%, $P = 0.001$, Figure 1)^[13].

The main drawback of CTC is radiation exposure. A single CTC study results in an estimated organ dose to the colon of 7 to 13 mSv, which is an additional 0.044% to the lifetime risk of colon cancer^[14]. More efficient low-dose protocols (estimated organ dose ranges of 5 to 8 mSv) have been shown to be feasible with encouraging results^[15].

Pre-treatment staging

Preoperative CT is typically performed for the following indications: (1) suspected haematogenous or distal nodal (e.g. paraaortic) metastases; (2) suspected invasion into adjacent organs or abscess formation; (3) unexplained or atypical symptoms; and (4) unusual histologic results. The major goal of CT is to determine if there is direct invasion of adjacent organs, enlargement of local nodes, or evidence of distant metastases^[16].

On CT, CRC commonly manifests as focal thickening of the bowel wall and luminal narrowing; hence adequate distension of the bowel is crucial for accurate assessment. CT has a role in the detection of potential complications, such as perforation, fistulation and intussusceptions, which may require early surgical intervention.

The clinical use of CT for local tumour (T) staging of rectal cancer is limited, with a reported accuracy of around 70%^[17]. This is attributable to the lack of attenuation differences between tumour and normal visceral soft

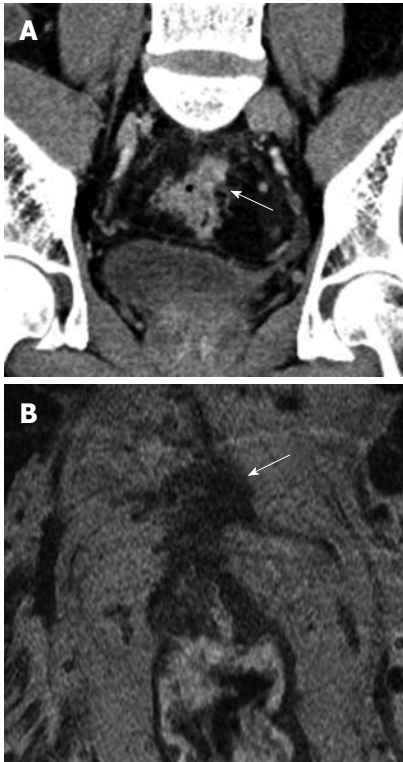


Figure 2 53-year-old male patient. Presented with lower gastrointestinal bleeding. Endoscopy revealed a fungating mass in the proximal rectum, preventing passage of the scope more proximally. A: Coronal reconstructed contrast-enhanced CT image reveals a spiculated mass at the rectosigmoid junction with a spiculated extraserosal nodular component (arrow); B: Corresponding T2 weighted high resolution magnetic resonance image in the axial plane confirms the findings of extraserosal extension of disease (arrow). The patient was referred for assessment of suitability for neoadjuvant chemoradiation treatment.

tissue. In a study by O'Neil looking at patients with rectal cancer, CT consistently overestimated tumour volume and underestimated distance from the anal verge compared to magnetic resonance imaging (MRI)^[18]. CT is also poor for the assessment of levator ani invasion in low rectal lesions, although it may assess the more proximal lesions with reasonable accuracy^[19] (Figure 2). Similarly, for the more proximal large bowel, CT fares suboptimally, with a sensitivity and specificity rate of 60% and 67%, respectively, for the detection of extramural spread of tumour^[20]. This is largely due to failure to detect microscopic disease.

CT can be considered to be more efficacious for nodal and metastases (N and M) staging than for T staging. A large meta-analysis by Bipat *et al*^[21] that included 90 studies showed similar accuracies between ultrasound, CT and MRI for the assessment of nodal involvement by rectal cancer. In a study of 137 patients, Valls *et al*^[22] showed good accuracy (85.1%), high positive predictive value (96.1%) and low positive predictive value (3.9%) of CT for the detection of liver metastases. For the detection of CRC metastases, CT imaging in the portal venous phase is the technique of choice. The addition of hepatic arterial phase imaging has been shown not to increase sensitivity, even though it improves the specific-

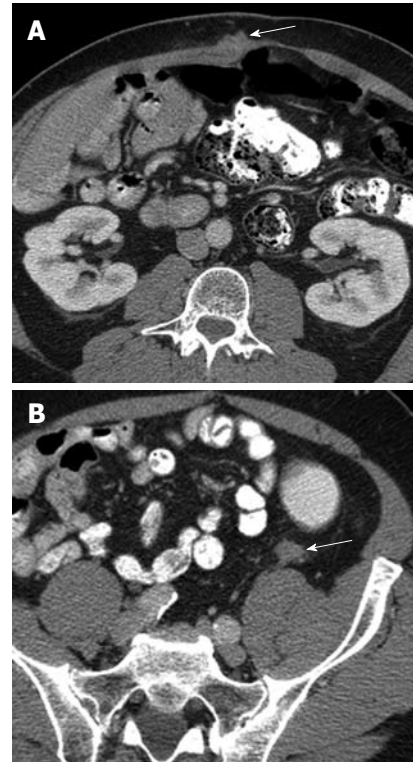


Figure 3 64-year-old male with metastatic adenocarcinoma of the colon. A: Surveillance axial contrast-enhanced CT image shows a metastatic deposit in the right rectus abdominis muscle (arrow); B: A second metastatic lesion is present in the left paracolic gutter (arrow). The high spatial resolution of CT and the contrast with the adjacent fat allows for easy detection of metastatic disease in these areas.

ity in diagnosing liver metastases in a small number of cases^[23].

At present, the optimal imaging strategy for the pre-treatment distant staging of CRC remains controversial. For instance, chest CT often detects indeterminate lung lesions, of which only a small proportion develop into definite metastases^[24]. Similarly, in rectal cancer, where pelvic MRI has already been performed, CT of the abdomen and pelvis will not provide additional value^[25]. Therefore, further studies are required to define optimal preoperative imaging.

Other than the liver, the peritoneum is a major site for metastatic disease (Figure 3). The presence of peritoneal metastasis predicts for a higher local recurrence rate^[26]. Furthermore, the Peritoneal Cancer Index, an assessment of the tumour burden attributed to peritoneal disease, has been recognized as an independent prognostic indicator for long-term outcomes. The role of CT in the detection of peritoneal carcinomatosis is limited for small metastases. In the study by de Bree *et al*^[27], CT detection of peritoneal metastases was only moderate (ranging from 9% for subcentimeter lesions to 66% for lesions larger than 5 cm) with significant interobserver differences. A more recent study by Koh *et al*^[28] echoed these findings, with a sensitivity of 11% for lesions smaller than 0.5 cm contrasting with 94% for le-

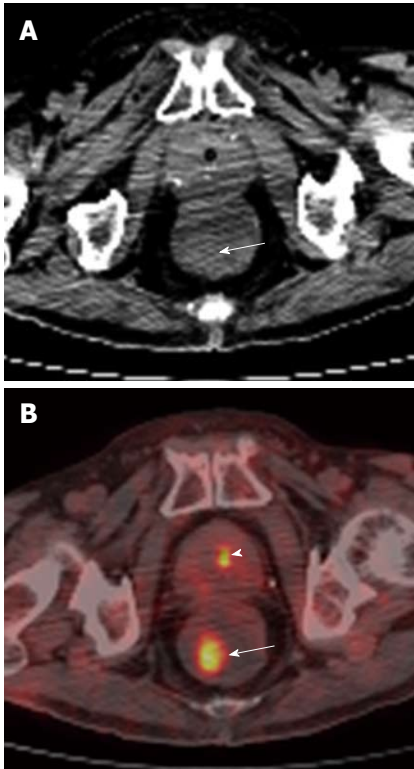


Figure 4 81-year-old male undergoing positron emission tomography (PET)/CT for restaging of diffuse large B cell lymphoma involving the duodenum. A: Axial non-contrast CT of the rectum showing an incidental subtle soft tissue density polypoid mass (arrow) in the right posterior lateral wall; B: This corresponded to a focal area of hypermetabolic activity (arrow), as demonstrated on fusion PET/CT. Biopsy returned as tubulovillous adenoma. This was excised. Smaller focus of increased tracer activity in keeping with normal physiologic excretion in the urine within the prostatic urethra (arrowhead).

sions larger than 5 cm, significantly underestimating the Peritoneal Cancer Index.

Post-treatment assessment

For routine surveillance, the American Society of Clinical Oncology currently recommends CEA assays every 3 mo for the first 3 years, CT scan of the chest, abdomen and pelvis annually for the first 3 years and colonoscopy at 3 years in patients with stage 2 and stage 3 CRC^[29].

Local disease recurrence is evidenced on CT by the serial progression of a mass, its nodular configuration and invasion of adjacent structures^[30]. However, CT cannot reliably differentiate tumour from post-treatment scar formation. For both local and nodal assessment of rectal cancer after neoadjuvant chemoradiation therapy, CT may not be able to reliably predict pathological response, and has a tendency to overstage disease. The study by Huh *et al.*^[31] looked at 80 rectal cancer patients following neoadjuvant chemoradiation therapy. It was found that the overall accuracy of CT for restaging the depth of tumour invasion and lymph node metastasis were 46.3% and 70.4%, respectively, while complete pathology-proved remission (11 patients) could not be correctly predicted.

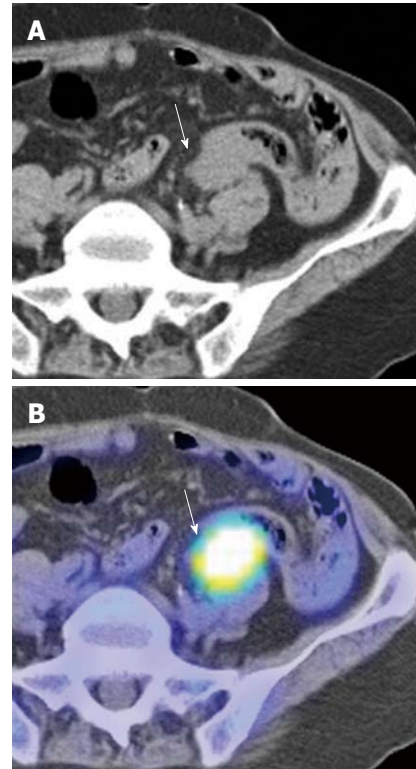


Figure 5 66-year-old Chinese male with adenocarcinoma of the rectum (not shown). A: Post-operative axial non-contrast CT component of a surveillance PET/CT study showing a soft tissue mass (arrow) abutting the sigmoid colon; B: Corresponding fusion PET/CT image of the lesion (arrow) demonstrates intense hypermetabolic activity consistent with tumour recurrence. (Case courtesy of Dr. Eik Hock Tan, Singapore).

Nevertheless, for the diagnosis of recurrent hepatic metastases, CT has already been shown to be more helpful than laboratory studies (liver function tests, measurement of CEA level)^[32]. Specifically, there is a 25% lower mortality in patients undergoing liver imaging compared with nonimaging strategies^[29]. This is further supported by the study of 530 patients conducted by Chau *et al.*^[33], in which routine post-treatment surveillance with CT and CEA levels in asymptomatic patients were shown to confer a median survival advantage of 13.8 mo over patients who were symptomatic. The reader should note however, given the increased costs, use of routine CT surveillance in these patients is only justified for those who are surgically fit to undergo metastasectomy. Therefore, CT currently still plays an important role in the postoperative surveillance of CRC.

FUNCTIONAL IMAGING BY CT

PET/CT

¹⁸Fluoro-deoxyglucose is the most widely used substrate for PET imaging. Fusion PET/CT combines the functional evaluation by PET with the anatomic detail provided by CT (Figures 4 and 5). PET/CT is increasingly shown to be superior to the other imaging modalities in demonstrating recurrent disease activity and has become

an integral part of the surveillance strategy for CRC. It has the potential to replace CT as the first-line diagnostic tool for restaging patients for recurrent CRC^[34]. In one study, PET/CT revealed unsuspected disease and modified the scope of surgery in around 10% of patients^[35]. In another study, FDG PET/CT altered treatment plans in 38% of patients largely through the detection of unsuspected lymphadenopathy^[36]. For local disease, PET/CT can improve preoperative target volume delineation by CT for conformal radiation therapy in rectal cancer^[37]. Preoperative PET/CT colonography may yield valuable information on the presence of synchronous tumors and for surgical planning^[38].

However, by far the greatest value of PET/CT in the management of CRC lies in its ability for whole body lesion detection. In one study, PET/CT showed high accuracy for the detection of liver metastases, with a reported accuracy of up to 99%, sensitivity up to 100% and specificity up to 98%^[39]. In the meta-analysis conducted by Kinkel *et al.*^[40] that included 110 studies, PET/CT afforded the highest mean weighted sensitivity (92%) and was significantly more sensitive for the detection of hepatic metastases from gastrointestinal cancers than CT. Rappeport *et al.*^[41] showed that PET/CT was superior to CT alone for the detection of extrahepatic metastases in CRC patients, with sensitivity and specificity rates of 83% and 96% for PET/CT and 58% and 87% for CT. Contrast-enhanced PET/CT and PET/CT colonography shows promise for improving accuracy in staging of disease^[42,43].

PET/CT can distinguish between tumour recurrence and post-surgical scar, as well as pinpoint the site of recurrence in cases with an unexplained rise in serum CEA^[44]. It is therefore recommended for evaluation of equivocal findings on serial CT and MRI^[45]. To detect recurrent nodal disease, PET/CT is superior to MRI, with a sensitivity of 93%^[46]. PET/CT is superior to contrast-enhanced CT in detecting local recurrences at the colorectal anastomosis, intrahepatic recurrences and extrahepatic disease, with sensitivity rates close to or exceeding 90%^[47]. Quantitative measurements of standardised uptake value and tumour volume may be used as a marker of tumour burden in cases of tumour recurrence^[48]. Note that PET/CT should be performed more than 6 wk following local therapy, as inflammatory changes can result in false positives.

In one study, PET/CT correctly assessed response of liver metastases to Bevacizumab-based therapy in 70% of cases compared to 35% by CT^[49]. For evaluation of liver metastases after radiofrequency ablation, PET/CT is comparable to MRI. In the study by Kuehl *et al.*^[50], the accuracy and sensitivity for the detection of liver metastases was 91% and 83% for PET/CT and 92% and 75% for MRI, respectively. After treatment of liver metastases with Y-90 microspheres, metabolic response on PET/CT correlates better with CEA levels than anatomic response with CT or MRI^[51]. This having

been said, it should be noted that complete metabolic response on FDG-PET after neoadjuvant chemotherapy does not necessarily imply complete pathologic response. Therefore, currently, curative resection of liver metastases should not be deferred solely on the basis of FDG-PET findings^[52,53].

Perfusion CT

Novel techniques such as perfusion CT^[54,55] and combined perfusion CT/PET CT^[56] show promise. Perfusion CT is performed at various time intervals after the injection of contrast. A precontrast scan is required for determination of increase in Hounsfield attenuation. Standard imaging protocols are to image at 45 and 130 s after contrast injection. For perfusion CT, iodinated contrast needs to be injected at a high rate, typically at 5 mL/s. Tissue blood flow, blood volume, mean transit time, and vascular permeability-surface area product are calculated based on the enhancement curves.

Aggressive tumors with poor differentiation are thought to be more vascular, and may therefore be distinguished from more well differentiated lesions with the use of perfusion CT. In the study by Sahani *et al.*^[57], rectal cancer showed higher tissue blood flow and shorter mean transit times than normal rectum. In another study, similar findings were echoed whereby CT perfusion was able to differentiate cancer from inflammation secondary to diverticulitis^[58].

An elevated liver perfusion index has also been found to be associated with the presence of hepatic metastases^[59]. Increased arterial perfusion appears to be an indicator of liver metastases, whereas reduced portal perfusion may indicate progressive disease^[60]. Perfusion CT may also play a role in predicting progression to metastatic disease. In the study by Goh *et al.*^[58], tumour blood flow differed significantly between disease-free and metastatic patients (76.0 mL/min per 100 g tissue *vs* 45.7 mL/min per 100 g tissue, respectively). Using blood flow < 64 mL/min per 100 g tissue as a cut-off, sensitivity and specificity for the development of metastases were 100% and 73%, respectively.

Perfusion CT has potential for predicting the response of rectal cancer to combined neoadjuvant chemotherapy and radiation therapy. In a study of 19 patients, blood flow, blood volume and permeability-surface area product significantly decreased after combined chemotherapy and radiation therapy ($P < 0.009$)^[61]. To date, however, the technique of perfusion CT remains the subject of research. The main drawback to this technique is the additional exposure to ionising radiation (estimated at 10 mSv). This translates to an added 1 in 2000 risk of lifetime cancer risk. To reduce the risk of ionising radiation, the radiation dose should be carefully optimised on a per patient basis.

There is also a need for standardisation of techniques. For example, the position and size of tumour region of interest analysis and observer variation have been found to substantially influence perfusion values. Region of inter-

est analysis for outlined entire tumour is more reliable for perfusion measurements and more appropriate clinically than use of arbitrarily determined smaller ROIs, although this may mean increased post-processing times^[62].

CONCLUSION

CT plays an important role in the management of CRC. The use of CT (colonography) as a screening tool for CRC has been validated and is expected to rise over time. The results of prior studies suggest that CT is suboptimal for the assessment of local T stage and moderate for N stage disease. Recent advances in CT technology are expected to lead to some improvement in staging accuracy. At present, the main role of CT in pre-treatment imaging assessment lies in its use for the detection of distant metastases, especially in the liver. In a select group of patients, routine post-treatment surveillance with CT confers survival benefits. The role of CT for post-treatment assessment has been radically altered and improved with the advent of fusion PET/CT. Perfusion CT shows promise as another functional imaging modality, but further experience with this technique is necessary before it can be applied to routine clinical practice.

REFERENCES

- 1 **Horner MJ**, Ries LAG, Krapcho M, Neyman N, Aminou R, Howlader N, Altekruse SF, Feuer EJ, Huang L, Mariotto A, Miller BA, Lewis DR, Eisner MP, Stinchcomb DG, Edwards BK, editors. SEER Cancer Statistics Review, 1975-2006. National Cancer Institute. Available from: URL: http://seer.cancer.gov/csr/1975_2006
- 2 **Espey DK**, Wu XC, Swan J, Wiggins C, Jim MA, Ward E, Wingo PA, Howe HL, Ries LA, Miller BA, Jemal A, Ahmed F, Cobb N, Kaur JS, Edwards BK. Annual report to the nation on the status of cancer, 1975-2004, featuring cancer in American Indians and Alaska Natives. *Cancer* 2007; **110**: 2119-2152
- 3 **Levin B**, Brooks D, Smith RA, Stone A. Emerging technologies in screening for colorectal cancer: CT colonography, immunochemical fecal occult blood tests, and stool screening using molecular markers. *CA Cancer J Clin* 2003; **53**: 44-55
- 4 **Duffy MJ**. Carcinoembryonic antigen as a marker for colorectal cancer: is it clinically useful? *Clin Chem* 2001; **47**: 624-630
- 5 **Pickhardt PJ**. Incidence of colonic perforation at CT colonography: review of existing data and implications for screening of asymptomatic adults. *Radiology* 2006; **239**: 313-316
- 6 **Burling D**, Halligan S, Slater A, Noakes MJ, Taylor SA. Potentially serious adverse events at CT colonography in symptomatic patients: national survey of the United Kingdom. *Radiology* 2006; **239**: 464-471
- 7 **Callstrom MR**, Johnson CD, Fletcher JG, Reed JE, Ahlquist DA, Harmsen WS, Tait K, Wilson LA, Corcoran KE. CT colonography without cathartic preparation: feasibility study. *Radiology* 2001; **219**: 693-698
- 8 **Hellström M**, Svensson MH, Lasson A. Extracolonic and incidental findings on CT colonography (virtual colonoscopy). *AJR Am J Roentgenol* 2004; **182**: 631-638
- 9 **Pickhardt PJ**, Choi JR, Hwang I, Butler JA, Puckett ML, Hildebrandt HA, Wong RK, Nugent PA, Mysliwiec PA, Schindler WR. Computed tomographic virtual colonoscopy to screen for colorectal neoplasia in asymptomatic adults. *N Engl J Med* 2003; **349**: 2191-2200

- 10 **Kim DH**, Pickhardt PJ, Hoff G, Kay CL. Computed tomographic colonography for colorectal screening. *Endoscopy* 2007; **39**: 545-549
- 11 **Kim DH**, Pickhardt PJ, Taylor AJ. Characteristics of advanced adenomas detected at CT colonographic screening: implications for appropriate polyp size thresholds for polypectomy versus surveillance. *AJR Am J Roentgenol* 2007; **188**: 940-944
- 12 **Moravec M**, Lieberman DA, Holub J, Michaels L, Eisen GM. Rate of advanced pathologic features in 6-9 mm polyps in patients referred for colonoscopy screening. *Gastrointest Endosc* 2007; **65**: AB127
- 13 **Chung DJ**, Huh KC, Choi WJ, Kim JK. CT colonography using 16-MDCT in the evaluation of colorectal cancer. *AJR Am J Roentgenol* 2005; **184**: 98-103
- 14 **Brenner DJ**, Georgsson MA. Mass screening with CT colonography: should the radiation exposure be of concern? *Gastroenterology* 2005; **129**: 328-337
- 15 **Macari M**, Bini EJ, Xue X, Milano A, Katz SS, Resnick D, Chandarana H, Krinsky G, Klingenberg K, Marshall CH, Megibow AJ. Colorectal neoplasms: prospective comparison of thin-section low-dose multi-detector row CT colonography and conventional colonoscopy for detection. *Radiology* 2002; **224**: 383-392
- 16 **Horton KM**, Abrams RA, Fishman EK. Spiral CT of colon cancer: imaging features and role in management. *Radiographics* 2000; **20**: 419-430
- 17 **Kwok H**, Bissett IP, Hill GL. Preoperative staging of rectal cancer. *Int J Colorectal Dis* 2000; **15**: 9-20
- 18 **O'Neill BD**, Salerno G, Thomas K, Tait DM, Brown G. MR vs CT imaging: low rectal cancer tumour delineation for three-dimensional conformal radiotherapy. *Br J Radiol* 2009; **82**: 509-513
- 19 **Wolberink SV**, Beets-Tan RG, de Haas-Kock DF, van de Jagt EJ, Span MM, Wiggers T. Multislice CT as a primary screening tool for the prediction of an involved mesorectal fascia and distant metastases in primary rectal cancer: a multicenter study. *Dis Colon Rectum* 2009; **52**: 928-934
- 20 **Acunaş B**, Rozanes I, Acunaş G, Celik L, Sayi I, Gökmen E. Preoperative CT staging of colon carcinoma (excluding the recto-sigmoid region). *Eur J Radiol* 1990; **11**: 150-153
- 21 **Bipat S**, Glas AS, Slors FJ, Zwinderman AH, Bossuyt PM, Stoker J. Rectal cancer: local staging and assessment of lymph node involvement with endoluminal US, CT, and MR imaging--a meta-analysis. *Radiology* 2004; **232**: 773-783
- 22 **Valls C**, Andía E, Sánchez A, Gumà A, Figueras J, Torras J, Serrano T. Hepatic metastases from colorectal cancer: preoperative detection and assessment of resectability with helical CT. *Radiology* 2001; **218**: 55-60
- 23 **Ch'en IY**, Katz DS, Jeffrey RB Jr, Daniel BL, Li KC, Beaulieu CF, Mindelzun RE, Yao D, Olcott EW. Do arterial phase helical CT images improve detection or characterization of colorectal liver metastases? *J Comput Assist Tomogr* 1997; **21**: 391-397
- 24 **Brent A**, Talbot R, Coyne J, Nash G. Should indeterminate lung lesions reported on staging CT scans influence the management of patients with colorectal cancer? *Colorectal Dis* 2007; **9**: 816-818
- 25 **Adeyemo D**, Hutchinson R. Preoperative staging of rectal cancer: pelvic MRI plus abdomen and pelvic CT. Does extrahepatic abdomen imaging matter? A case for routine thoracic CT. *Colorectal Dis* 2009; **11**: 259-263
- 26 **Shepherd NA**, Baxter KJ, Love SB. The prognostic importance of peritoneal involvement in colonic cancer: a prospective evaluation. *Gastroenterology* 1997; **112**: 1096-1102
- 27 **de Bree E**, Koops W, Kröger R, van Ruth S, Witkamp AJ, Zoetmulder FA. Peritoneal carcinomatosis from colorectal or appendiceal origin: correlation of preoperative CT with in-

- traoperative findings and evaluation of interobserver agreement. *J Surg Oncol* 2004; **86**: 64-73
- 28 **Koh JL**, Yan TD, Glenn D, Morris DL. Evaluation of preoperative computed tomography in estimating peritoneal cancer index in colorectal peritoneal carcinomatosis. *Ann Surg Oncol* 2009; **16**: 327-333
- 29 **Desch CE**, Benson AB 3rd, Somerfield MR, Flynn PJ, Krause C, Loprinzi CL, Minsky BD, Pfister DG, Virgo KS, Petrelli NJ. Colorectal cancer surveillance: 2005 update of an American Society of Clinical Oncology practice guideline. *J Clin Oncol* 2005; **23**: 8512-8519
- 30 **McCarthy SM**, Barnes D, Deveney K, Moss AA, Goldberg HI. Detection of recurrent rectosigmoid carcinoma: prospective evaluation of CT and clinical factors. *AJR Am J Roentgenol* 1985; **144**: 577-579
- 31 **Huh JW**, Park YA, Jung EJ, Lee KY, Sohn SK. Accuracy of endorectal ultrasonography and computed tomography for restaging rectal cancer after preoperative chemoradiation. *J Am Coll Surg* 2008; **207**: 7-12
- 32 **Freeny PC**, Marks WM, Ryan JA, Bolen JW. Colorectal carcinoma evaluation with CT: preoperative staging and detection of postoperative recurrence. *Radiology* 1986; **158**: 347-353
- 33 **Chau I**, Allen MJ, Cunningham D, Norman AR, Brown G, Ford HE, Tebbutt N, Tait D, Hill M, Ross PJ, Oates J. The value of routine serum carcino-embryonic antigen measurement and computed tomography in the surveillance of patients after adjuvant chemotherapy for colorectal cancer. *J Clin Oncol* 2004; **22**: 1420-1429
- 34 **Soyka JD**, Veit-Haibach P, Strobel K, Breitenstein S, Tschopp A, Mende KA, Lago MP, Hany TF. Staging pathways in recurrent colorectal carcinoma: is contrast-enhanced 18F-FDG PET/CT the diagnostic tool of choice? *J Nucl Med* 2008; **49**: 354-361
- 35 **Llamas-Elvira JM**, Rodríguez-Fernández A, Gutiérrez-Sáinz J, Gomez-Rio M, Bellon-Guardia M, Ramos-Font C, Rebollo-Aguirre AC, Cabello-García D, Ferrón-Orihuela A. Fluorine-18 fluorodeoxyglucose PET in the preoperative staging of colorectal cancer. *Eur J Nucl Med Mol Imaging* 2007; **34**: 859-867
- 36 **Gearhart SL**, Frassica D, Rosen R, Choti M, Schulick R, Wahl R. Improved staging with pretreatment positron emission tomography/computed tomography in low rectal cancer. *Ann Surg Oncol* 2006; **13**: 397-404
- 37 **Bassi MC**, Turri L, Sacchetti G, Loi G, Cannillo B, La Mattina P, Brambilla M, Inglese E, Krengli M. FDG-PET/CT imaging for staging and target volume delineation in preoperative conformal radiotherapy of rectal cancer. *Int J Radiat Oncol Biol Phys* 2008; **70**: 1423-1426
- 38 **Nagata K**, Ota Y, Okawa T, Endo S, Kudo SE. PET/CT colonography for the preoperative evaluation of the colon proximal to the obstructive colorectal cancer. *Dis Colon Rectum* 2008; **51**: 882-890
- 39 **Nahas CS**, Akhurst T, Yeung H, Leibold T, Riedel E, Markowitz AJ, Minsky BD, Paty PB, Weiser MR, Temple LK, Wong WD, Larson SM, Guillem JG. Positron emission tomography detection of distant metastatic or synchronous disease in patients with locally advanced rectal cancer receiving preoperative chemoradiation. *Ann Surg Oncol* 2008; **15**: 704-711
- 40 **Kinkel K**, Lu Y, Both M, Warren RS, Thoeni RF. Detection of hepatic metastases from cancers of the gastrointestinal tract by using noninvasive imaging methods (US, CT, MR imaging, PET): a meta-analysis. *Radiology* 2002; **224**: 748-756
- 41 **Rappeport ED**, Loft A, Berthelsen AK, von der Recke P, Larsen PN, Mogensen AM, Wettergren A, Rasmussen A, Hillingsøe J, Kirkegaard P, Thomsen C. Contrast-enhanced FDG-PET/CT vs. SPIO-enhanced MRI vs. FDG-PET vs. CT in patients with liver metastases from colorectal cancer: a prospective study with intraoperative confirmation. *Acta Radiol* 2007; **48**: 369-378
- 42 **Vriens D**, de Geus-Oei LF, van der Graaf WT, Oyen WJ. Tailoring therapy in colorectal cancer by PET-CT. *Q J Nucl Med Mol Imaging* 2009; **53**: 224-244
- 43 **Potter KC**, Husband JE, Houghton SL, Thomas K, Brown G. Diagnostic accuracy of serial CT/magnetic resonance imaging review vs. positron emission tomography/CT in colorectal cancer patients with suspected and known recurrence. *Dis Colon Rectum* 2009; **52**: 253-259
- 44 **Schmidt GP**, Baur-Melnyk A, Haug A, Utzschneider S, Becker CR, Tiling R, Reiser MF, Hermann KA. Whole-body MRI at 1.5 T and 3 T compared with FDG-PET-CT for the detection of tumour recurrence in patients with colorectal cancer. *Eur Radiol* 2009; **19**: 1366-1378
- 45 **Selzner M**, Hany TF, Wildbrett P, McCormack L, Kadry Z, Clavien PA. Does the novel PET/CT imaging modality impact on the treatment of patients with metastatic colorectal cancer of the liver? *Ann Surg* 2004; **240**: 1027-1034; discussion 1035-1036
- 46 **Choi MY**, Lee KM, Chung JK, Lee DS, Jeong JM, Park JG, Kim JH, Lee MC. Correlation between serum CEA level and metabolic volume as determined by FDG PET in postoperative patients with recurrent colorectal cancer. *Ann Nucl Med* 2005; **19**: 123-129
- 47 **Badiee S**, Franc BL, Webb EM, Chu B, Hawkins RA, Coakley F, Singer L. Role of IV iodinated contrast material in 18F-FDG PET/CT of liver metastases. *AJR Am J Roentgenol* 2008; **191**: 1436-1439
- 48 **Veit-Haibach P**, Kuehle CA, Beyer T, Stergar H, Kuehl H, Schmidt J, Börsch G, Dahmen G, Barkhausen J, Bockisch A, Antoch G. Diagnostic accuracy of colorectal cancer staging with whole-body PET/CT colonography. *JAMA* 2006; **296**: 2590-2600
- 49 **Goshen E**, Davidson T, Zwas ST, Aderka D. PET/CT in the evaluation of response to treatment of liver metastases from colorectal cancer with bevacizumab and irinotecan. *Technol Cancer Res Treat* 2006; **5**: 37-43
- 50 **Kuehl H**, Antoch G, Stergar H, Veit-Haibach P, Rosenbaum-Krumme S, Vogt F, Frilling A, Barkhausen J, Bockisch A. Comparison of FDG-PET, PET/CT and MRI for follow-up of colorectal liver metastases treated with radiofrequency ablation: initial results. *Eur J Radiol* 2008; **67**: 362-371
- 51 **Wong CY**, Salem R, Raman S, Gates VL, Dworkin HJ. Evaluating 90Y-glass microsphere treatment response of unresectable colorectal liver metastases by [18F]FDG PET: a comparison with CT or MRI. *Eur J Nucl Med Mol Imaging* 2002; **29**: 815-820
- 52 **Tan MC**, Linehan DC, Hawkins WG, Siegel BA, Strasberg SM. Chemotherapy-induced normalization of FDG uptake by colorectal liver metastases does not usually indicate complete pathologic response. *J Gastrointest Surg* 2007; **11**: 1112-1119
- 53 **Lubezky N**, Metser U, Geva R, Nakache R, Shmueli E, Klausner JM, Even-Sapir E, Figer A, Ben-Haim M. The role and limitations of 18-fluoro-2-deoxy-D-glucose positron emission tomography (FDG-PET) scan and computerized tomography (CT) in restaging patients with hepatic colorectal metastases following neoadjuvant chemotherapy: comparison with operative and pathological findings. *J Gastrointest Surg* 2007; **11**: 472-478
- 54 **Wu GY**, Ghimire P. Perfusion computed tomography in colorectal cancer: protocols, clinical applications and emerging trends. *World J Gastroenterol* 2009; **15**: 3228-3231
- 55 **Goh V**, Halligan S, Wellsted DM, Bartram CI. Can perfusion CT assessment of primary colorectal adenocarcinoma blood flow at staging predict for subsequent metastatic disease? A pilot study. *Eur Radiol* 2009; **19**: 79-89

- 56 **Veit-Haibach P**, Treyer V, Strobel K, Soyka JD, Husmann L, Schaefer NG, Tschopp A, Hany TF. Feasibility of integrated CT-liver perfusion in routine FDG-PET/CT. *Abdom Imaging* 2009; Epub ahead of print
- 57 **Sahani DV**, Kalva SP, Hamberg LM, Hahn PF, Willett CG, Saini S, Mueller PR, Lee TY. Assessing tumor perfusion and treatment response in rectal cancer with multisection CT: initial observations. *Radiology* 2005; **234**: 785-792
- 58 **Goh V**, Halligan S, Taylor SA, Burling D, Bassett P, Bartram CI. Differentiation between diverticulitis and colorectal cancer: quantitative CT perfusion measurements versus morphologic criteria—initial experience. *Radiology* 2007; **242**: 456-462
- 59 **Ballantyne KC**, Charnley RM, Perkins AC, Pye G, Whalley DR, Wastie ML, Hardcastle JD. Hepatic perfusion index in the diagnosis of overt metastatic colorectal cancer. *Nucl Med Commun* 1990; **11**: 23-28
- 60 **Leggett DA**, Kelley BB, Bunce IH, Miles KA. Colorectal cancer: diagnostic potential of CT measurements of hepatic perfusion and implications for contrast enhancement protocols. *Radiology* 1997; **205**: 716-720
- 61 **Bellomi M**, Petralia G, Sonzogni A, Zampino MG, Rocca A. CT perfusion for the monitoring of neoadjuvant chemotherapy and radiation therapy in rectal carcinoma: initial experience. *Radiology* 2007; **244**: 486-493
- 62 **Goh V**, Halligan S, Gharpuray A, Wellsted D, Sundin J, Bartram CI. Quantitative assessment of colorectal cancer tumor vascular parameters by using perfusion CT: influence of tumor region of interest. *Radiology* 2008; **247**: 726-732

S- Editor Cheng JX L- Editor Webster JR E- Editor Zheng XM

Magnetic resonance imaging staging of nasopharyngeal carcinoma in the head and neck

Ann Dorothy King, Kunwar Suryaveer Singh Bhatia

Ann Dorothy King, Kunwar Suryaveer Singh Bhatia, Department of Diagnostic Radiology and Organ Imaging, Faculty of Medicine, The Chinese University of Hong Kong, Prince of Wales Hospital, Shatin, 30-32 Ngan Shing Street, New Territories, Hong Kong, China

Author contributions: King AD participated in conception, design, literature search, drafting and revision of the manuscript; Bhatia KSS searched the literature, prepared the image and revised the paper.

Correspondence to: Ann Dorothy King, FRCR, Department of Diagnostic Radiology and Organ Imaging Faculty of Medicine, The Chinese University of Hong Kong, Prince of Wales Hospital, Shatin, New Territories, Hong Kong, China. b834756@mailserv.cuhk.edu.hk

Telephone: +1-852-26322290 Fax: +1-852-26322290

Received: March 31, 2010 Revised: April 26, 2010

Accepted: May 3, 2010

Published online: May 28, 2010

Abstract

Magnetic resonance imaging (MRI) is the modality of choice for staging nasopharyngeal carcinoma in the head and neck. This article will review the patterns of primary and nodal spread on MRI with reference to the latest 7th edition of the International Union Against Cancer/American Joint Committee on Cancer staging system.

© 2010 Baishideng. All rights reserved.

Key words: Lymph nodes; Magnetic resonance imaging; metastases; Nasopharyngeal carcinoma; Staging

Peer reviewers: Juebin Huang, MD, PhD, Assistant Professor, Department of Neurology, The University of Mississippi Medical Center, 2500 N. State Street, Jackson, MS 39216, United States; Rivka R Colen, MD, Department of Radiology, Brigham and Women's Hospital, 75 Francis St, Boston, MA 02115, United States; Meng Law, MD, MBBS, FRACR, Professor of Radiology and Neurological Surgery, Director of Neuroradiology, Keck School of Medicine, University of Southern California, 1500 San Pablo St, Los Angeles, CA 90033, United States

King AD, Bhatia KSS. Magnetic resonance imaging staging of nasopharyngeal carcinoma in the head and neck. *World J Radiol* 2010; 2(5): 159-165 Available from: URL: <http://www.wjgnet.com/1949-8470/full/v2/i5/159.htm> DOI: <http://dx.doi.org/10.4329/wjr.v2.i5.159>

INTRODUCTION

Nasopharyngeal carcinoma (NPC) is an uncommon cancer but pockets of high prevalence are found in regions of the world such as southern China, North Africa, Greenland and Alaska. In the Chinese population, the tumor is usually a non-keratinizing undifferentiated carcinoma (Type III) with a peak age incidence of 40-70 years, and is the form of the disease described in this review. Undifferentiated NPC is linked to infection with the Epstein Bar virus and has additional risk factors including diet and a genetic predisposition in family members. Because the nasopharynx is a relatively clinically silent region, patients often do not present until late when the tumor has spread into the deep tissues or to nodes in the neck. Nevertheless, this tumor is highly responsive to radiotherapy and the overall 5 years progression-free and cancer specific survival are 63% and 80%, respectively^[1]. The diagnosis of NPC is made by endoscopy and confirmed on endoscopically-guided biopsy before the patient is referred for imaging to stage the cancer and plan treatment.

Head and neck computed tomography (CT) and magnetic resonance imaging (MRI) are used to stage the primary and nodal NPC, but the latter is preferred^[2-5] because it is superior in terms of delineating small anatomical structures that make up the boundary of the nasopharynx, mapping tumor extent in the skull base, paranasal sinuses and brain, and discriminating between the primary tumor and adjacent retropharyngeal nodes. In some centers, fluorodeoxyglucose positron emission tomography integrated with CT (PET/CT) is advocated for NPC staging, because it may increase the accuracy of the assessment of cervical nodal metastases as well as re-

placing other conventional imaging techniques which are used to screen for metastases at distant sites outside the head and neck^[6]. However, in these circumstances PET/CT is performed as an additional imaging modality to head and neck MRI, because MRI is superior for assessing primary tumor extent and retropharyngeal nodes^[6,7].

The MRI scan should cover the head and neck from just above the skull base to just below the suprasternal notch. The protocol will vary between centers but in general T2-weighted sequences are performed in the coronal plane and axial planes, the latter with fat saturation, together with T1-weighted images in the axial +/- sagittal planes. Following a bolus injection of intravenous contrast, T1-weighted post-contrast scans are performed in at least two planes, and these should include at least one sequence without fat saturation using a 512 matrix, and one with fat saturation.

This review of staging NPC using MRI will follow the TNM staging system according to the latest 7th edition of the International Union Against Cancer/American Joint Committee on Cancer (UICC/AJCC) Cancer staging manual published in 2009/2010^[8,9] which stages the primary tumor from stage T0 to T4 and the nodal metastases from N0 to N3.

MRI STAGING OF THE PRIMARY TUMOUR (T-STAGE)

Stage T0 and T1 disease

Tumor confined to the nasopharynx: The nasopharynx consists of a roof, posterior wall, lateral walls and inferior wall formed by the palate. MRI is a very sensitive technique for identifying NPC, therefore it is rare to find patients in whom the primary tumor cannot be identified (stage T0)^[10]. In addition, the recent widespread use of serological testing in high risk patients with a family history of NPC is leading to the early detection of tumors^[11], some of which can be clearly depicted by MRI but may be missed by endoscopy or endoscopic guided biopsy, because they are submucosal or buried deep in the lateral pharyngeal recess^[10]. The latter site, also known as the fossa of Rosenmuller, lies posterior to the opening of the eustachian tube and is the most common site for NPC to arise (Figure 1)^[10,12]. Mucosal spread of primary tumors tends to involve the superior portion of the nasopharynx rather than the inferior portion and palatal wall. Deep infiltrating tumors may be found even when the nasopharyngeal component is small, while other primary tumors may reach a large size and fill the nasopharyngeal cavity without extending outside the nasopharynx. However, in the non-serology screening setting, most NPCs have already spread to adjacent sites at diagnosis and so disease confined to the nasopharynx (stage T1) is only found in about a fifth of patients^[13].

Tumor spread to the nasal cavity and oropharynx: In the latest edition of the UICC/AJCC classification, superficial spread to the nasal cavity and oropharynx has been

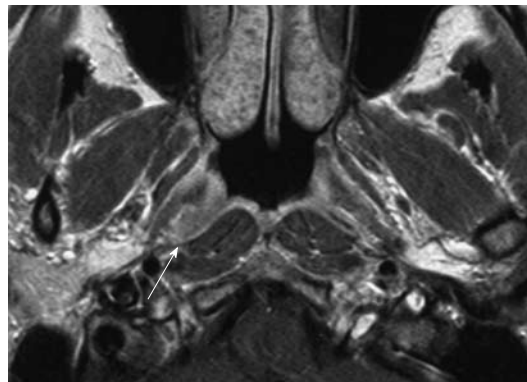


Figure 1 Axial post-contrast T1 weighted magnetic resonance imaging (MRI) showing a small nasopharyngeal carcinoma within the right lateral pharyngeal recess (arrow). This is a frequent site for early cancer.

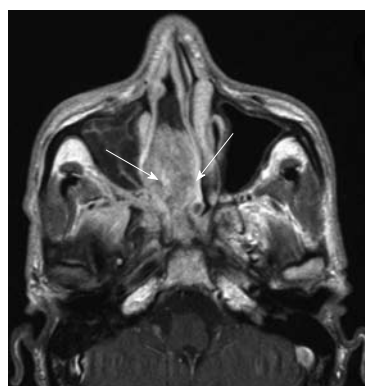


Figure 2 Axial post-contrast T1 weighted MRI showing a bulky nasopharyngeal carcinoma with gross extension into the right nasal cavity (arrows).

down staged from T2 to T1 disease. The nasal cavity is commonly involved by this carcinoma because it lies directly anterior to the nasopharynx. Minimal invasion with tumor just crossing the margin of the choanal orifice is common, while more bulky disease extending into the main body of the nasal cavity is encountered less frequently (Figure 2). The nasal septum should always be scrutinized on the axial and coronal images as tumor in the nasopharyngeal roof may spread centrally along the septum.

Inferior superficial extension down to the mucosa of the oropharynx is uncommon, tumors preferentially spreading superiorly to the skull base. Therefore, invasion of the oropharynx rarely occurs as an isolated event and is not usually an early sign of disease because it is already associated with tumor spread to sites such as the parapharyngeal region, skull base and cranium^[13,14] (Figure 3).

Stage T2 disease

Tumor spread to the parapharynx: Deep extension into the parapharyngeal region has been changed from stage T2b to stage T2. Parapharyngeal spread occurs when tumor spreads posterolaterally from the nasopharynx and usually involves lateral penetration through the levator palatini muscle and pharyngobasilar fascia to involve the

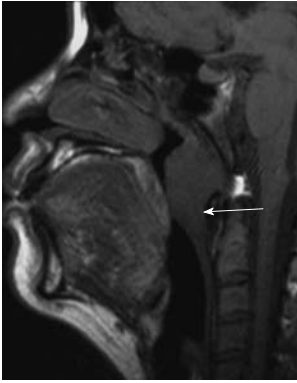


Figure 3 Sagittal T1 weighted MRI showing a bulky nasopharyngeal carcinoma with inferior extension, crossing the C1/2 level, along the posterior wall into the oropharynx (arrow).

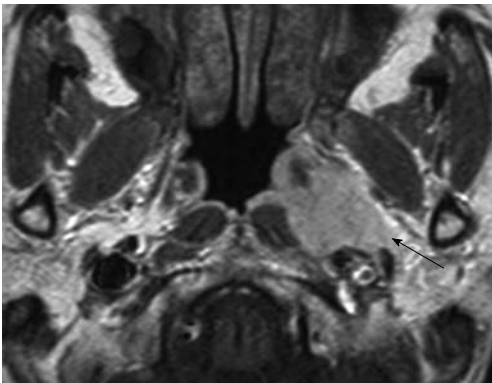


Figure 4 Axial post-contrast T1 weighted MRI showing a nasopharyngeal carcinoma directly infiltrating into the left parapharyngeal space (arrow).

tensor palatini muscle and parapharyngeal fat space which contains the pharyngeal venous plexus. Parapharyngeal invasion is associated with an increased risk of distant metastases, tumor recurrence and survival^[15-17]. MRI is able to distinguish between a primary tumor confined to the nasopharynx that is only bulging into the fat space (stage T1), a primary tumor confined to the nasopharynx which is abutting a metastatic retropharyngeal node (stage T1N1), and a primary tumor that is directly invading the parapharyngeal region (stage T2) (Figure 4)^[18]. Parapharyngeal involvement can lead to compression of the eustachian tube resulting in a middle ear and mastoid effusion. Further posterolateral spread may also involve the carotid space and encase the carotid artery.

Directly posterior to the nasopharynx is the retropharyngeal region, longus capitis muscles, prevertebral space and clivus (Figure 5). Direct posterior extension into these sites may be the only site of invasion outside the nasopharynx. In some patients this posterior extension is the preferred pattern of tumor spread with bulky disease continuing down to the foramen magnum and upper cervical spine. This region contains lymphatics and a venous plexus and so invasion of the prevertebral space is associated with an increased risk of distant metastases and decreased survival^[19].

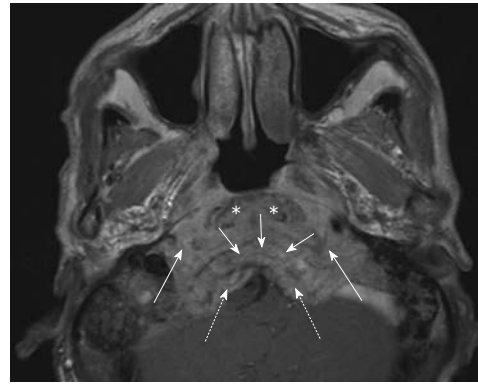


Figure 5 Axial post-contrast T1-weighted MRI showing a nasopharyngeal carcinoma with gross posterior retropharyngeal extension in the longus capitis muscles (asterisks), prevertebral space (long arrows), clivus (short arrows) and posterior cranial fossa (broken arrows).

Stage T3 disease

Tumor spread to the skull base: Tumor invasion into the skull base or paranasal sinuses remains stage T3 disease in the latest edition of the UICC/AJCC classification. NPC has a propensity to invade bone and over 60% of patients have skull base invasion at diagnosis^[13]. The number of bony sites may influence prognosis^[20] and can vary from extensive invasion involving multiple sites to only a small localized area, which in some patients may be the only site of extra nasopharyngeal spread. The clivus, pterygoid bones, body of the sphenoid and apices of the petrous temporal bones are most commonly invaded. The axial T1 weighted image provides a good overview of the extent of any skull base invasion and interrogation relies on identifying five key regions of high T1 signal fatty bone marrow which comprise the clivus; right pterygoid base; left pterygoid base; right petrous apex; left petrous apex (Figure 6A and B). The body of the sphenoid is more difficult to assess because it forms a thin shelf around the sphenoid sinus but can be studied on the coronal images. After identification of the major sites of bony invasion, other sites including the sphenoid wings and upper cervical spine should be assessed before scrutinizing the skull base foramina and fissures. The skull base foramina form an unimpeded channel for tumor spread, but there is often direct invasion of the bones bordering these foramina. The foramina are assessed best on the coronal images, and passing from the anterior to the posterior skull base they consist of the foramen rotundum (V² nerve) and vidian canal (vidian nerve) (Figure 7A); the foramen ovale (V³ nerve) (Figure 7B); and foramen lacerum (which lies below the horizontal portion of the internal carotid artery) (Figure 7C). The foramen ovale and lacerum are two commonly involved foramina which provide a route of tumor spread into the cranium^[2,13,21].

Inferior spread of tumor to involve the hypoglossal nerve canal (XII nerve) and jugular foramen (IX-XI nerves) is less common, but in the case of the hypoglossal nerve canal, denervation of the hemitongue may be found.

Tumor may also involve the pterygomaxillary fissure, which lies posterior to the maxillary sinus, and the

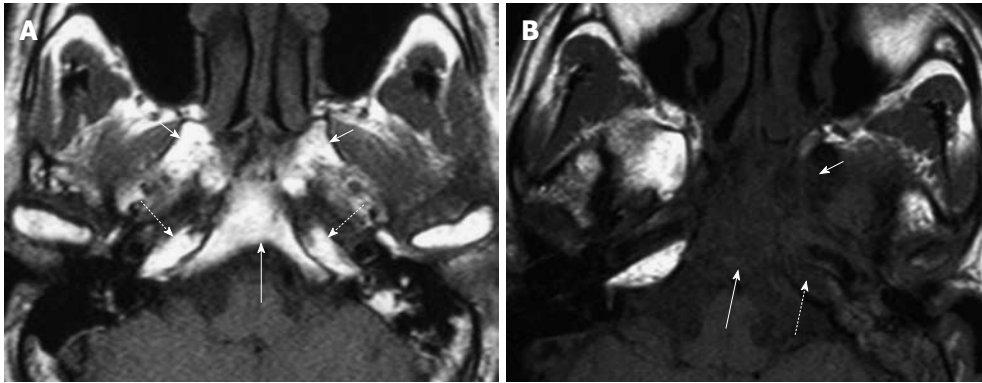


Figure 6 Axial T1 weighted MRI of the skull base showing five key bony sites to check for tumor invasion. A: Normal skull base showing T1W weighted signal of normal fatty bone marrow within the clivus (long arrow), bilateral pterygoid bases (short arrows) and petrous apices (broken arrows); B: Abnormal skull base showing loss of normal high T1 weighted signal due to tumor invasion of the clivus (long arrow), left pterygoid base (short arrow) and left petrous apex (broken arrow).

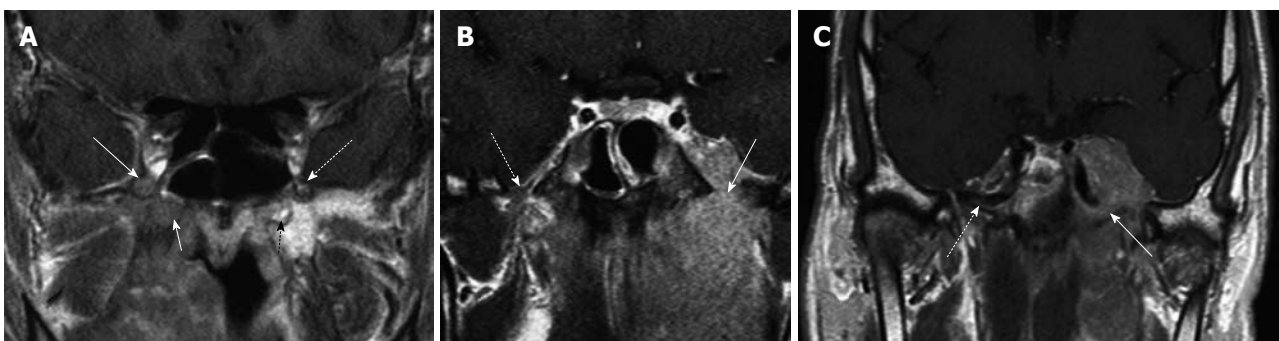


Figure 7 Coronal post-contrast T1 weighted MRIs of nasopharyngeal carcinoma in three patients illustrating tumor extension in the foramina from the anterior (A) to the posterior (C) skull base. A: The right foramen rotundum and vidian canal (solid long and short arrows, respectively); B: Left foramen ovale (solid arrow); C: Left foramen lacerum (solid arrow). The uninvolved foramina on the contralateral sides are indicated by broken arrows.

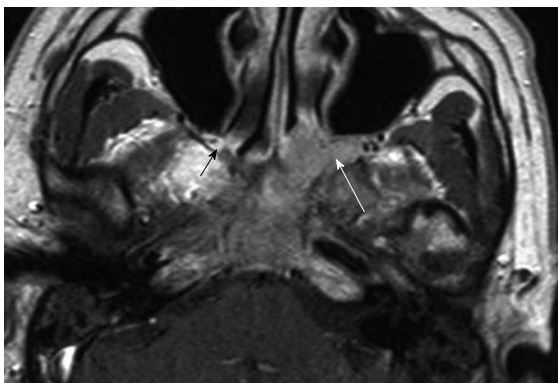


Figure 8 Axial post-contrast T1 weighted MRI showing contiguous extension of nasopharyngeal carcinoma into the left pterygopalatine fossa which is expanded (long arrow). Compare this with the normal hyperintense fat signal in the narrow pterygopalatine fossa on the contralateral side (short arrow).

petroclival fissure. Finally, positioned in the central skull base is the pterygopalatine fossa (Figure 8) which forms a very important crossroads connecting the skull base to the face and brain. This fossa can be located in the most medial aspect of the pterygomaxillary fissure on the axial images and provides a route of tumor spread to the orbit (*via* the inferior orbital fissure), infratemporal fossa (*via*

the pterygomaxillary fissure), oral cavity (*via* the pterygopalatine canal), nasal cavity (*via* the sphenopalatine foramen), foramen lacerum (*via* the vidian canal) and middle cranial fossa (*via* foramen rotundum).

Tumor spread to the paranasal sinuses: Mucosal inflammatory changes in the paranasal sinuses are common in patients with NPC, and MRI has the advantage over CT of providing better discrimination between tumor and these benign changes. The sphenoid sinus is frequently invaded by NPC because it lies immediately above the roof of the nasopharynx from which it is separated by a thin plate of bone (Figure 9). Tumor invasion of the ethmoid sinuses usually occurs from direct spread from the sphenoid sinus or nasal cavity, and invasion at this site may reduce the chance of shielding the optic nerve from the radiotherapy field. The maxillary sinus is rarely involved except as a late event when there is usually extensive invasion elsewhere, not only within the nasal cavity, but also the sphenoid and ethmoid sinuses, skull base and brain^[13].

Stage T4 disease

Tumor spread to the intracranium, cranial nerves and orbit: NPC invades the cavernous sinus (Figure 9) and dura^[2,15], while direct invasion of the brain at diagnosis is rare. Invasion of the cavernous sinus can lead to multiple cranial

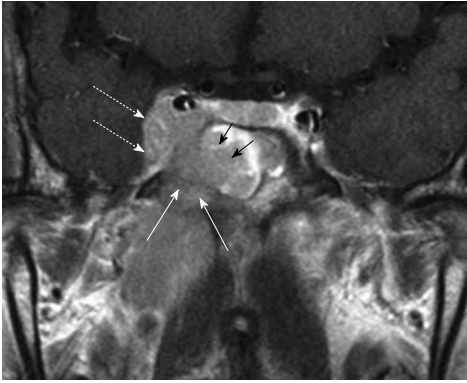


Figure 9 Coronal post-contrast T1 weighted MRI showing a nasopharyngeal carcinoma with direct infiltration through the sphenoid body (long arrows) into the sphenoid sinus (short arrows) and right cavernous sinus (broken arrows).

nerve palsies involving cranial nerves III, IV, V¹, V² and VI. NPC may spread into the cavernous sinus from multiple directions including posteriorly from tumor surrounding the horizontal portion of the internal carotid artery, anteriorly from the orbital fissures or through the skull base in the region of the foramen ovale or sphenoid sinus. Dural invasion usually involves the floor of the middle cranial fossa adjacent to the cavernous sinus and foramen ovale, while posterior fossa invasion occurs along the posterior aspect of the clivus and occasionally along the tentorium.

Cranial nerve involvement is a clinical rather than radiological sign for staging, although tumor may be seen on MRI on the post-contrast T1-weighted images with fat saturation, especially around the V³ and V² nerves in the foramen ovale and rotundum, respectively. True perineural spread, in which tumor extends a long distance along the nerve away from the primary tumor site and foramina in the skull base, is occasionally found, but in general is uncommon in the pre-treatment setting. Orbital invasion is also a marker of the most extensive form of NPC and is usually invaded by tumor in the pterygopalatine fossa travelling *via* the inferior orbital fissure or directly from the cavernous sinus.

Tumor spread to the infratemporal fossa/masticator space and hypopharynx: Invasion of the medial and lateral pterygoid muscles, infratemporal fat and temporalis muscle is denoted as T4 disease and is usually found when tumors extend laterally from the parapharyngeal space, pterygoid base or the pterygomaxillary fissure. The hypopharynx is the most inferior site of tumor invasion included in the staging classification, but it is very rarely involved at diagnosis because, as noted above, NPC has a preference for extending superiorly to the skull base rather than inferiorly to the oropharynx and then hypopharynx.

MRI STAGING OF NODAL METASTASES (N-STAGE)

Patterns of nodal spread

NPC has a propensity to spread to nodes with over 75%

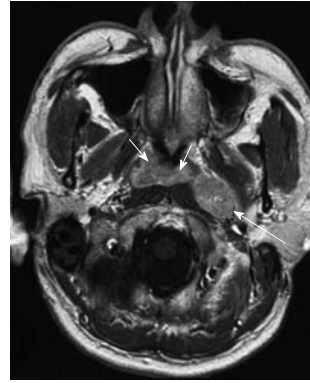


Figure 10 Axial post-contrast T1 weighted MRI showing a nasopharyngeal carcinoma (short arrows) and a grossly enlarged metastatic left retropharyngeal lymph node at the level of the nasopharynx (long arrow).

of patients having nodal metastases at presentation and enlarged nodes may be the first clinical manifestation of disease. Nodal metastases are not necessarily related to the size^[22] or stage of the primary tumor because patients with small tumors may have extensive nodal metastases while some bulky tumors invading the skull base show no nodal spread. Nodal metastases from NPC have a tendency for bilateral neck spread. Lateral retropharyngeal nodes, which lie medial to the carotid artery (Figure 10), are one of the most common sites of nodal spread from NPC^[23] and are easily identified on MRI^[24,25] and as such have been considered the first echelon of metastatic spread^[23,25]. However, it has now been shown that metastatic nodal spread may bypass these nodes and spread directly to the non-retropharyngeal nodes in the upper neck, usually to the level II nodes^[26-29]. It should also be noted that the metastatic lateral retropharyngeal nodes can be identified on MRI from the skull base to the level of C3^[25], and therefore they frequently extend deep to the oropharyngeal wall (Figure 11). The median group of retropharyngeal nodes does not form a discrete nodal chain^[30] and as such are not usually identified on MRI in NPC^[24,25].

Skip metastases to the lower neck have been described^[29] but usually nodal metastases spread in an orderly fashion^[31] down the neck involving the nodal groups along the internal jugular chain (level II to IV), and spinal accessory chain in the posterior triangle (Va and Vb). Metastatic nodes posterior to the jugular vein in the upper neck (Figure 11) are the most common site for non-retropharyngeal nodes^[27] and are designated as high internal jugular nodes (level II a or b), although at this site the internal jugular and spinal accessory nodal chains converge. Nodes in the submandibular and parotid/periparotid region are far less common at diagnosis but should be searched for because of the implications for planning radiotherapy especially intensity modulated radiotherapy. Nodes at these sites may be found when there are bulky upper cervical nodes (Figure 12) which obstruct the normal routes of lymphatic drainage^[25,29]. Once the nodal metastases reach the supraclavicular fossa there is an increased incidence of distant metastases.

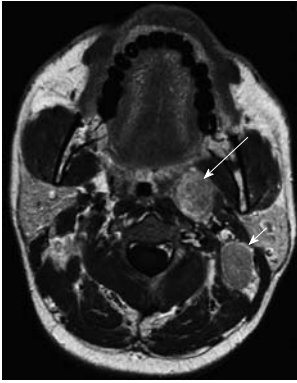


Figure 11 Axial post-contrast T1 weighted MRI in a patient with nasopharyngeal carcinoma showing an enlarged left sided metastatic retropharyngeal node deep to the oropharynx (long arrow). An enlarged metastatic left upper internal jugular node posterior to the left internal jugular vein (level IIB) is also present which is a very common site of nodal metastases (short arrow).

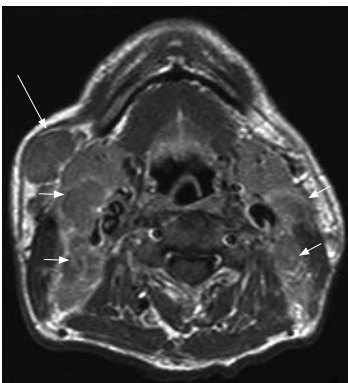


Figure 12 Axial post-contrast T1 weighted MRI in a patient with nasopharyngeal carcinoma showing bulky metastatic nodes in the internal jugular chains (short arrows) and right submandibular region (long arrow).

Diagnosis of nodal metastases

MRI diagnoses nodal metastases on the basis of size if the shortest nodal axial diameter reaches 5 mm or greater in the lateral retropharyngeal region^[25,32], 11 mm in the jugulodigastric region or 10 mm in other non-retropharyngeal nodes of the neck, or if there are a group of three or more nodes which are borderline in size^[33]. However, it should be noted that normal nodes become progressively smaller moving caudally in the neck and therefore a size of 5-7 mm is sometimes used as a cut-off in the lower neck. NPC nodes are often necrotic and show extracapsular spread and these signs are used by MRI to identify metastatic nodes irrespective of size^[33,34]. Extracapsular spread has also been shown to be an independent prognostic factor for overall survival and distant metastases failure-free survival^[35].

Staging

Staging of nodal metastases from NPC differs from that of other carcinomas in the head and neck. The most recent 7th edition UICC/AJCC classification includes the retropharyngeal nodes which have been shown to have a negative effect on prognosis^[36], and is classified as N1

irrespective of whether they are unilateral or bilateral. All other cervical nodes are considered to be stage N1 if unilateral and stage N2 if bilateral, unless they are greater than 6 cm in size or reach the supraclavicular fossa, in which case they are designated as stage N3a or N3b, respectively. Unlike other carcinomas in the neck, N2 is not further divided into substages according to the number of nodes or bilateral/contralateral involvement. Matted nodes forming a nodal mass of greater than 6 cm is rare and therefore most patients with stage N3 are diagnosed on the basis of supraclavicular nodes.

MRI STAGING OF DISTANT METASTASES IN THE HEAD AND NECK (M-STAGE)

Distant metastases are found in about 5% of patients^[37] at diagnosis and are most frequently found in the skeletal system followed by the thorax (lymph nodes and lungs) and then the liver. Although distant metastases are uncommon at diagnosis, head and neck MRI studies should always be assessed for evidence of spread to the bones in this region or lung apices, especially in patients with risk factors such as metastatic cervical nodes which extend to the supraclavicular fossa.

CONCLUSION

Head and neck MRI is the best modality for staging locoregional NPC, and the common sites for local primary tumor invasion and patterns of nodal spread have been described. Recent minor changes to the latest 7th edition of the UICC/AJCC cancer staging manual have seen primary tumor spread to the nasal cavity and oropharynx down staged from stage T2A to stage T1, and parapharyngeal spread changed from stage T2a to T2, while for nodal staging the retropharyngeal nodes have now been incorporated officially into the staging system as stage N1 disease, irrespective of whether they are unilateral or bilateral.

REFERENCES

- 1 **Lee AW**, Sze WM, Au JS, Leung SF, Leung TW, Chua DT, Zee BC, Law SC, Teo PM, Tung SY, Kwong DL, Lau WH. Treatment results for nasopharyngeal carcinoma in the modern era: the Hong Kong experience. *Int J Radiat Oncol Biol Phys* 2005; **61**: 1107-1116
- 2 **Chong VF**, Fan YF, Khoo JB. Nasopharyngeal carcinoma with intracranial spread: CT and MR characteristics. *J Comput Assist Tomogr* 1996; **20**: 563-569
- 3 **Chong VF**, Fan YF. Skull base erosion in nasopharyngeal carcinoma: detection by CT and MRI. *Clin Radiol* 1996; **51**: 625-631
- 4 **Liao XB**, Mao YP, Liu LZ, Tang LL, Sun Y, Wang Y, Lin AH, Cui CY, Li L, Ma J. How does magnetic resonance imaging influence staging according to AJCC staging system for nasopharyngeal carcinoma compared with computed tomography? *Int J Radiat Oncol Biol Phys* 2008; **72**: 1368-1377
- 5 **Chung NN**, Ting LL, Hsu WC, Lui LT, Wang PM. Impact of magnetic resonance imaging versus CT on nasopharyngeal

- carcinoma: primary tumor target delineation for radiotherapy. *Head Neck* 2004; **26**: 241-246
- 6 **Ng SH**, Chan SC, Yen TC, Chang JT, Liao CT, Ko SF, Liu FY, Chin SC, Fan KH, Hsu CL. Staging of untreated nasopharyngeal carcinoma with PET/CT: comparison with conventional imaging work-up. *Eur J Nucl Med Mol Imaging* 2009; **36**: 12-22
 - 7 **King AD**, Ma BB, Yau YY, Zee B, Leung SF, Wong JK, Kam MK, Ahuja AT, Chan AT. The impact of 18F-FDG PET/CT on assessment of nasopharyngeal carcinoma at diagnosis. *Br J Radiol* 2008; **81**: 291-298
 - 8 **Sobin LH**, Gospodarowicz MK, Wittekind C. TNM classification of malignant tumours. 7th ed. Hoboken: Wiley-Blackwell, 2010: 30-38
 - 9 **Edge SB**, Byrd DR, Compton CC, Fritz AG, Greene FL, Trotti A. AJCC Cancer Staging Manual. 7th ed. New York: Springer-Verlag, 2010: 41-49
 - 10 **King AD**, Vlantis AC, Tsang RK, Gary TM, Au AK, Chan CY, Kok SY, Kwok WT, Lui HK, Ahuja AT. Magnetic resonance imaging for the detection of nasopharyngeal carcinoma. *AJNR Am J Neuroradiol* 2006; **27**: 1288-1291
 - 11 **Ng WT**, Choi CW, Lee MC, Law LY, Yau TK, Lee AW. Outcomes of nasopharyngeal carcinoma screening for high risk family members in Hong Kong. *Fam Cancer* 2010; **9**: 221-228
 - 12 **Sham JS**, Wei WI, Zong YS, Choy D, Guo YQ, Luo Y, Lin ZX, Ng MH. Detection of subclinical nasopharyngeal carcinoma by fiberoptic endoscopy and multiple biopsy. *Lancet* 1990; **335**: 371-374
 - 13 **King AD**, Lam WW, Leung SF, Chan YL, Teo P, Metreweli C. MRI of local disease in nasopharyngeal carcinoma: tumour extent vs tumour stage. *Br J Radiol* 1999; **72**: 734-741
 - 14 **Teo P**, Shiu W, Leung SF, Lee WY. Prognostic factors in nasopharyngeal carcinoma investigated by computer tomography--an analysis of 659 patients. *Radiother Oncol* 1992; **23**: 79-93
 - 15 **Teo P**, Lee WY, Yu P. The prognostic significance of parapharyngeal tumour involvement in nasopharyngeal carcinoma. *Radiother Oncol* 1996; **39**: 209-221
 - 16 **Cheng SH**, Tsai SY, Yen KL, Jian JJ, Feng AC, Chan KY, Hong CF, Chu NM, Lin YC, Lin CY, Tan TD, Hsieh CY, Chong V, Huang AT. Prognostic significance of parapharyngeal space venous plexus and marrow involvement: potential landmarks of dissemination for stage I-III nasopharyngeal carcinoma. *Int J Radiat Oncol Biol Phys* 2005; **61**: 456-465
 - 17 **Ho HC**, Lee MS, Hsiao SH, Hwang JH, Hung SK, Lee CC, Chou P. Prognostic influence of parapharyngeal extension in nasopharyngeal carcinoma. *Acta Otolaryngol* 2008; **128**: 790-798
 - 18 **King AD**, Teo P, Lam WW, Leung SF, Metreweli C. Paranasopharyngeal space involvement in nasopharyngeal cancer: detection by CT and MRI. *Clin Oncol (R Coll Radiol)* 2000; **12**: 397-402
 - 19 **Lee CC**, Chu ST, Chou P, Lee CC, Chen LF. The prognostic influence of prevertebral space involvement in nasopharyngeal carcinoma. *Clin Otolaryngol* 2008; **33**: 442-449
 - 20 **Lu JC**, Wei Q, Zhang YQ, Li F. Influence of MRI abnormality in skull base bone on prognosis of nasopharyngeal carcinoma. *Cancer Radiother* 2004; **8**: 230-233
 - 21 **Liang SB**, Sun Y, Liu LZ, Chen Y, Chen L, Mao YP, Tang LL, Tian L, Lin AH, Liu MZ, Li L, Ma J. Extension of local disease in nasopharyngeal carcinoma detected by magnetic resonance imaging: improvement of clinical target volume delineation. *Int J Radiat Oncol Biol Phys* 2009; **75**: 742-750
 - 22 **Fuwa N**, Arijji Y, Daimon T, Wakisaka M, Matsumoto A, Kodaira T, Tachibana H, Nakamura T, Satou Y. Relationship between the growth pattern of nasopharyngeal cancer and the cervical lymph nodes based on MRI findings: can the cervical radiation field be reduced in patients with nasopharyngeal cancer? *Br J Radiol* 2006; **79**: 725-729
 - 23 **Rouviere H**. Lymphatic system of the head and neck. In: Tobias MJ, editor. Anatomy of the human lymphatics system. Ann Arbor: Edward Brothers, 1938: 5-28
 - 24 **Chong VF**, Fan YF, Khoo JB. Retropharyngeal lymphadenopathy in nasopharyngeal carcinoma. *Eur J Radiol* 1995; **21**: 100-105
 - 25 **King AD**, Ahuja AT, Leung SF, Lam WW, Teo P, Chan YL, Metreweli C. Neck node metastases from nasopharyngeal carcinoma: MR imaging of patterns of disease. *Head Neck* 2000; **22**: 275-281
 - 26 **Wang XS**, Hu CS, Ying HM, Zhou ZR, Ding JH, Feng Y. Patterns of retropharyngeal node metastasis in nasopharyngeal carcinoma. *Int J Radiat Oncol Biol Phys* 2009; **73**: 194-201
 - 27 **Mao YP**, Liang SB, Liu LZ, Chen Y, Sun Y, Tang LL, Tian L, Lin AH, Liu MZ, Li L, Ma J. The N staging system in nasopharyngeal carcinoma with radiation therapy oncology group guidelines for lymph node levels based on magnetic resonance imaging. *Clin Cancer Res* 2008; **14**: 7497-7503
 - 28 **Liu LZ**, Zhang GY, Xie CM, Liu XW, Cui CY, Li L. Magnetic resonance imaging of retropharyngeal lymph node metastasis in nasopharyngeal carcinoma: patterns of spread. *Int J Radiat Oncol Biol Phys* 2006; **66**: 721-730
 - 29 **Ng SH**, Chang JT, Chan SC, Ko SF, Wang HM, Liao CT, Chang YC, Yen TC. Nodal metastases of nasopharyngeal carcinoma: patterns of disease on MRI and FDG PET. *Eur J Nucl Med Mol Imaging* 2004; **31**: 1073-1080
 - 30 **Smoker WRK**, Gentry LR. Computed tomography of the nasopharynx and related spaces. *Semin Ultrasound CT MR* 1986; **7**: 107-130
 - 31 **Sham JS**, Choy D, Wei WI. Nasopharyngeal carcinoma: orderly neck node spread. *Int J Radiat Oncol Biol Phys* 1990; **19**: 929-933
 - 32 **Lam WW**, Chan YL, Leung SF, Metreweli C. Retropharyngeal lymphadenopathy in nasopharyngeal carcinoma. *Head Neck* 1997; **19**: 176-181
 - 33 **van den Brekel MW**, Stel HV, Castelijns JA, Nauta JJ, van der Waal I, Valk J, Meyer CJ, Snow GB. Cervical lymph node metastasis: assessment of radiologic criteria. *Radiology* 1990; **177**: 379-384
 - 34 **Som PM**. Lymph nodes of the neck. *Radiology* 1987; **165**: 593-600
 - 35 **Mao YP**, Li WF, Chen L, Sun Y, Liu LZ, Tang LL, Cao SM, Lin AH, Hong MH, Lu TX, Liu MZ, Li L, Ma J. [A clinical verification of the Chinese 2008 staging system for nasopharyngeal carcinoma] *Aizheng* 2009; **28**: 1022-1028
 - 36 **Ma J**, Liu L, Tang L, Zong J, Lin A, Lu T, Cui N, Cui C, Li L. Retropharyngeal lymph node metastasis in nasopharyngeal carcinoma: prognostic value and staging categories. *Clin Cancer Res* 2007; **13**: 1445-1452
 - 37 **Teo PM**, Kwan WH, Lee WY, Leung SF, Johnson PJ. Prognosticators determining survival subsequent to distant metastasis from nasopharyngeal carcinoma. *Cancer* 1996; **77**: 2423-2431

S- Editor Cheng JX L- Editor Webster JR E- Editor Zheng XM

Update on the natural history of intracranial atherosclerotic disease: A critical review

Ricardo J Komotar, Christopher P Kellner, Daniel M Raper, Dorothea Strozyk, Randall T Higashida, Philip M Meyers

Ricardo J Komotar, Christopher P Kellner, Daniel M Raper, Dorothea Strozyk, Randall T Higashida, Philip M Meyers, Departments of Neurological Surgery and Radiology, Columbia College of Physicians and Surgeons, New York, NY 10032, United States; Sydney Medical School, Northern Clinical School, Level 7, Kolling Building, Royal North Shore Hospital, Reserve Road, St Leonards NSW 2065, Australia

Author contributions: Komotar RJ, Kellner CP and Raper DM participated in research background, design concept and draft creation; Strozyk D and Higashida RT contributed to analysis, background research and paper revisions; Meyers PM participated in the whole process.

Correspondence to: Philip M Meyers, MD, FAHA, Associate Professor, Departments of Neurological Surgery and Radiology, Columbia College of Physicians and Surgeons, 710 West 168th Street, Suite 428, New York, NY 10032, United States. pmm2002@columbia.edu

Telephone: +212-305-6384 Fax: +212-342-1229

Received: March 23, 2010 Revised: April 29, 2010

Accepted: May 6, 2010

Published online: May 28, 2010

Abstract

Intracranial atherosclerotic disease (ICAD) contributes to a significant number of ischemic strokes. There is debate in the recent literature concerning the impact of the location of stenosis in ICAD on outcome. Some reports have suggested that disease processes and outcomes vary by vessel location, potentially altering the natural history and indications for intervention. Here we have performed a comprehensive, critical review of the natural history of ICAD by vessel in an attempt to assess the differences in disease specific to each of the vascular territories. Our assessment concludes that only minor differences exist between patients with different vessels affected in vessel-specific ICAD. We have found that middle cerebral artery disease confers a lower mortality than vessel-specific ICAD in other intracranial vessels, asymptomatic disease follows a more benign course than symptomatic disease, and

that plaque progression or the detection of microemboli on transcranial Doppler may predict poor outcome. Given the expanding indications for treatment of ICAD and rapidly developing endovascular techniques to confront this disease, a thorough understanding of the natural history of ICAD aids the interventional neuro-radiologist in determining when to treat and how to predict outcome in this patient population.

© 2010 Baishideng. All rights reserved.

Key words: Intracranial atherosclerosis; Natural history; Stenosis

Peer reviewers: Ender Uysal, MD, Sisli Etfal Training and Research Hospital. Clinic of Radiology, Sisli Etfal Eğitim ve Araştırma Hastanesi Radyoloji Kliniği, Etfal sok. Sisli, Istanbul 34377, Turkey; Hadi Rokni Yazdi, MD, Associate Professor, Department of radiology, Central Radiology, Imam Khomeini Hospital, Tehran University of Medical Sciences, Keshavarz Blvd, Tehran, 1419733141, Iran

Komotar RJ, Kellner CP, Raper DM, Strozyk D, Higashida RT, Meyers PM. Update on the natural history of intracranial atherosclerotic disease: A critical review. *World J Radiol* 2010; 2(5): 166-171 Available from: URL: <http://www.wjgnet.com/1949-8470/full/v2/i5/166.htm> DOI: <http://dx.doi.org/10.4329/wjr.v2.i5.166>

INTRODUCTION

Patients with stroke or transient ischaemic attack (TIA) are found to have intracranial atherosclerotic disease (ICAD) in at least 9% of cases^[1]. Depending on the populations studied, and particularly in Asian populations, ICAD may account for up to 29% of all ischemic events^[2-4]. Besides race and ethnicity, medical risk factors associated with ICAD include insulin-dependent diabetes mellitus, hypercholesterolemia, cigarette smoking and hypertension^[1,5,6].

Despite advances in endovascular and pharmaceutical technology, the prognosis for patients with ICAD remains poor. We have previously characterized the natural history of ICAD on a vessel-by-vessel basis^[7] in an effort to identify the potentially variable risk represented by stenosis of the different intracranial vessels. Care should be taken when interpreting the finding of single stenosed intracranial vessels, since intracranial atherosclerosis is likely to be a diffuse process affecting multiple locations^[8]. For this reason, atherosclerotic stenosis identified in any one vessel also confers an increased risk of subsequent stroke in other vascular distributions. The location of stenosis has no clear effect on stenosis progression and stroke^[7].

Though most recent reports on ICAD aggregate stenoses at all locations in the intracranial arteries in their outcome assessment, some investigators have identified pathogenic differences that may contribute to the observed survival discrepancies identified in the literature. Bang *et al*^[9], investigated the mechanisms underlying stroke in patients with atherosclerotic lesions in the internal carotid artery and proximal atherosclerotic lesions (MCA), finding that biomarkers of inflammation were more elevated in those with carotid stenosis ($P < 0.01$). These authors concluded that atherosclerotic intracranial carotid stenosis may be prone to instability with plaque rupture and subsequent ischemic stroke while atherosclerotic stenosis of the MCA appears more stable and less prone to plaque rupture.

Because of apparent differences in morbidity and mortality based upon location in the intracranial circulation, we critically review the natural history of ICAD using a vessel-by-vessel approach, and discuss the possible common features and management.

EPIDEMIOLOGY AND PATHOGENESIS OF ICAD

The proportion of patients with atherosclerotic stenoses in the major vessels varies widely in the medical literature. Mazighi *et al*^[10], reported on a series of patients with stenosis $> 30\%$: the ICA was affected in 16.3%, MCA in 18.3%, basilar artery (BA) in 15.9% and vertebral artery (VA) in 7.6%. In a prospective series of 267 patients with intracranial large vessel occlusion, the MCA was affected in 38%, ICA in 6%, ACA in 1.3%, and posterior circulation arteries in 7%^[11]. However, the Groupe d'Etude des Stenoses Intra-Craniennes Athéromateuses symptomatiques (GESICA) was a prospective series including 102 patients with symptomatic intracranial stenosis and showed relatively equal distribution of disease affecting VA, BA, MCA and ICA^[12].

ICAD occurs more commonly in patients of Asian, African or Hispanic origin than in Caucasians. Studies in Chinese, Thai, Korean, Japanese and Singaporean patients with stroke have demonstrated rates of ICAD between 30%-50%^[13]. By contrast, approximately 8 to 9% of strokes are attributable to ICAD in Caucasians, while African- and Hispanic-Americans were shown to have a relative risk of 5 to 6 for ICAD-related stroke compared

to Caucasians^[14]. The development of this racial difference has been hypothesized to be related to the emergence of a stroke-suppressor genotype among Europeans that has primarily affected intracranial arteries^[15].

The prevalence and true impact of ICAD is likely underestimated because most patients are evaluated using primarily cross-sectional imaging studies such as computed tomography^[16] or magnetic resonance imaging^[17] rather than catheter angiography which can most accurately diagnose and characterized intracranial stenoses. In particular, recent studies suggest that even stenoses $< 50\%$ can potentially be associated with ischemic stroke and may be significant^[10]. Nevertheless, the Warfarin-Aspirin Symptomatic Intracranial Diseases (WASID) Trial showed that intracranial stenosis 70%-99% were associated with the greatest risk of stroke^[3], and an autopsy study of 339 consecutive patients who died of stroke found in intracranial stenoses in 43% of cases, not all of which were symptomatic^[10].

Controversy remains about the prognostic significance of ICAD, either discovered prior to a stroke or secondarily identified post-stroke or TIA. Since the risk factors for ICAD are similar to those for arterial disease in other parts of the body (diabetes, hypertension, cigarette smoking, and hypercholesterolemia^[1,18,19]), it is not surprising that patients with ICAD have increased rates of vascular occlusive disease in other vascular territories.

ICAD is part of a generalized vasculopathy due to genetic and environmental factors that puts these patients at a significantly higher risk for a range of vascular events. ICAD has been associated with high levels of circulating pro-inflammatory cytokines and inhibitors of fibrinolysis^[20]. In particular, increased levels of C-reactive protein and PAI-1 predicted progression to symptomatic ICAD. High levels of lipoprotein-(a) and diabetes have been found to predict higher levels of ICAD and may be useful markers of risk for this disease^[21].

INTERNAL CAROTID ARTERY ICAD

A number of retrospective studies have investigated annual mortality and ipsilateral stroke rates following diagnosis of intracranial ICA atherosclerotic disease in the 1980s^[22-25]. The reported rates of annual mortality ranged from 7.8% to 17.2%, with recurrent ipsilateral stroke occurring at a rate of 3.1 to 8.1%. These reports have limitations because the patient populations investigated were heterogeneous with baseline stenosis ranging from 20%-70%, longitudinal evaluation varied from 25.5-50 mo, and the series were small, with fewer than 100 symptomatic and asymptomatic patients. The primary outcomes are difficult to compare because there is no common objective measure of stroke severity. In aggregate, these case series can only be considered Level 2b evidence by the Oxford Centre for Evidence Based Medicine scheme^[26].

A number of important hypotheses emerged from this early work on carotid ICAD. Craig *et al*^[22] found that recurrent cerebral ischemic events were more frequent in patients with symptomatic rather than asymptomatic

ICA stenosis. Wechsler *et al*^[25] showed that impaired flow on angiography in symptomatic patients due to hemodynamically significant carotid siphon stenosis contributed to TIA symptomatology, while strokes primarily resulted from distal embolization from the stenosis. Even though ICAD occurs in the condition of diffuse vascular disease, strokes subsequent to the diagnosis of ICAD occurred primarily in the same vascular territory supplied by the area of lesion identified^[23,24]. In a prospective series of patients with suspected stroke, multivariate analysis demonstrated that the location of stenosis is associated with clinical outcome: ICAD at the internal carotid terminus was significantly associated with poor outcome (modified Rankin scale score 3-6) over a 23-mo follow-up^[11].

MIDDLE CEREBRAL ARTERY ICAD

The early, retrospective cohorts investigating the natural history of MCA ICAD show a 12.5%-24% risk of recurrent stroke during 6.5 years follow-up^[27,28]. The annual stroke rate ranged from 2.8%-3.7%, and in some cases occurred very quickly, prior to initiation of medical therapy^[27]. More recently, a number of prospective series have investigated the same population. Sub-group analysis of the extracranial-intracranial bypass study population^[29] reported an annual stroke rate of 5%, with 25% of 138 patients experiencing stroke during 55.8 mo follow-up. The patients in this group had > 70% stenosis at the beginning of the study, and may represent a higher risk group than the earlier cohorts including patients with < 50% stenosis. Arenillas *et al*^[20] showed that stenosis progression, as measured by transcranial Doppler (TCD), independently predicted stroke recurrence in symptomatic patients with MCA ICAD. Subsequently, Gao *et al*^[30] showed that the presence of microembolic signals (MES) on TCD ultrasonography in symptomatic patients with known MCA stenoses predicted recurrent ipsilateral stroke. The annual ipsilateral stroke rate was 7.8% and annual mortality was 7.0%^[30]. The results of these two studies suggest that symptomatic MCA ICAD is a condition with significant risk of death or recurrent stroke, which is primarily embolic in origin. Furthermore, regular evaluation using TCD, including evaluation of MES, may be valuable in identifying high-risk patients with MCA stenosis.

Stroke prevention in symptomatic ICAD patients remains a subject of discussion and on-going research. Generally, systemic anti-coagulation is no longer primary therapy based on WASID and Warfarin-Aspirin Recurrent Stroke Study (WARSS)^[3,31]. The Aspirin or anticoagulants in stenosis of the middle cerebral artery (MCA) (AVASIS) trial, which was intended to clarify the findings of WASID concerning efficacy of aspirin *vs* warfarin was halted due to slow enrollment. Neither group reached the primary endpoint in a final analysis of the collected data^[32]. In the United States, an update of the American Heart Association/American Stroke Association summarizes existing data on stroke prevention in patients with prior stroke or TIA^[33].

VERTEBROBASILAR ICAD

The second most common location for ICAD is the vertebrobasilar arteries^[2]. ICAD at this location confers a substantial risk of subsequent ischemic events. In GESICA, BA atherosclerosis conferred the highest risk for recurrent stroke over an average 23-mo follow up^[12]. In a prospective series of patients presenting with suspected stroke, basilar and internal carotid terminus occlusions independently predicted poorer outcome on multivariate analysis (relative risk for a good outcome was 0.4 for basilar occlusion and 0.47 for ICA occlusion)^[11]. Data from the WASID study group demonstrated that BA stenosis conferred a higher risk of subsequent events than VA stenosis^[34]. The posterior circulation has also been found to have significantly higher rates of complications after angioplasty and stenting than ICAD affecting the anterior circulation^[35].

Most of the data regarding the natural history of vertebrobasilar ICAD comes from retrospective cohorts. In four retrospective series published over the last 20 years, the rates of annual stroke mortality ranged from 1.1%-14.3%^[34,36-39]. The annual vertebrobasilar-territory stroke rate and overall annual stroke rate ranged from 0%-8.7% and 3%-14.3%, respectively. Kaplan-Meier analysis revealed that the majority of symptomatic patients experienced a stroke and/or death within 5 years of initial presentation. The best data specifically about posterior circulation stroke likely comes from the New England Stroke Registry^[40]. In this study of 407 registry patients, 59% had posterior circulation strokes without TIA, 24% presented with TIAs then strokes, and only 16% had TIAs, 14% of which were due to intra-arterial lesions^[40].

Voetsch *et al*^[41] performed a subgroup analysis of patients with basilar stenosis artery in the New England Stroke Registry. Mortality was lower than expected (2.6%) and 62% had minor or no permanent deficits at follow-up over an 8 years period. Longer-term follow up from this cohort would be welcomed, but has not been reported to date. It has been proposed that, as for ICAD in other regions, the risk of recurrent ischemia is highest in the first 2 years following a stroke^[36]. Indeed, Thijs *et al*^[42] showed that the risk of recurrent stroke and death on treatment can be quite high. In a series of 52 patients with TIA or stroke due to ICAD, 56% had recurrent events during treatment with antithrombotic or anti-platelet medications. 52% of these events occurred within 36 d (median) and 15% were major strokes or death. However, an analysis of the WASID cohort failed to reveal any difference in patients who were on or off (i.e. had failed) antithrombotic therapy at the time of the initial stroke^[43].

MEDICAL AND INTERVENTIONAL MANAGEMENT OF ICAD

Optimal management of ICAD continues to evolve but currently focuses on the use of anti-aggregating (anti-platelet) medications as first line therapy and revascular-

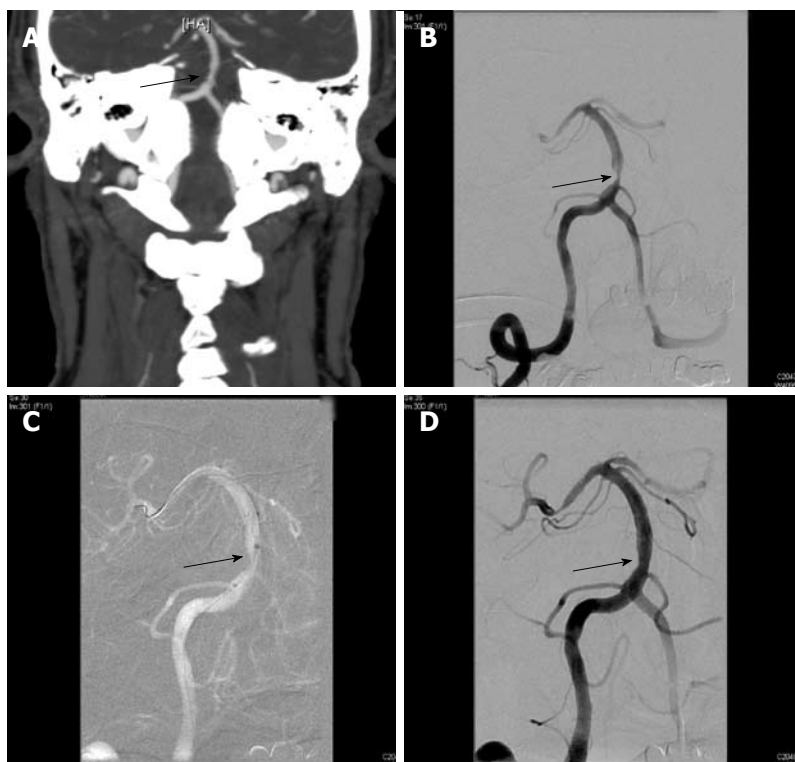


Figure 1 Seventy-nine years old man with hypertension and hyperlipidemia developed episodic dizziness, visual distortion, dysarthria, and somnolence refractory to anti-platelet therapy using aspirin and dipyridamole. A: Computed tomography of the brain with contrast, CTA protocol and coronal reconstructions, shows severe focal stenosis of the basilar artery (arrow); B: Catheter arteriography of the right vertebral artery during arterial phase in frontal projection confirms 80% stenosis the proximal basilar artery (arrow); C: Fluororadiography during endovascular revascularization using stent angioplasty shows placement of a 3.0 mm × 15 mm Wingspan® self-expanding nitinol stent (arrow) symmetrically across the stenosis after angioplasty using a 2.5 mm × 9 mm Gateway® angioplasty balloon catheter; D: Catheter arteriography of the right vertebral artery during the arterial phase in frontal projection at the conclusion of the procedure shows residual 40% stenosis of the basilar artery after angioplasty and stent placement (arrow). Out-patient follow-up with non-invasive imaging using transcranial Doppler ultrasonography shows stable normal velocities in the treated artery. The patient remains stable on aspirin and clopidogrel.

ization procedures (usually endovascular) for refractory cases. Recent medical management, which evolved from the treatment of systemic atherosclerosis has included combinations of aspirin, dipyridamole, statins, ticlopidine, clopidogrel, warfarin and angiotensin-converting enzyme inhibitors^[2,42]. Since the publication of the WASID and the WARSS trial, the benefit of warfarin over aspirin has been questioned^[3,31]. For example, WASID was stopped prematurely by its safety monitoring committee due to a significantly increased risk of hemorrhage in the warfarin group. At a mean follow-up of 1.8 years, there was no difference in the primary endpoint of ischemic stroke, brain hemorrhage or death from other vascular causes, but the rates of each endpoint individually were significantly lower in the aspirin group. Although some commentators have voiced concerns about the study design and applicability of outcome and complication measures^[44], use of warfarin to treat this group of high-risk patients based on the foregoing data requires caution.

For patients who develop recurrent symptoms on antithrombotic therapy, the risk of recurrent stroke or TIA is believed to be extremely high and revascularization is often considered (Figure 1). The efficacy of angioplasty^[45] or stent-supported angioplasty (PTAS) for ICAD remains controversial. Marks *et al*^[46], reported clinical outcomes in their series of 120 patients with 124 symptomatic intracranial stenoses using PTA alone. Including periprocedural strokes and deaths, the annual stroke rate in the territory of treatment was 3.2% and 4.4% overall^[46]. However, PTA alone is not always successful. In Marks' series, 12.9% of patients required immediate stenting when angioplasty failed^[46].

There are also numerous series reviewing single and multi-center experience with intracranial stent angioplasty. SSYLVIA (Stenting of symptomatic atherosclerotic lesions in the vertebral or intracranial arteries) was a prospective multi-center non-randomized feasibility trial to evaluate the NeuroLink® intracranial stent (Guidant, Indianapolis, IN). Sixty one patients underwent treatment with 95% technical success, 6.6% stroke and 0% mortality. Unfortunately, the incidence of stroke increased to 7.3% between 30 d and 1 year with a 35% rate of restenosis in the treated arteries^[47]. In 2005, Henkes *et al*^[48] reported on the use of a novel self-expanding stent called Wingspan® (Boston Scientific, Fremont, CA). Forty five patients underwent treatment for ICAD > 50% stenosis with 98% technical success, composite 30-d ipsilateral or death of 4.5%, and 6-mo all cause stroke rate of 9.5%. Based on these data, the FDA granted Boston Scientific a humanitarian device exemption to treat symptomatic patients with ICAD stenosis > 50% and refractory to medical therapy. Fiorella *et al*^[49], reported on 78 patients with 82 intracranial stenoses > 50% who were treated with Wingspan®. With a technical success rate of nearly 99%, there were 6.1% major peri-procedural complications or deaths with good target artery revascularization but a 32% rate of in-stent restenosis^[50]. The SAMMPRIS (Stenting *vs* aggressive medical management for preventing recurrent stroke in intracranial stenosis) is a National Institute of Health-funded randomized trial comparing best medical therapy with stent-angioplasty using the Wingspan device plus best medical therapy and is now enrolling in the United States^[51].

Across centers in the Americas and Europe, the results of PTA/PTAS have not been uniform. Recent non-

randomized, retrospective studies have found no significant difference in vascular ischemic endpoints between patients with ICAD treated with medical therapy or PTA/PTAS^[52]. In a systematic review of PTAS for ICAD, Gröschel *et al.*^[35], concluded that the use of PTA/PTAS outside the context of randomized, controlled trials cannot be recommended due to the widely variable complication rates of PTA/PTAS, the natural history of the ICAD, and lack of clear effect on patient outcome. A comprehensive review of this area is beyond the scope of this review, and is covered in detail elsewhere^[17,53].

CONCLUSION

Symptomatic ICAD is associated with a significant risk of stroke despite medical therapy. Vessel-specific patterns of outcome have emerged in the old and recent literature on ICAD. Studies examining the ICA terminus have shown that stenosis in this region predicts poor outcome, arguing for intervention in some cases. Stenosis specific to the MCA distribution confers a lower rate of morbidity and mortality than other vessels, suggesting that medical management may play a larger role in this vessel. The presence of ICAD in the vertebrobasilar system confers the highest rate of stroke, but interventional neuroradiologists also report the highest rate of complications following angioplasty and stenting in these vessels. Within the posterior circulation, the ICAD of the BA has the highest rate of mortality and morbidity.

Examination of the natural history of ICAD evidences the new potential role for endovascular revascularization of the most severe intracranial stenoses. Percutaneous transluminal angioplasty and stent-supported angioplasty are now feasible with modern microcatheter technologies. Studies designed to compare complication rates of medical and interventional therapies are now underway. Restenosis with stent-supported angioplasty may be less frequent than after angioplasty alone at early follow-up evaluations. However, the long-term patency of stented cerebral arteries and rates of recurrent stroke remain unclear. For these reasons, a multi-disciplinary approach to patients with symptomatic ICAD is important to achieve optimal outcomes across the spectrum of cerebrovascular occlusive diseases.

REFERENCES

- 1 Sacco RL, Kargman DE, Gu Q, Zamanillo MC. Race-ethnicity and determinants of intracranial atherosclerotic cerebral infarction. The Northern Manhattan Stroke Study. *Stroke* 1995; **26**: 14-20
- 2 Chimowitz MI, Kokkinos J, Strong J, Brown MB, Levine SR, Silliman S, Pessin MS, Weichel E, Sila CA, Furlan AJ. The Warfarin-Aspirin Symptomatic Intracranial Disease Study. *Neurology* 1995; **45**: 1488-1493
- 3 Chimowitz MI, Lynn MJ, Howlett-Smith H, Stern BJ, Hertzberg VS, Frankel MR, Levine SR, Chaturvedi S, Kasner SE, Benesch CG, Sila CA, Jovin TG, Romano JG. Comparison of warfarin and aspirin for symptomatic intracranial arterial stenosis. *N Engl J Med* 2005; **352**: 1305-1316
- 4 Rundek T, Elkind MS, Chen X, Boden-Albala B, Paik MC, Sacco RL. Increased early stroke recurrence among patients with extracranial and intracranial atherosclerosis: the Northern Manhattan Stroke Study. *Neurology* 1998; **50** Suppl 4: A75
- 5 Caplan LR, Gorelick PB, Hier DB. Race, sex and occlusive cerebrovascular disease: a review. *Stroke* 1986; **17**: 648-655
- 6 Ingall TJ, Homer D, Baker HL Jr, Kottke BA, O'Fallon WM, Whisnant JP. Predictors of intracranial carotid artery atherosclerosis. Duration of cigarette smoking and hypertension are more powerful than serum lipid levels. *Arch Neurol* 1991; **48**: 687-691
- 7 Komotar RJ, Wilson DA, Mocco J, Jones JE, Connolly ES Jr, Lavine SD, Meyers PM. Natural history of intracranial atherosclerosis: a critical review. *Neurosurgery* 2006; **58**: 595-601; discussion 595-601
- 8 Arenillas JF, Alvarez-Sabín J. Basic mechanisms in intracranial large-artery atherosclerosis: advances and challenges. *Cerebrovasc Dis* 2005; **20** Suppl 2: 75-83
- 9 Bang OY, Lee PH, Yoon SR, Lee MA, Joo IS, Huh K. Inflammatory markers, rather than conventional risk factors, are different between carotid and MCA atherosclerosis. *J Neurol Neurosurg Psychiatry* 2005; **76**: 1128-1134
- 10 Mazighi M, Labreuche J, Gongora-Rivera F, Duyckaerts C, Hauw JJ, Amarenco P. Autopsy prevalence of intracranial atherosclerosis in patients with fatal stroke. *Stroke* 2008; **39**: 1142-1147
- 11 Smith WS, Lev MH, English JD, Camargo EC, Chou M, Johnston SC, Gonzalez G, Schaefer PW, Dillon WP, Koroshetz WJ, Furie KL. Significance of large vessel intracranial occlusion causing acute ischemic stroke and TIA. *Stroke* 2009; **40**: 3834-3840
- 12 Mazighi M, Tanasescu R, Ducrocq X, Vicaut E, Bracard S, Houdart E, Woimant F. Prospective study of symptomatic atherothrombotic intracranial stenoses: the GESICA study. *Neurology* 2006; **66**: 1187-1191
- 13 Wong LK. Global burden of intracranial atherosclerosis. *Int J Stroke* 2006; **1**: 158-159
- 14 White H, Boden-Albala B, Wang C, Elkind MS, Rundek T, Wright CB, Sacco RL. Ischemic stroke subtype incidence among whites, blacks, and Hispanics: the Northern Manhattan Study. *Circulation* 2005; **111**: 1327-1331
- 15 Mak W, Cheng TS, Chan KH, Cheung RT, Ho SL. A possible explanation for the racial difference in distribution of large-arterial cerebrovascular disease: ancestral European settlers evolved genetic resistance to atherosclerosis, but confined to the intracranial arteries. *Med Hypotheses* 2005; **65**: 637-648
- 16 McTaggart RA, Jayaraman MV, Haas RA, Feldmann E. Intracranial atherosclerotic disease: epidemiology, imaging and treatment. *Med Health R I* 2009; **92**: 412-414
- 17 Leung TW, Kwon SU, Wong KS. Management of patients with symptomatic intracranial atherosclerosis. *Int J Stroke* 2006; **1**: 20-25
- 18 Segura T, Serena J, Castellanos M, Teruel J, Vilar C, Dávalos A. Embolism in acute middle cerebral artery stenosis. *Neurology* 2001; **56**: 497-501
- 19 Wityk RJ, Lehman D, Klag M, Coresh J, Ahn H, Litt B. Race and sex differences in the distribution of cerebral atherosclerosis. *Stroke* 1996; **27**: 1974-1980
- 20 Arenillas JF, Alvarez-Sabín J, Molina CA, Chacón P, Fernández-Cadenas I, Ribó M, Delgado P, Rubiera M, Penalba A, Rovira A, Montaner J. Progression of symptomatic intracranial large artery atherosclerosis is associated with a proinflammatory state and impaired fibrinolysis. *Stroke* 2008; **39**: 1456-1463
- 21 Arenillas JF, Molina CA, Chacón P, Rovira A, Montaner J, Coscojuela P, Sánchez E, Quintana M, Alvarez-Sabín J. High lipoprotein (a), diabetes, and the extent of symptomatic intracranial atherosclerosis. *Neurology* 2004; **63**: 27-32
- 22 Craig DR, Meguro K, Watridge C, Robertson JT, Barnett HJ, Fox AJ. Intracranial internal carotid artery stenosis. *Stroke* 1982; **13**: 825-828
- 23 Marzewski DJ, Furlan AJ, St Louis P, Little JR, Modic MT,

- Williams G. Intracranial internal carotid artery stenosis: longterm prognosis. *Stroke* 1982; **13**: 821-824
- 24 **Bogousslavsky J.** Prognosis of carotid siphon stenosis. *Stroke* 1987; **18**: 537
- 25 **Wechsler LR,** Kistler JP, Davis KR, Kaminski MJ. The prognosis of carotid siphon stenosis. *Stroke* 1986; **17**: 714-718
- 26 **Heneghan C.** EBM resources on the new CEBM website. *Evid Based Med* 2009; **14**: 67
- 27 **Feldmeyer JJ,** Merendaz C, Regli F. [Symptomatic stenoses of the middle cerebral artery] *Rev Neurol (Paris)* 1983; **139**: 725-736
- 28 **Hinton RC,** Mohr JP, Ackerman RH, Adair LB, Fisher CM. Symptomatic middle cerebral artery stenosis. *Ann Neurol* 1979; **5**: 152-157
- 29 Failure of extracranial-intracranial arterial bypass to reduce the risk of ischemic stroke. Results of an international randomized trial. The EC/IC Bypass Study Group. *N Engl J Med* 1985; **313**: 1191-1200
- 30 **Gao S,** Wong KS, Hansberg T, Lam WW, Droste DW, Ringelstein EB. Microembolic signal predicts recurrent cerebral ischemic events in acute stroke patients with middle cerebral artery stenosis. *Stroke* 2004; **35**: 2832-2836
- 31 **Mohr JP,** Thompson JL, Lazar RM, Levin B, Sacco RL, Furie KL, Kistler JP, Albers GW, Pettigrew LC, Adams HP Jr, Jackson CM, Pullicino P. A comparison of warfarin and aspirin for the prevention of recurrent ischemic stroke. *N Engl J Med* 2001; **345**: 1444-1451
- 32 **Martí-Fàbregas J,** Cocho D, Martí-Vilalta JL, Gich I, Belvis R, Bravo Y, Millán M, Castellanos M, Rodríguez-Campello A, Egido J, Geffner D, Gil-Núñez A, Marta J, Navarro R, Obach V, Palomeras E. Aspirin or anticoagulants in stenosis of the middle cerebral artery: A randomized trial. *Cerebrovasc Dis* 2006; **22**: 162-169
- 33 **Adams RJ,** Albers G, Alberts MJ, Benavente O, Furie K, Goldstein LB, Gorelick P, Halperin J, Harbaugh R, Johnston SC, Katzan I, Kelly-Hayes M, Kenton EJ, Marks M, Sacco RL, Schwamm LH. Update to the AHA/ASA recommendations for the prevention of stroke in patients with stroke and transient ischemic attack. *Stroke* 2008; **39**: 1647-1652
- 34 Prognosis of patients with symptomatic vertebral or basilar artery stenosis. The Warfarin-Aspirin Symptomatic Intracranial Disease (WASID) Study Group. *Stroke* 1998; **29**: 1389-1392
- 35 **Gröschel K,** Schnaudigel S, Pilgram SM, Wasser K, Kastrup A. A systematic review on outcome after stenting for intracranial atherosclerosis. *Stroke* 2009; **40**: e340-e347
- 36 **Moufarrij NA,** Little JR, Furlan AJ, Leatherman JR, Williams GW. Basilar and distal vertebral artery stenosis: long-term follow-up. *Stroke* 1986; **17**: 938-942
- 37 **Pessin MS,** Kwan ES, DeWitt LD, Hedges TR 3rd, Gale D, Caplan LR. Posterior cerebral artery stenosis. *Ann Neurol* 1987; **21**: 85-89
- 38 **Pessin MS,** Gorelick PB, Kwan ES, Caplan LR. Basilar artery stenosis: middle and distal segments. *Neurology* 1987; **37**: 1742-1746
- 39 **Qureshi AI,** Ziai WC, Yahia AM, Mohammad Y, Sen S, Agarwal P, Zaidat OO, Suarez JI, Wityk RJ. Stroke-free survival and its determinants in patients with symptomatic vertebro-basilar stenosis: a multicenter study. *Neurosurgery* 2003; **52**: 1033-1039; discussion 1039-1040
- 40 **Caplan LR,** Wityk RJ, Glass TA, Tapia J, Pazdera L, Chang HM, Teal P, Dashe JF, Chaves CJ, Breen JC, Vemmos K, Amarenco P, Tettenborn B, Leary M, Estol C, Dewitt LD, Pessin MS. New England Medical Center Posterior Circulation registry. *Ann Neurol* 2004; **56**: 389-398
- 41 **Voetsch B,** DeWitt LD, Pessin MS, Caplan LR. Basilar artery occlusive disease in the New England Medical Center Posterior Circulation Registry. *Arch Neurol* 2004; **61**: 496-504
- 42 **Thijs VN,** Albers GW. Symptomatic intracranial atherosclerosis: outcome of patients who fail antithrombotic therapy. *Neurology* 2000; **55**: 490-497
- 43 **Turan TN,** Maida L, Cotsonis G, Lynn MJ, Romano JG, Levine SR, Chimowitz MI. Failure of antithrombotic therapy and risk of stroke in patients with symptomatic intracranial stenosis. *Stroke* 2009; **40**: 505-509
- 44 **Koroshetz WJ.** Warfarin, aspirin, and intracranial vascular disease. *N Engl J Med* 2005; **352**: 1368-1370
- 45 **Kassab MY,** Gupta R, Majid A, Farooq MU, Giles BP, Johnson MD, Graybeal DF, Rappard G. Extent of intra-arterial calcification on head CT is predictive of the degree of intracranial atherosclerosis on digital subtraction angiography. *Cerebrovasc Dis* 2009; **28**: 45-48
- 46 **Marks MP,** Wojak JC, Al-Ali F, Jayaraman M, Marcellus ML, Connors JJ, Do HM. Angioplasty for symptomatic intracranial stenosis: clinical outcome. *Stroke* 2006; **37**: 1016-1020
- 47 Stenting of Symptomatic Atherosclerotic Lesions in the Vertebral or Intracranial Arteries (SSYLVA): study results. *Stroke* 2004; **35**: 1388-1392
- 48 **Henkes H,** Miloslavski E, Lowens S, Reinartz J, Liebig T, Kühne D. Treatment of intracranial atherosclerotic stenoses with balloon dilatation and self-expanding stent deployment (WingSpan). *Neuroradiology* 2005; **47**: 222-228
- 49 **Fiorella D,** Levy EI, Turk AS, Albuquerque FC, Niemann DB, Aagaard-Kienitz B, Hanel RA, Woo H, Rasmussen PA, Hopkins LN, Masaryk TJ, McDougall CG. US multicenter experience with the wingspan stent system for the treatment of intracranial atheromatous disease: periprocedural results. *Stroke* 2007; **38**: 881-887
- 50 **Albuquerque FC,** Levy EI, Turk AS, Niemann DB, Aagaard-Kienitz B, Pride GL Jr, Purdy PD, Welch BG, Woo HH, Rasmussen PA, Hopkins LN, Masaryk TJ, McDougall CG, Fiorella DJ. Angiographic patterns of Wingspan in-stent restenosis. *Neurosurgery* 2008; **63**: 23-27; discussion 27-28
- 51 SAMMPRIS (Stenting vs. Aggressive Medical Management for Preventing Recurrent Stroke in Intracranial Stenosis). 2008. Available from: URL: <http://www.strokecenter.org/trials/TrialDetail.aspx?tid=819>
- 52 **Samaniego EA,** Hetzel S, Thirunarayanan S, Aagaard-Kienitz B, Turk AS, Levine R. Outcome of symptomatic intracranial atherosclerotic disease. *Stroke* 2009; **40**: 2983-2987
- 53 **Meyers PM,** Schumacher HC, Tanji K, Higashida RT, Caplan LR. Use of stents to treat intracranial cerebrovascular disease. *Annu Rev Med* 2007; **58**: 107-122

S- Editor Cheng JX L- Editor Lalor PF E- Editor Zheng XM

Imaging in male-factor obstructive infertility

Ragab H Donkol

Ragab H Donkol, Department of Radiology, Aseer Central Hospital, PO Box 34, 31911, Abha, Saudi Arabia; Department of Radiology, Faculty of Medicine, Cairo University, Kasr Al-Ainy, 1 Al-Saray Street, Al-Manial, 11559, Cairo, Egypt

Author contributions: Donkol RH contributed to design of manuscript, as well as review of articles, collection of data and manuscript writing.

Correspondence to: Ragab H Donkol, Professor, Department of Radiology, Aseer Central Hospital, PO Box 34, 31911, Abha, Saudi Arabia. donkol@gawab.com

Telephone: +966-7-2201169 Fax: +966-7-2248092

Received: March 19, 2010 Revised: April 24, 2010

Accepted: May 1, 2010

Published online: May 28, 2010

Abstract

The main purpose of imaging evaluation in male infertility is to identify and treat correctable causes of infertility, such as obstruction of the seminal tract. Various imaging modalities are available to evaluate men with obstructive infertility including scrotal ultrasonography, transrectal ultrasound (TRUS), vasography, magnetic resonance imaging, seminal vesicle aspiration, seminal tract washout, and seminal vesiculography. To date the most reliable and accurate diagnostic technique for obstructive infertility is unclear. In this review article, we report the role of these modalities in diagnosis of obstructive infertility. Scrotal sonography is the initial modality, and if patient results indicate non obstructive azoospermia as varicocele or testicular pathology they will be treated according to standard protocols for management of these pathologies. If the patient findings indicate proximal obstructive azoospermia, they can be managed by vasoepididymostomy. If the scrotal ultrasound is normal, TRUS is the second imaging modality. Accordingly, they are classified into patients with criteria of obstructive infertility without urogenital cysts where TRUS-guided aspiration and seminal vesiculography can be performed and transurethral resection of the ejaculatory ducts (TURED) will be the management of choice. In patients with urogenital cyst, TRUS-guided cyst aspiration and opacification are performed. If

the cyst is communicating with the seminal tract, management will be transurethral incision of the cyst. If the cyst is not in communication, the obstruction may be relieved after cyst aspiration. If the obstruction is not relieved, TURED will be the management of choice. Sperm harvested during aspiration may be stored and used in assisted reproduction techniques. If the results of TRUS are inconclusive or doubtful, endorectal magnetic resonance imaging should be performed to serve as a "detailed map" for guiding corrective operative interventions.

© 2010 Baishideng. All rights reserved.

Key words: Male fertility; Obstructive infertility; Transrectal ultrasonography; Seminal vesiculography; Endorectal magnetic resonance imaging

Peer reviewer: Cem Onal, MD, Department of Radiation Oncology, Adana Research and Treatment Centre, Baskent University Medical Faculty, 01120 Yuregir, Adana, Turkey

Donkol RH. Imaging in male-factor obstructive infertility. *World J Radiol* 2010; 2(5): 172-179 Available from: URL: <http://www.wjgnet.com/1949-8470/full/v2/i5/172.htm> DOI: <http://dx.doi.org/10.4329/wjr.v2.i5.172>

INTRODUCTION

Fertility is a two-person phenomenon and successful conception depends on a complex set of interactions between the male and the female reproductive tracts. Infertility is defined as failure to conceive after 1 year of unprotected intercourse. Infertility is a relatively common problem that affects approximately 15% of the reproductive age range population^[1]. More couples now seek infertility evaluations, which may reflect the increased availability of infertility-related services and an increased media focus on medical advances in reproductive technology. Male and female factors coexist in about one third of cases, whilst one third of cases are secondary to

male factors only^[2]. Therefore the man should be evaluated concurrently with the woman, since a male factor is the primary or contributing cause in 40% to 60% of cases. In addition to detecting treatable abnormalities, evaluation of the infertile man is critical to uncover life-threatening problems associated with the symptom of infertility, as well as genetic conditions associated with male infertility that could be transmitted to offspring with assisted reproduction. New diagnostic tests have been developed and surgical techniques refined resulting in improved treatment results and patient care^[3].

A large body of literature describes the causes, investigations, and treatment of infertility. This paper reviews the causes of infertility in men with obstruction of the seminal tract, describes medical imaging investigations, and suggests guidelines for referral to infertility specialists.

CAUSES OF MALE INFERTILITY

Male infertility has many causes, which may be pre-testicular, testicular, and post-testicular. From the practical point of view, abnormalities that cause testicular failure and impaired spermatogenesis cannot be corrected while obstructive processes involving the sperm transport system are potentially correctable. Post-testicular causes include obstruction of the sperm delivery route (male factor obstructive infertility) anti-sperm antibodies and retrograde ejaculation^[4]. Obstruction can occur at any level either proximal, affecting the epididymis or distal, affecting the ejaculatory duct^[5,6].

It is important to distinguish non-obstructive azoospermia from obstructive azoospermia, because infertile men with obstructive azoospermia may be amenable to surgical or interventional correction. On the other hand, in those with primary testicular failure, it may be reasonable to proceed directly to an advanced assisted reproductive technique such as intracytoplasmic sperm injection^[7]. Obstruction of the seminal tract represents 6% of cases^[3]. Men with obstructive azoospermia typically have normal-sized testes, possible epididymal fullness, and a normal serum follicle stimulating hormone (FSH). Men with non-obstructive azoospermia present frequently with small or soft testes and an elevated FSH^[8-10].

Seminal tract obstruction can be classified according to the level of obstruction, into proximal seminal tract obstruction, including epididymis and scrotal portions of the vas deferens and distal seminal tract obstruction including inguinal, pelvic and ampullary portions of the vas deferens, and ejaculatory ducts. Pathology from complete ejaculatory duct obstruction (EDO) occurs in < 1% of infertile men, whereas the frequency of incomplete obstructive pathologies is reportedly 4.4%^[11]. Seminal tract obstruction may be congenital or acquired. Congenital causes include atresia or stenosis as well as midline prostatic cystic lesions, e.g. utricular, Müllerian and ejaculatory duct cysts. Acquired causes may be of inflammatory or traumatic origin, including calculus formation and stenosis after transurethral resection of the prostate^[5].

Fortunately, fifty percent of the causes of male infer-

tility are potentially correctable^[12]. The main purpose of imaging evaluation in cases of male infertility is to identify these correctable causes. Treatment of correctable male-factor pathology is cost effective, does not increase the risk of multiple births, and can spare the woman invasive procedures and the potential complications associated with assisted reproductive technologies^[13].

MEDICAL IMAGING IN MALE INFERTILITY

Various imaging modalities are available to evaluate men with obstructive infertility such as scrotal ultrasonography, transrectal ultrasound (TRUS), vasography, magnetic imaging resonance, seminal vesicle aspiration, seminal tract washout (STW), and seminal vesiculography. The imaging and analysis of infertility in males has become more common in recent years. The practicing radiologist should be familiar with the evaluation of the infertile man and the common radiologic findings and disease processes associated with infertility^[14-16].

Scrotal ultrasound

Ultrasound (US) is a widely used and well tolerated imaging modality for evaluation of pathologic conditions in male factor infertility. Recent technical advances in US applications and post processing developments have enabled new aspects in the structural and functional analysis of testicular tissue, varicocele and seminal tract. US is being used with increased frequency in the evaluation of the infertile male. Scrotal US is considered the primary imaging modality for the evaluation of scrotal abnormalities^[17-19]. Scrotal US can be helpful in determining whether azoospermia is non-obstructive or obstructive, because it can directly detect abnormalities in the testis, mediastinum testis, epididymis, and the proximal vas deferens.

Scrotal US findings in non obstructive Azoospermia:

Testicular pathologies causing infertility include; cryptorchidism, atrophy, torsion/infarction, inflammation, mumps, tuberculosis, neoplasm, trauma, microlithiasis, hydrocele, and varicocele. Varicoceles are the most frequent physical finding in infertile men; indeed, they may be responsible for nearly one-third of cases of male infertility^[20]. Scrotal US is a good diagnostic tool for diagnosis of varicocele (sensitivity 97%, specificity 94%)^[21]. The commonly accepted color Doppler US criterion for varicocele with a maximal vein diameter of 3 mm or greater had a sensitivity of 53% and specificity of 91% compared to physical examination^[22]. Varicocele management, however, has always been a controversial issue because very few randomized, controlled studies have been performed to examine varicolectomy as an infertility treatment. Significant evidence suggests that varicoceles have a harmful effect on the testis and that varicolectomy can not only prevent progressive decline in testicular function but also reverse the damage^[23-25].

However, the degree to which varicocele repair improves pregnancy rates and the success of assisted reproductive technology remains controversial. Varicoceles

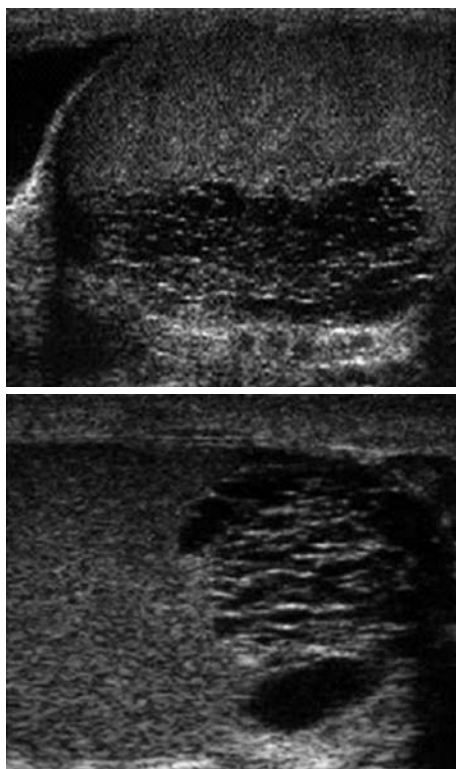


Figure 1 Ultrasound of both testes (sagittal images) demonstrates ectasia of the testes with formation of intratesticular cysts. These findings are suggestive of a seminal tract obstructive etiology which should be managed by epididymo-vasotomy.

are associated with infertility but the significance of this relationship is uncertain; surgical or radiological repair of varicoceles is not recognized as appropriate treatment for infertility^[20,26-29].

Scrotal US is used to examine the testes in at least two planes, the transverse and longitudinal; the size is measured and the echotexture is evaluated^[30]. Recent technical advances in US applications and post processing developments have enabled new aspects in the structural and functional analysis of testicular tissue and therefore male fertility^[31].

Testicular volume measured by testicular US correlates significantly with testicular function. Increased resistive index and pulsatility index of capsular branches of the testicular arteries on unenhanced color Doppler US examination may be an indicator of impaired testicular microcirculation^[19]. Also, if a testis is non-palpable, scrotal US can determine whether it is congenitally absent, cryptorchid, atrophic, or ectopic^[18].

Scrotal US findings in obstructive Azoospermia: Scrotal US can directly demonstrate abnormalities in the proximal portion of the seminal duct and can also depict secondary changes of the proximal seminal duct caused by obstruction in the distal part of the seminal duct. Evaluation of the proximal genital duct and measurement of testicular volume with scrotal US are helpful in distinguishing obstructive azoospermia from nonobstructive azoospermia in infertile men. Testicular volume measured

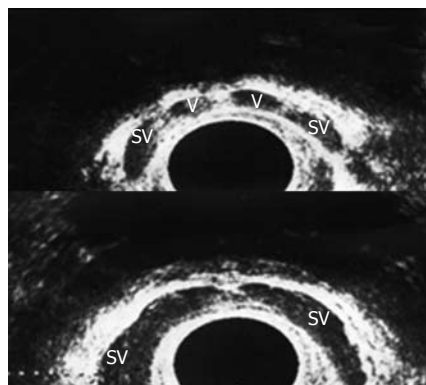


Figure 2 Transrectal ultrasound (TRUS) in the axial plane showed normal both vasal ampullae (V) and seminal vesicles (SV).

at scrotal US is higher for obstructive azoospermia than for nonobstructive azoospermia. The median testicular volume in obstructive azoospermia was 11.6 mL (range, 7.7-25.8 mL) and that in nonobstructive azoospermia was 8.3 mL (range, 1.2-16.4 mL) ($P < 0.05$)^[7].

Scrotal US also can diagnose obstruction in an azoospermic patient by directly demonstrating dilatation in the proximal seminal duct (mediastinum testis, epididymis, and intrascrotal portion of the vas deferens) as seen in Figure 1. The epididymal abnormalities depicted with scrotal US are significantly associated with obstructive azoospermia ($P = 0.001$)^[7]. Scrotal US may also depict secondary changes of the proximal genital duct caused by distal genital duct obstruction (terminal vas deferens, ampulla of the vas deferens, seminal vesicle, and ejaculatory duct)^[26]. Thus, evaluation of the epididymis and testicular volume with scrotal US are important in distinguishing obstructive azoospermia from nonobstructive azoospermia in infertile men. Sensitivity, specificity, and accuracy of scrotal US for differentiation of obstructive from nonobstructive azoospermia were 82.1%, 100% and 87.5%, respectively^[7].

TRUS

TRUS can clearly visualize the distal genital tract as vassal ampullae, seminal vesicles and ejaculatory ducts (Figure 2). Seminal vesicles are thought to be normal when > 25 mm in length, hypoplastic when > 16 mm but < 25 mm and atrophic when < 16 mm. TRUS proved to be a reliable diagnostic tool in men with obstructive infertility, especially when combined with seminal analysis. TRUS is most commonly performed if the diagnosis of distal seminal tract obstruction is being considered^[5,32]. The role TRUS is now firmly established in diagnosing post testicular causes of infertility.

Pathologic findings were detected in 75% of patients with azoospermia on TRUS. However TRUS did not reveal any pathologies in 64.7% of patients with nonazoospermia. The incidences of hypoplastic/atrophic seminal vesicles and vasal agenesis were significantly higher in the azoospermic subgroup ($P < 0.002$)^[33].

Currently, the most important indication for TRUS to assess for obstruction and the absence or hypoplasia

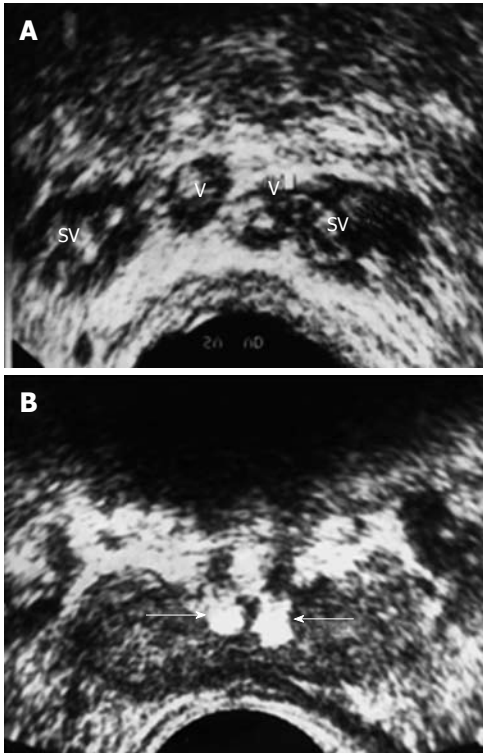


Figure 3 Twenty five years infertile man with azospermia. A: Multiple calculi within the SV and V; B: Bilateral echogenic calculi impacted within the ejaculatory ducts (arrows).

of the seminal vesicles and the ejaculatory ducts, is low ejaculate volume. TRUS has proved invaluable in visualizing and evaluating the patency of the ductal system. The advantage of TRUS is that it is non invasive, well accepted by patients and aids in visualizing the normal and abnormal seminal vesicles, the vasa deferentia, ejaculatory ducts and the prostate. Congenital abnormalities of the vas are the most common finding on TRUS in men with azoospermia and low ejaculate volume. Agenesis of the vas deferens is reported to occur in between 1.0%-2.5% of cases. It may be partial, complete, unilateral or bilateral. Other vasal abnormalities that may be seen on TRUS in infertility are: echogenic vas (fibrosis, calcification), cysts of the vas deferens and calculi (Figure 3). Obstructive findings are also seen in seminal vesicles secondary to midline urogenital cysts as utricle and Mullerian duct cysts. Seminal vesicles are thought to be absent when no tissue is identified. Seminal vesicular cysts are commonly congenital rather than acquired. The obstructed ejaculatory duct as seen as a hypoechoic tubular structure, is best seen in the saggital plane. The US features of EDO are: ejaculatory duct cyst, calcification, dilatation and seminal vesicular dilatation^[17]. Transrectal ultrasonography is the initial investigation method used to visualize and locate the presence of a cyst or calcifications that may contribute to the obstruction. Transurethral resection of the ejaculatory ducts (TURED) represents the best treatment modality, resulting in marked improvement in the semen parameters and pregnancy rate in well selected cases^[34].

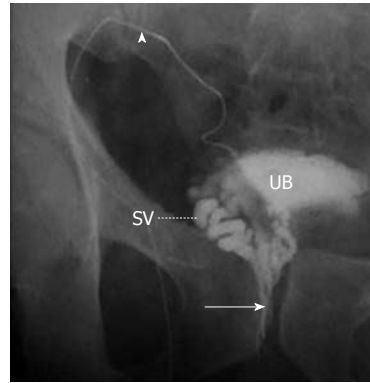


Figure 4 Percutaneous vasography shows normal right sided vasogram with opacification of the right vas (arrowhead), SV and ejaculatory duct (arrow) with retrograde opacification of the urinary bladder (UB).



Figure 5 Percutaneous right vasography in a patient with obstructed infertility shows complete obstruction of the ejaculatory duct with retention of the dye in the vas (arrowhead) and SV and non opacification of the urinary bladder.

Vasography

Traditionally vasography (vesiculodeferentography) has been considered the gold standard radiological imaging modality used for evaluation of the patency of the seminal tract (Figure 4). It can clearly demonstrate the site of obstruction along the seminal tract (Figure 5). Unfortunately, it has the complication of possible iatrogenic vasal stricture^[35]. This complication has narrowed its clinical use in obstructive infertility. Vasography has been considered the reference standard for the evaluation of the distal genital duct, but is an invasive procedure which carries the risk of genital duct scarring. Vasography was used in the past to evaluate suspected cases of obstruction of the seminal ducts. Over the years, numerous attempts have been made to improve the technique used to perform this examination and to render it less invasive. Bilateral dilatations of the seminal vesicles and/or dilated ejaculatory ducts with no contrast flow into the urethra are the common findings of complete EDO on vasography. In contrast, vasography may not always confirm a diagnosis of partial EDO, as the contrast medium used in this method may pass into the bladder on partial obstruction, similar to the flow seen in patients with no obstruction^[36,37]. Currently, the use of



Figure 6 TRUS-right seminal vesiculography shows normal opacification of right SV and ejaculatory duct (arrow). The injected dye is seen in the posterior urethra and UB denoting patency of the right ejaculatory duct.

vasography is indicated in selected cases, where it is combined with functional studies like STW and followed by immediate interventions to correct the obstruction^[38].

STW

In cases of distal seminal tract obstruction, there are retained spermatozoa within the seminal tract anywhere downstream of the epididymis. In these instances the technique of STW may be useful. This technique involves cannulation of the vas deferens and subsequent antegrade washing of the vas with collection of sperm from the bladder^[36-40]. The advent of TRUS has greatly facilitated the accurate diagnosis of distal seminal tract obstruction being less invasive. TRUS can provide information about the exact location of any cyst, or the level of obstructed ejaculatory duct, which is very helpful during TURED^[32].

Endorectal magnetic resonance imaging

In patients with male infertility, endorectal surface coil magnetic resonance imaging (MRI) is superior to TRUS in delineating the anatomy of the prostate and distal seminal tract (vassal ampullae, seminal vesicles and ejaculatory ducts) due to its high soft tissue contrast and multiplanar capability. A MR image serves as a “detailed map” for guiding interventional diagnostic or corrective procedures. Pitfalls in the interpretation of MR images can be avoided by familiarity with normal and abnormal findings in patients with male infertility^[41,42].

Causes of male infertility like Wolffian duct abnormalities include agenesis of the kidney, vas deferens, or seminal vesicle and cysts of the vas deferens, seminal vesicle, or urogenital sinus-ejaculatory duct. Müllerian duct abnormalities such as müllerian duct cysts and utricle cysts can be easily diagnosed by MRI. MRI can clearly demonstrate the level and cause of EDO (Figure 6). However, endorectal MR imaging is expensive and less available than TRUS and should be reserved for selected patients in whom results of TRUS are not conclusive^[34]. TRUS is a good method for initial evaluation of infertile patients especially those with complete obstruction. Endorectal MR



Figure 7 A 29-year-old man with primary obstructive infertility. TRUS (upper image) and endorectal magnetic resonance imaging (middle image) show a well-defined midline urogenital cyst with intra- and extraprostatic components. TRUS-seminal vesiculography (lower image) shows the seminal vesicle is communicating with the urogenital cyst with non opacification of the urethra or urinary bladder denoting complete distal obstruction (N.B. the left vas and seminal vesicles were absent). Trans-urethral incision of the cyst lead to improvement of sperm count.

imaging should be reserved for selected patients in whom results of TRUS are not conclusive^[42]. Recently, with the increased awareness of functional obstruction of ejaculatory ducts, reports have been focusing on the diagnosis of partial or functional obstruction and abnormalities of the ejaculatory duct related to infertility by increased use of magnetic resonance imaging^[43]. Pathologic findings were detected in 61% of patients with azoospermia by MR imaging. MR imaging did not reveal any pathologies in 59.1% of patients with nonazoospermia^[33].

TRUS-guided seminal vesiculography

TRUS-guided seminal vesiculography is a technique that couples US with radiography to evaluate male-factor infertility. Seminal vesiculography is performed after needle puncture of the seminal vesicle to inject contrast material for radiography (Figure 7). Seminal vesiculography has helped imaging of the distal male reproductive tract (vas deferens, seminal vesicles, and ejaculatory ducts)^[39,44]. TRUS has also been used to guide aspiration of seminal vesicles to diagnose EDO. The presence of sperm in the aspirated fluid documents the presence

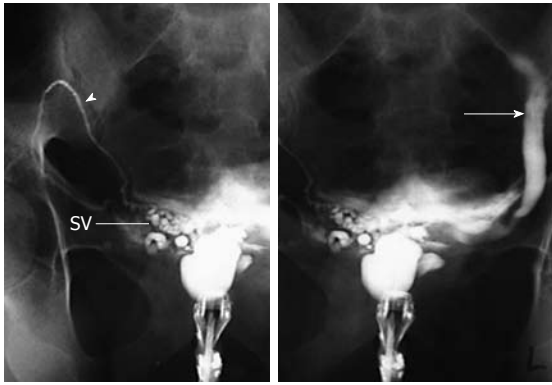


Figure 8 A 33-year-old man with primary infertility. TRUS-guided contrast opacification of midline prostatic cyst shows the presence of a large cyst communicating on the right side with the right vas (arrowhead) and right SV. On the left side the cyst is communicating with a blind tubular structure (arrow), which proved to be an ectopic short ureter of a hypoplastic left kidney.

of obstruction, confirms the presence of intact spermatogenesis, and rules out more proximal obstruction. Normal fertile men do not have significant numbers of motile sperm in the seminal vesicles immediately after ejaculation but, in the presence of an anatomical or functional distal obstruction, sperm reflux may occur and sperm can be detected within the seminal vesicles. The presence of more than three motile sperm per high-power field in the seminal vesicle aspirate obtained immediately after ejaculation indicates obstruction^[39,45]. A comparative analysis done by Purohit *et al*^[32], compared the four common diagnostic tests used to evaluate patients with distal seminal duct obstruction which are TRUS and three dynamic tests (chromotubation, seminal vesicle aspiration and seminal vesiculography). They concluded that TRUS alone has poor specificity for diagnosis of distal seminal duct obstruction as obstruction on TRUS was confirmed in only 52%, 48% and 36% of vesiculography, seminal vesicle aspiration and duct chromotubation studies, respectively. Thus incorporation of dynamic tests into the algorithm for diagnosis of distal seminal duct obstruction may decrease unnecessary duct resection procedures and improve the success of the resection procedures that are indicated. Some urogenital cysts communicate with the seminal tract and if TRUS-guided aspiration is done for these patients it reveals the presence of sperm (Figures 7 and 8). In other patients the ejaculatory ducts are compressed and obstructed by virtue of the urogenital cysts (Figure 9) and after cyst aspiration, the compression is released and EDO is relieved^[46].

TRUS alone is not a reliable tool for the diagnosis of EDO. For this reason, seminal vesicle aspiration should be used as an adjunctive technique in patients with seminal vesicle dilation or a prostatic midline/ED cyst to confirm the diagnosis before surgery. Engin *et al*^[33], studied 70 patients with suspected EDO; they found 55 patients (78.6%) had evidence of EDO on diagnostic TRUS. However, obstruction on TRUS was confirmed in 49.1% (27 of 55) of the patients with seminal vesicle aspiration.

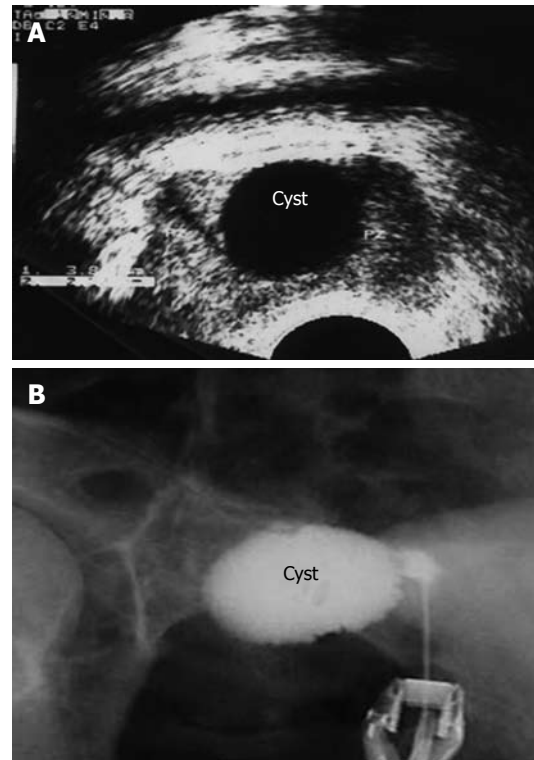


Figure 9 A 27-year-old with primary infertility. A: TRUS shows a 3 cm × 2 cm thin walled midline intraprostatic urogenital cyst; B: TRUS-guided contrast opacification of the cyst revealed that the cyst was blind with no communication with the seminal tract. Semen analysis showed improvement of the sperm count 3 d after complete cyst aspiration.

TREATMENT OF MALE OBSTRUCTIVE INFERTILITY

Management of patients with obstructive disorders of the seminal tract is one of the most rapidly growing fields in medicine in recent years. Numerous changes in diagnostic and therapeutic decision-making strategies for these patients have been made. Seminal tract obstruction is one of the correctable causes of male infertility. Treatment for proximal seminal tract obstruction is by vasoepididymostomy anastomosis operation to overcome the obstruction. Vasoepididymostomy has a lower cost burden per birth than does intracytoplasmic sperm injection, and natural pregnancy initiated with surgical correction may filter some chromosomal or genetic abnormalities. Moreover, epididymal damage that can happen during sperm retrieval could be prevented^[7].

The treatment of choice for distal seminal tract obstruction is TURED. Approximately half of the men undergoing this procedure for EDO show improvement of their semen parameters and half of the men who improve achieve a subsequent pregnancy^[11]. Although the assisted reproduction technique (ART) has been considered the cutting edge in management of male infertility in recent years, men should investigate the cause of their male factor infertility for many reasons. In addition to detecting treatable abnormalities, evaluation of

the infertile man is critical to uncover life-threatening problems associated with the symptom of infertility, as well as genetic conditions associated with male infertility that could be transmitted to offspring with assisted reproductive techniques^[3]. Analysis of the genetic factors that impact male factor infertility will provide valuable insights into the creation of targeted treatments for patients and the determination of the causes of idiopathic infertility. Novel technologies that analyze the influence of genetics from a global perspective may lead to further developments in the understanding of the etiology of male factor infertility through the identification of specific infertile phenotype signatures^[47,48].

CONCLUSION

Thorough evaluation of infertile men is mandatory to identify patients with potentially correctable defects such as obstructive infertility from patients with nonobstructive azoospermia to eliminate unnecessary investigations and interventions.

In men with the clinical and laboratory findings of suspected seminal tract blockage, scrotal sonography should be the initial diagnostic procedure performed. If they have findings of non obstructive azoospermia such as varicocele or testicular pathology they will be managed according to the standard protocol for management of these pathologies. If the patients have findings of proximal obstructive azoospermia they can be managed surgically by vasoepididymostomy. If the scrotal US is normal or they have findings of distal obstructive azoospermia, they should be evaluated by TRUS. According to the TRUS results, the patients are classified into patients with sonographic criteria of obstructive infertility without urogenital cysts where TRUS-guided aspiration of the seminal vesicles is performed and TURED will be the management of choice. If a urogenital cyst is seen by sonography, TRUS-guided cyst aspiration and contrast opacification are performed. If the cyst is communicating with the seminal tract, management will be transurethral incision of the cyst. If the cyst is not in communication, obstructive infertility may be relieved after cyst aspiration. If the obstruction is not cured, TURED will be the management of choice. Also, sperm harvested during TRUS-guided aspiration may be stored and used for the ART which is the cutting edge in management of male infertility. If the results of TRUS are inconclusive or doubtful, endorectal MRI should be performed to serve as a “detailed map” for guiding interventional diagnostic or corrective procedures.

REFERENCES

- 1 **Fisch H**, Kang YM, Johnson CW, Goluboff ET. Ejaculatory duct obstruction. *Curr Opin Urol* 2002; **12**: 509-515
- 2 **Sigman M**, Lipshultz LI, Howards SS. Evaluation of the subfertile male. In: Lipshultz LI, Howards SS, editors. *Infertility in the male*. 3rd ed. St. Louis: Mosby, 1997: 173-193
- 3 **Schlegel PN**. Evaluation of male infertility. *Minerva Ginecol* 2009; **61**: 261-283
- 4 **Turek PJ**, Magana JO, Lipshultz LI. Semen parameters

- before and after transurethral surgery for ejaculatory duct obstruction. *J Urol* 1996; **155**: 1291-1293
- 5 **Goluboff ET**, Stifelman MD, Fisch H. Ejaculatory duct obstruction in the infertile male. *Urology* 1995; **45**: 925-931
- 6 **Brugh VM 3rd**, Lipshultz LI. Male factor infertility: evaluation and management. *Med Clin North Am* 2004; **88**: 367-385
- 7 **Moon MH**, Kim SH, Cho JY, Seo JT, Chun YK. Scrotal US for evaluation of infertile men with azoospermia. *Radiology* 2006; **239**: 168-173
- 8 **Jarow JP**, Espeland MA, Lipshultz LI. Evaluation of the azoospermic patient. *J Urol* 1989; **142**: 62-65
- 9 **Worischek JH**, Parra RO. Transrectal ultrasound in the evaluation of men with low volume azoospermia. *J Urol* 1993; **149**: 1341-1344
- 10 **Littrup PJ**, Lee F, McLeary RD, Wu D, Lee A, Kumasaka GH. Transrectal US of the seminal vesicles and ejaculatory ducts: clinical correlation. *Radiology* 1988; **168**: 625-628
- 11 **Schlegel PN**. Management of ejaculatory duct obstruction. In: Lipshultz LI, Howards SS, editors. *Infertility in the male*. 3rd ed. St. Louis: Mosby, 1997: 385-394
- 12 **Kolettis PN**. Evaluation of the subfertile man. *Am Fam Physician* 2003; **67**: 2165-2172
- 13 **Schenker JG**, Ezra Y. Complications of assisted reproductive techniques. *Fertil Steril* 1994; **61**: 411-422
- 14 **Simpson WL Jr**, Rausch DR. Imaging of male infertility: pictorial review. *AJR Am J Roentgenol* 2009; **192**: S98-S107 (Quiz S108-11)
- 15 **Simpson WL Jr**, Rausch DR. Imaging of male infertility: self-assessment module. *AJR Am J Roentgenol* 2009; **192**: S108-S111
- 16 **Jhaveri KS**, Mazrani W, Chawla TP, Filobos R, Toi A, Jarvi K. The Role of Cross-sectional Imaging in Male Infertility: A Pictorial Review. *Can Assoc Radiol J* 2010; **61**: 144-155
- 17 **Joshi M**. Role of ultrasound in assessment of male infertility. *Biomed Imaging Interv J* 2007; **3**: e12-e47
- 18 **Mathers MJ**, Sperling H, Rübber H, Roth S. The undescended testis: diagnosis, treatment and long-term consequences. *Dtsch Arztebl Int* 2009; **106**: 527-532
- 19 **Schurich M**, Aigner F, Frauscher F, Pallwein L. The role of ultrasound in assessment of male fertility. *Eur J Obstet Gynecol Reprod Biol* 2009; **144** Suppl 1: S192-S198
- 20 **Cocuzza M**, Cocuzza MA, Bragais FM, Agarwal A. The role of varicocele repair in the new era of assisted reproductive technology. *Clinics (Sao Paulo)* 2008; **63**: 395-404
- 21 **Trum JW**, Gubler FM, Laan R, van der Veen F. The value of palpation, varicoscreen contact thermography and colour Doppler ultrasound in the diagnosis of varicocele. *Hum Reprod* 1996; **11**: 1232-1235
- 22 **Chiou RK**, Anderson JC, Wobig RK, Rosinsky DE, Matamoros A Jr, Chen WS, Taylor RJ. Color Doppler ultrasound criteria to diagnose varicoceles: correlation of a new scoring system with physical examination. *Urology* 1997; **50**: 953-956
- 23 **Zorba UO**, Sanli OM, Tezer M, Erdemir F, Shavakhov S, Kadioglu A. Effect of infertility duration on postvaricocelectomy sperm counts and pregnancy rates. *Urology* 2009; **73**: 767-771
- 24 **Romeo C**, Santoro G. Varicocele and infertility: why a prevention? *J Endocrinol Invest* 2009; **32**: 559-561
- 25 **Zheng YQ**, Gao X, Li ZJ, Yu YL, Zhang ZG, Li W. Efficacy of bilateral and left varicocelectomy in infertile men with left clinical and right subclinical varicoceles: a comparative study. *Urology* 2009; **73**: 1236-1240
- 26 **Beddy P**, Geoghegan T, Browne RF, Torreggiani WC. Testicular varicoceles. *Clin Radiol* 2005; **60**: 1248-1255
- 27 **Donkol RH**, Salem T. Paternity after varicocelectomy: preoperative sonographic parameters of success. *J Ultrasound Med* 2007; **26**: 593-599
- 28 **Kim HH**, Goldstein M. Adult varicocele. *Curr Opin Urol* 2008; **18**: 608-612
- 29 **Youssef T**, Abd-Elaal E, Gaballah G, Elhanbly S, Eldosoky E. Varicocelectomy in men with nonobstructive azoospermia:

- is it beneficial? *Int J Surg* 2009; **7**: 356-360
- 30 **Edey AJ**, Sidhu PS. Male infertility: role of imaging in the diagnosis and management. *Imaging* 2008; **20**: 139-146
- 31 **Caretta N**, Palego P, Schipilliti M, Torino M, Pati M, Ferlin A, Foresta C. Testicular contrast harmonic imaging to evaluate intratesticular perfusion alterations in patients with varicocele. *J Urol* 2010; **183**: 263-269
- 32 **Purohit RS**, Wu DS, Shinohara K, Turek PJ. A prospective comparison of 3 diagnostic methods to evaluate ejaculatory duct obstruction. *J Urol* 2004; **171**: 232-235; discussion 235-236
- 33 **Engin G**, Kadioğlu A, Orhan I, Akdöl S, Rozanes I. Transrectal US and endorectal MR imaging in partial and complete obstruction of the seminal duct system. A comparative study. *Acta Radiol* 2000; **41**: 288-295
- 34 **Heshmat S**, Lo KC. Evaluation and treatment of ejaculatory duct obstruction in infertile men. *Can J Urol* 2006; **13** Suppl 1: 18-21
- 35 **Goldstein M**. Vasography. In: Goldstein M, editor. *Surgery of male infertility*. Philadelphia: Saunders, 1995: 26-32
- 36 **Colpi GM**, Negri L, Patrizio P, Pardi G. Fertility restoration by seminal tract washout in ejaculatory duct obstruction. *J Urol* 1995; **153**: 1948-1950
- 37 **Jarow JP**. Seminal vesicle aspiration in the management of patients with ejaculatory duct obstruction. *J Urol* 1994; **152**: 899-901
- 38 **Solivetti FM**, Drusco A, Pizzi G, Elia F, de Mutiis C, Teoli M, Bacaro D. Percutaneous vesiculodeferentography in the diagnosis of male infertility: A review of our results and the data reported in the literature. *J Ultrasound* 2008; **11**: 102-106
- 39 **Jarow JP**. Seminal vesicle aspiration of fertile men. *J Urol* 1996; **156**: 1005-1007
- 40 **Jarow JP**. Transrectal ultrasonography in the diagnosis and management of ejaculatory duct obstruction. *J Androl* 1996; **17**: 467-472
- 41 **Schnall MD**, Pollack HM, Van Arsdalen K, Kressel HY. The seminal tract in patients with ejaculatory dysfunction: MR imaging with an endorectal surface coil. *AJR Am J Roentgenol* 1992; **159**: 337-341
- 42 **Parsons RB**, Fisher AM, Bar-Chama N, Mitty HA. MR imaging in male infertility. *Radiographics* 1997; **17**: 627-637
- 43 **Onur MR**, Orhan I, Firdolas F, Onur R, Kocakoç E. Clinical and radiological evaluation of ejaculatory duct obstruction. *Arch Androl* 2007; **53**: 179-186
- 44 **Jones TR**, Zagoria RJ, Jarow JP. Transrectal US-guided seminal vesiculography. *Radiology* 1997; **205**: 276-278
- 45 **Orhan I**, Onur R, Cayan S, Koksall IT, Kadioğlu A. Seminal vesicle sperm aspiration in the diagnosis of ejaculatory duct obstruction. *BJU Int* 1999; **84**: 1050-1053
- 46 **Stricker HJ**, Kunin JR, Faerber GJ. Congenital prostatic cyst causing ejaculatory duct obstruction: management by transrectal cyst aspiration. *J Urol* 1993; **149**: 1141-1143
- 47 **McKie R**. Assisted reproduction means male infertility will continue for years to come. *BMJ* 2010; **340**: c1073
- 48 **O'Flynn O'Brien KL**, Varghese AC, Agarwal A. The genetic causes of male factor infertility: a review. *Fertil Steril* 2010; **93**: 1-12

S- Editor Cheng JX L- Editor Lalor PF E- Editor Zheng XM

Multi-parametric MR imaging of transition zone prostate cancer: Imaging features, detection and staging

Arda Kayhan, Xiaobing Fan, Jacob Oommen, Aytekin Oto

Arda Kayhan, Xiaobing Fan, Jacob Oommen, Aytekin Oto, Department of Radiology, University of Chicago, Chicago, IL 60637, United States

Author contributions: Kayhan A wrote the article; Fan X organized the references and drafted the article; Oommen J collected and assembled the data; Oto A revised the article.

Correspondence to: Arda Kayhan, MD, Department of Radiology, University of Chicago, Chicago, IL, United States. arda_kayhan@yahoo.com

Telephone: +1-773-7021310 Fax: +1-773-8347448

Received: March 30, 2010 Revised: April 21, 2010

Accepted: April 28, 2010

Published online: May 28, 2010

Samsung Medical Center, Sungkyunkwan University School of Medicine, 50 Ilwon-dong, Kangnam-gu, Seoul 135-710, South Korea

Kayhan A, Fan X, Oommen J, Oto A. Multi-parametric MR imaging of transition zone prostate cancer: Imaging features, detection and staging. *World J Radiol* 2010; 2(5): 180-187 Available from: <http://www.wjgnet.com/1949-8470/full/v2/i5/180.htm> DOI: <http://dx.doi.org/10.4329/wjr.v2.i5.180>

Abstract

Magnetic resonance (MR) imaging has been increasingly used in the evaluation of prostate cancer. As studies have suggested that the majority of cancers arise from the peripheral zone (PZ), MR imaging has focused on the PZ of the prostate gland thus far. However, a considerable number of cancers (up to 30%) originate in the transition zone (TZ), substantially contributing to morbidity and mortality. Therefore, research is needed on the TZ of the prostate gland. Recently, MR imaging and advanced MR techniques have been gaining acceptance in evaluation of the TZ. In this article, the MR imaging features of TZ prostate cancers, the role of MR imaging in TZ cancer detection and staging, and recent advanced MR techniques will be discussed in light of the literature.

© 2010 Baishideng. All rights reserved.

Key words: Multi-parametric magnetic resonance imaging; Prostate cancer; Transition zone

Peer reviewers: James Chow, PhD, Radiation Physicist, Radiation Medicine Program, Princess Margaret Hospital, 610 University Avenue, Toronto, ON, M5G 2M9, Canada; Chan Kyo Kim, MD, Assistant Professor, Department of Radiology,

INTRODUCTION

It is important to localize prostate gland tumors to evaluate the transcapsular spread and staging in order to plan treatment protocols and avoid positive anterior surgical margins during radical prostatectomy. Prostate cancer arises from the peripheral zone (PZ) in 75%-85% of patients^[1]. Cancers arising from the transition zone (TZ) represent 40% of autopsy series and 25%-30% of radical prostatectomy series^[1]. The utility of magnetic resonance (MR) imaging in prostate cancer is currently under investigation, and it has been shown to be an excellent technique for evaluating prostate cancers, particularly PZ cancers^[2,3]. As TZ cancers are less frequent than PZ cancers, MR imaging in TZ cancers has not been widely used. However, recent studies attempting to identify MR characteristics of the TZ, by means of emerging techniques, have shown that MR can be used to delineate TZ cancers accurately^[4-7]. Herein, the MR imaging features of TZ tumors, the role of MR imaging in detection and staging, and recent advanced MR techniques in the evaluation of TZ cancers will be discussed including a review of literature.

ANATOMY AND MR IMAGING OF THE PROSTATE GLAND

According to zonal anatomy, the prostate is composed of anterior fibromuscular stroma, periurethral glandular

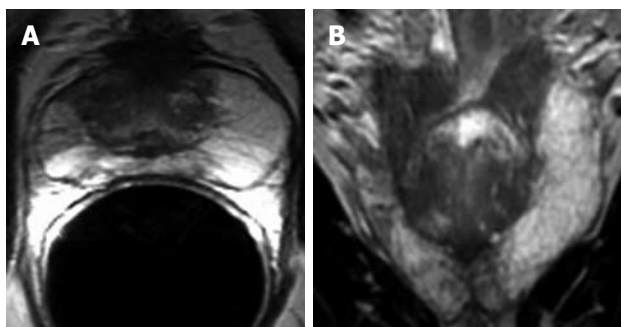


Figure 1 Magnetic resonance (MR) images demonstrating zonal anatomy of prostate gland. A: Axial T2-weighted (T2W) MR image depicts the central gland and peripheral zone (PZ). Central gland is hypointense compared to hyperintense PZ; B: Coronal T2W MR image shows hyperintense PZ and hypointense central gland.

tissue, the TZ, central zone (CZ) and PZ. The TZ is the inner prostate and forms 5% of the gland. It surrounds the anterior and lateral parts of the proximal urethra. In younger men this zone is small, however, with aging it enlarges and compresses the CZ due to hyperplastic changes. The CZ is the outer prostate forming approximately 25% of the gland in young men^[8]. It is less clearly distinguished histologically from the PZ. The PZ is the outer prostate and forms 70% of the gland^[8]. Radiologically, the prostate has been divided into two parts: the PZ and the central gland which is composed of the PZ, TZ and CZ^[9]. In young men, the gland is mainly composed of the CZ. With aging, the TZ is enlarged due to benign prostatic hyperplasia (BPH) which commonly arises from the TZ^[10].

MR imaging enables differentiation between the PZ, CZ and TZ. In young adults, normal prostate is homogenous, whereas with aging the differentiation between the PZ and the central gland is more clearly depicted. T1-weighted (T1W) images distinguish between the prostatic parenchyma and the surrounding periprostatic fat and vascular plexus. On T1W images, the homogenous gland has an intermediate-to-low signal intensity, and zonal differentiation can not be identified^[11]. Post-biopsy hemorrhage has high signal-intensity on T1W images. On T2-weighted (T2W) images, better tissue differentiation is achieved and zonal anatomy is better depicted^[12]. As the glandular components are more prominent in the PZ, it has a homogeneously high signal intensity and is surrounded by a capsule which is seen as a thin, hypointense rim on T2W images. Both the CZ and TZ are hypointense compared to the PZ because of their stroma which consists of compact muscle fiber bundles. MR also enables multiplanar imaging of the prostate (Figure 1).

MR imaging has been increasingly used in the evaluation of prostate cancer^[13-18]. It enables multiplanar imaging and is superior to ultrasound and computed tomography in anatomic and volumetric evaluation of the gland^[19]. It is more accurate than digital rectal examination and transectal ultrasound (TRUS)-guided biopsy for cancer detection and localization. In a recent study, the detectability of

prostate cancer using MR imaging prior to TRUS-guided biopsy was determined by calculating the sensitivity and positive predictive value of TRUS, T2W imaging, diffusion weighted imaging (DWI), apparent diffusion coefficient (ADC) map and biopsy^[20]. The relationship between the detectability on each sequence and cancer location, Gleason score, and the short and long axis diameter of the tumor were also evaluated. The sensitivities were 26.9%, 41.2%, 56.7%, 57.7% and 75.1%, respectively. The sensitivity of each sequence increased as the Gleason score and the short- and long-axis diameters of the tumors increased. It was stated that MR imaging prior to biopsy has a high detectability for prostate cancer. MR imaging is used to guide targeted biopsy when prostate cancer is clinically suspected and previous ultrasound-guided biopsy results are negative. MR imaging also enables the localization and staging of prostate cancer. The high soft tissue resolution of MR imaging helps to show extracapsular extension and seminal vesicle invasion. It may be used in planning a roadmap for therapeutic approaches and for residual or locally recurrent cancer after treatment. MR imaging has mainly been used as a diagnostic tool for the detection of PZ cancers^[18-21]. It is considered insufficient for evaluating the TZ, as BPH, which causes a heterogeneous signal intensity, especially in elderly men, also originates from the TZ leading to conspicuous findings on T2W images^[2,22,23]. Recent studies using MR imaging of TZ cancers have shown that it can be used in the detection of TZ tumors that are not sampled during TRUS-guided biopsy and also for localization and staging^[4].

MR IMAGING OF TZ CANCERS

Prostate cancer begins as a small focus of carcinoma within the gland which grows very slowly^[24]. Approximately 75%-85% of cancers arise from the PZ, 25% arise from the TZ and 10% arise from the CZ^[1,25,26]. As there is no clear demarcation between the CZ and the PZ, most pathologists do not routinely recognize tumors as originating from the CZ. For that reason, comparison is generally focused on the distinctions between PZ and TZ cancers. TZ tumors are located anteriorly, far from the rectum and they are more difficult to detect compared to PZ tumors. These tumors can be of a large volume and are associated with high serum prostate specific antigen (PSA) levels but they are confined to the gland^[27]. They are mostly low grade and relatively non-aggressive. Most TZ tumors are found incidentally in resection specimens. It is important to accurately distinguish TZ cancers to guide biopsy and to avoid positive anterior surgical margins at radical prostatectomy.

Currently, the PZ is the primary target in most biopsies^[28]. However, in patients with elevated PSA levels with negative biopsy results, it should be kept in mind that the tumor focus may be in the central gland. Therefore, it has been suggested that TZ-targeted biopsy should be performed in patients with multiple negative biopsy results. As a result, although tumor zonal origin is

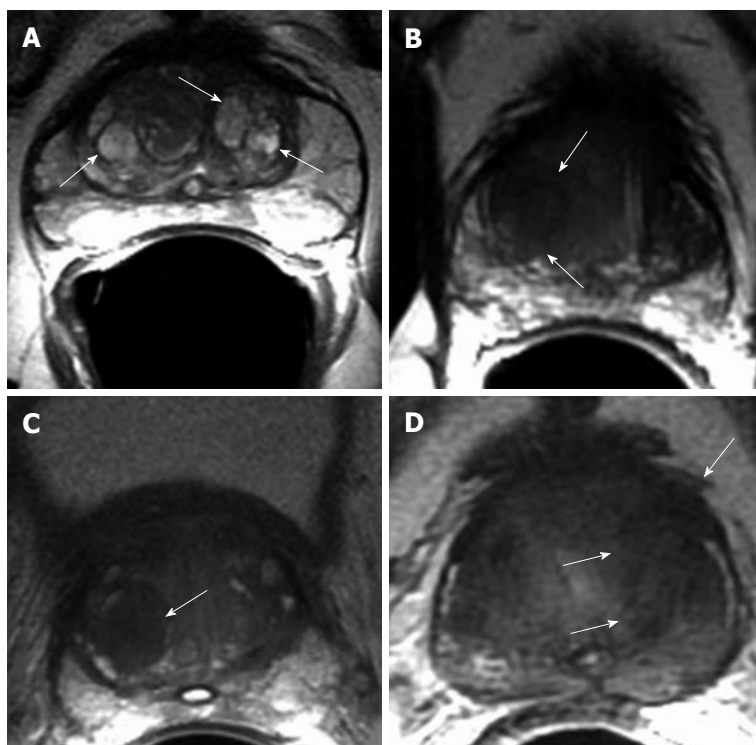


Figure 2 Axial T2W MR image. A: Multiple, well defined hyperintense glandular benign prostatic hyperplasia (BPH) nodules in central gland (arrows); B: Well defined, amorphous, hypointense TZ tumor (arrows); C: Hypointense stromal BPH nodule in the right transition zone (TZ) (arrow); D: Hypointense TZ tumor with extracapsular extension (arrows).

not an independent determinant of biochemical failure, it is helpful in predicting the route of cancer spread. If the zonal origin can be determined preoperatively, the cure rate may be increased by modification of the surgical approach.

The central gland has a heterogeneously variable signal intensity appearance in older men due to the presence of BPH or other coexisting benign diseases. BPH nodules occur almost exclusively in the TZ. As hypertrophied TZ tissue might also show metabolic heterogeneity similar to BPH nodules, it may be difficult to differentiate them from carcinoma. Discrimination between BPH and central gland tumors is important for staging. BPH is an enlargement of the TZ (central gland) which gives a heterogeneous appearance on MR imaging^[29,30]. BPH nodules may be seen as hypointense, isointense or hyperintense on T2W images, depending on the ratio of glandular to stromal tissue^[31]. It has been shown that, high signal intensity is due to hyperplastic glandular elements which are filled with secretion and the presence of cystic ectasia (Figure 2A). Low signal intensity is due to the presence of prominent sclerotic, fibrous or muscular elements^[22,29] (Figure 2B).

TZ cancers tend to have uniform low intensity on T2W imaging, but their diagnosis is not certain in the presence of coexisting benign disease^[31,32] (Figure 2C and D). It has been shown that, unless cancers in the TZ are of a large dimension, their detection on MR imaging is very difficult^[33]. Akin *et al.*^[4] determined the accuracy of MR imaging in detection and local staging in 148 patients. Features indicative of TZ cancers were defined as: homogenous low T2 signal intensity, ill defined margins, lack of capsule, lenticular shape, and invasion of anterior fibromuscular stroma. For identification of patients with

TZ cancer, the sensitivity of MR imaging was 75%-80% and the specificity was 78%-87%. The area under the receiver operating characteristic curve was 0.75 for detection and localization of tumor. For detection of extra-prostatic extension, the sensitivity and specificity of MR imaging were 28%-56% and 93%-94%, respectively. Li *et al.*^[5] determined the conventional MR findings of TZ lesions in 86 patients, of which 53 were cancers and 33 were benign, by comparing T2W and contrast-enhanced T1W images. Lesions were classified as uniform, low signal intensity on T2W images, lesions with homogeneous contrast enhancement and lesions with irregular margins on both gadolinium enhanced T1 and T2W images. Sensitivity, specificity and accuracy for cancer were 50%, 51% and 51%, respectively, for the uniform low T2 signal intensity criterion; 68%, 75% and 71% for homogeneous gadolinium enhancement; 60%, 72% and 65% for irregular margins on both T2W and gadolinium enhanced images.

ADVANCED MR TECHNIQUES

TZ cancers are difficult to diagnose particularly in the presence of BPH. Even in the PZ, some cancers such as those with a more permeative pattern can not be detected. Moreover, focal prostatic atrophy or prostatitis may also mimic cancer and may cause false-positive results. To increase the accuracy of MR imaging and to improve the detection of prostate cancer at an earlier stage, special techniques such as DWI, dynamic contrast-enhanced MR imaging (DCE-MRI), MR spectroscopy (MRS) and high-field-strength (3.0-T) MR imaging have been increasingly used. It has also been shown that these techniques may play a role in the detection of prostate tumor

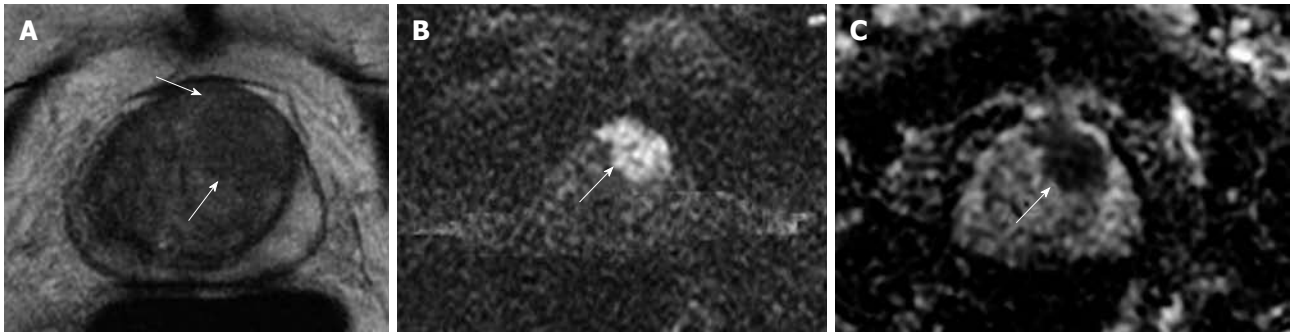


Figure 3 Tumor in the left mid prostate gland demonstrated by MR. A: Axial T2W image shows ill defined, amorphous, hypointense tumor (arrows); B: Diffusion weighted imaging (DWI) reveals focal area of bright signal consistent with tumor (arrow); C: Apparent diffusion coefficient (ADC) map reveals clear focal mass with dark signal consistent with decreased ADC (arrow).

foci in patients with persistently elevated PSA levels and prior to negative random TRUS-guided biopsy^[34].

DWI

DWI is a technique sensitive to molecular translation of water in biologic tissues due to the random thermal motion of molecules. The rapid changes in the movement of water in tissues and the measurement of the flow of water molecules can be identified by calculating the ADC^[35]. When the flow of water or diffusion is restricted, ADC is decreased. If ADC values are increased, there is no restriction in water flow. The ADC has been determined for tumor growth. It has been shown that, in proliferating cells, cellular density increases and extra- as well as intra-cellular space decreases leading to decreased ADC^[36]. In recent years, an increased number of studies have evaluated the utility of DWI in prostate cancer diagnosis^[37-44]. It has been shown that cancer tissues show higher signal intensity on DWI and thus a lower ADC compared with BPH nodules and normal tissue due to replacement of normal tissue (composed of water rich acinar structures) with densely packed malignant epithelial cells. TZ tumors have also been shown to have lower ADC values than the surrounding tissue^[37] (Figure 3). Namiki *et al.*^[45] stated that different b factors may effect the detection of tumors. Noworolski *et al.*^[41] showed that glandular-ductal tissues (glandular BPH) had lower peak enhancement and higher ADC values than the stromal-low ductal tissues (stromal BPH and central gland). Oto *et al.*^[46] showed significant ADC differences between tumor, stromal BPH and glandular BPH (lowest in tumor, highest in glandular BPH). These authors stated that there were differences between the perfusion parameters of tumor, stromal and glandular BPH, with the exception of the k-trans values between tumor and glandular BPH. Tamada *et al.*^[47] compared the ADC values in peripheral and transitional zones between normal and malignant prostatic tissues. Mean ADC values were significantly lower in both the PZ and TZ than in the corresponding normal regions. Ren *et al.*^[48] investigated the diagnostic value of DWI and ADC values in normal and pathologic prostate tissues. They showed that BPH nodules had a lower and non-homogenous signal intensity than the PZ. Prostate cancer showed high signal intensity

while prostate cyst showed low intensity. ADC values of BPH nodules were larger than prostate cancer foci and normal central gland. They stated that DWI and ADC values for normal central gland, PZ, prostate cyst, BPH nodules and cancer foci showed significant differences and could be used in the differential diagnosis of diseases of the prostate gland. Yoshizako *et al.*^[6] determined the clinical value of DWI and DCE-MRI in combination with T2W images, for the diagnosis of TZ tumors. They found that adding DWI to T2W images improved the sensitivity, specificity, accuracy and positive predictive value of diagnosing TZ tumors. In a recent study, the need for biexponential signal decay modeling for prostate cancer diffusion signal decays with b-factor over an extended b-factor range was evaluated. The researchers found that the fast and slow ADC values of cancer were significantly lower than those of the TZ and PZ, and the apparent fraction of the fast diffusion component was significantly smaller in cancer than in the PZ. It was stated that biexponential diffusion decay functions were required for prostate cancer diffusion signal decay curves when sampled over an extended b-factor range, enabling specific tissue characterization of prostate cancers^[49].

DCE-MRI

DCE-MRI was introduced to effectively visualize the pharmacokinetics of gadolinium uptake in the prostate gland. It depicts the physiological function of the tumor microcirculation. There is a relationship between contrast material uptake and microvascular structures in tumors, in which tumor angiogenesis is correlated with the parameters of signal intensity-time curves. As the reliability of T2W MR imaging in distinguishing prostate cancer of the PZ and TZ is limited, several studies have been performed to delineate the enhancement characteristics of prostate cancer to achieve more accurate information^[2,50-53]. In a recent study, the accuracy of T2W and DCE-MRI for cancer detection in 18 prostate cancer patients were compared prior to prostatectomy^[54]. The accuracy of DCE-MRI for cancer detection was calculated by a pixel-by-pixel correlation of quantitative DCE-MRI parameter maps and pathology. It was shown that DCE-MRI was more sensitive than T2W images for

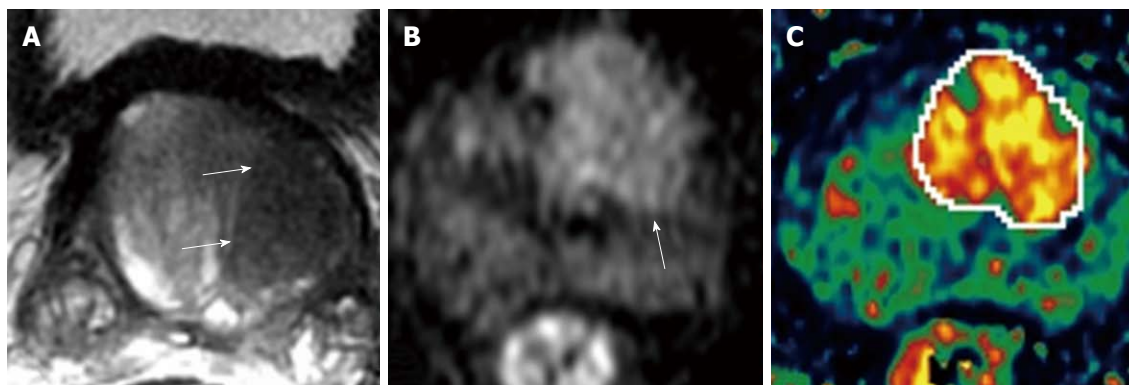


Figure 4 Left TZ tumor of prostate gland demonstrated by MR. A: Axial T2W image depicts ill defined, round, homogenous hypointense tumor (arrows); B: DWI depicts focal area of bright signal on left mid gland (arrow); C: K-trans map in dynamic contrast-enhanced MR imaging (DCE-MRI) clearly localizes the tumor and reveals some internal heterogeneity.

tumor localization (50% *vs* 21%) and more specific (85% *vs* 81%). The researchers stated that due to its higher sensitivity and specificity, DCE-MRI could be used to guide radiotherapy boosts in prostate cancer patients. Due to increased microvessel density (MVD) in carcinomatous tissue, the enhancement curve of prostate tumors was shown to be different when compared to the PZ and BPH. Engelbrecht *et al*^[55] found that in both the PZ and TZ, the relative peak enhancement was the optimal parameter when compared to other parameters such as onset time, time to peak, peak enhancement and wash-out. Yoshizako *et al*^[61] stated that the addition of DCE-MRI to T2W images and DWI improved the specificity and positive predictive value of diagnosing TZ cancer (93.8% and 94.7%, respectively). Turnbull *et al*^[2] found significant differences in amplitude of the initial enhancement and wash-out patterns between carcinoma and BPH. In both the PZ and the central gland, relative peak enhancement was the optimal parameter. The combination of relative peak enhancement with other dynamic parameters (onset time, time to peak, peak enhancement, and washout) did not yield a significant gain in discriminatory performance. Ogura *et al*^[56] demonstrated a sensitivity, specificity and accuracy rate of 37%, 97% and 63%, respectively, for the detection of TZ cancer. In another study, it was shown that the glandular-ductal tissues had lower peak enhancement than the stromal-low ductal tissues suggesting that gadolinium-DTPA does not enter healthy prostatic tissues^[2]. Ren *et al*^[57] examined DCE-MRI parameters in 21 patients with prostate cancer and 29 patients with BPH by means of signal intensity-time curves and angiogenesis. Prostate cancer showed stronger enhancement with an earlier peak time, higher enhancement and enhancement rate. The vascular endothelial growth factor (VEGF) and MVD expression levels in cancer were higher than in BPH. They found a negative correlation between peak time and the expression levels of VEGF and MVD, however, the degree of enhancement and enhancement rate showed positive correlations.

In cancerous tissues, there is uncontrolled angiogenesis and the permeability of vascular structures is markedly

increased resulting in significantly different pharmacokinetics compared to surrounding normal tissue. Pharmacokinetic parameter mapping clearly identifies pathologic areas in heterogeneously enhanced prostate. K-trans maps enable the identification of tumor within heterogeneously enhanced PZ and can reveal the extent of extra-glandular involvement. These maps may also be useful in providing a biopsy target and in revealing intra-tumoral heterogeneity (Figure 4).

MRS

MRS imaging is an emerging technique used in combination with MRI in the evaluation of prostate cancer^[58-63]. This technique allows the metabolites within tissues to be identified and provides information on the biochemical and metabolic environment of tissues. As prostate is composed of different types of glands and tissues, it is difficult to study the gland using MRS. However; there are sophisticated chemical shift filtering techniques and three dimensional chemical shift imaging which allow examination of the entire prostate at one time and the selection of particular chemicals for diagnosis^[59,64]. It has been shown that stromal and glandular tissue have the same resonances with different relative peak height intensities^[65]. In addition, it has been stated that citrate is produced by glandular epithelial cells and the amount of glandular elements can affect tissue citrate levels. Glandular BPH has higher levels of citrate than stromal BPH^[66]. It has also been stated that citrate levels show the degree of tissue differentiation, in that poorly differentiated tumors have lower citrate levels than well differentiated tumors^[67]. Healthy PZ is known to have high citrate content, whereas in cancer tissues, the resonance signal from citrate is reduced or even absent. Adenocarcinomatous tissue in the prostate gland also shows a similar spectrum to adenocarcinoma in other organs (except for citrate)^[68], which show elevated choline relative to creatine due to the increased cell proliferation associated with malignant tumors^[69]. In their series performed in 40 patients, Zakian *et al*^[7] studied the mean values of choline + creatine/citrate, choline/creatinine and choline/citrate in TZ cancer

and normal tissue, in which a significant difference was found. It was shown that 56% of patients had tumor voxels with at least one detectable choline peak, while control voxels showed only choline peaks.

3.0-T MR imaging

High-field-strength MR imaging has recently been investigated in prostate imaging. The introduction of 3.0-T MR scanners has resulted in an increase in the in-plane resolution of anatomic T2W imaging due to higher signal to noise ratio. Higher magnetic field strengths have been shown to enable structural imaging of the prostate with improved spatial resolution leading to improved detection and staging of PZ tumors^[70-72]. Moreover, functional imaging such as DWI, DCE-MRI or MRS at high field strength is thought to improve the detection of CZ and TZ cancers, prevent false-positive diagnoses and help less experienced readers to improve their local staging performance^[73,74].

CONCLUSION

TZ cancers demonstrate similar imaging features to BPH and are therefore more difficult to diagnose on MR imaging. However, certain imaging features (alone or in combination) on multi-parametric MR imaging can help in the differentiation between cancerous and benign TZ tissue. MR imaging can also provide reliable local staging of TZ cancers. By the addition of emerging MR techniques, such as DWI, DCE-MRI, MRS and high-field-strength (3.0-T) MR imaging to standard T2W images, MR imaging has now become a promising technique in the evaluation of TZ tumors.

REFERENCES

- 1 **McNeal JE**, Redwine EA, Freiha FS, Stamey TA. Zonal distribution of prostatic adenocarcinoma. Correlation with histologic pattern and direction of spread. *Am J Surg Pathol* 1988; **12**: 897-906
- 2 **Turnbull LW**, Buckley DL, Turnbull LS, Liney GP, Knowles AJ. Differentiation of prostatic carcinoma and benign prostatic hyperplasia: correlation between dynamic Gd-DTPA-enhanced MR imaging and histopathology. *J Magn Reson Imaging* 1999; **9**: 311-316
- 3 **Tamada T**, Sone T, Nagai K, Jo Y, Gyoten M, Imai S, Kajihara Y, Fukunaga M. T2-weighted MR imaging of prostate cancer: multishot echo-planar imaging vs fast spin-echo imaging. *Eur Radiol* 2004; **14**: 318-325
- 4 **Akin O**, Sala E, Moskowitz CS, Kuroiwa K, Ishill NM, Pucar D, Scardino PT, Hricak H. Transition zone prostate cancers: features, detection, localization, and staging at endorectal MR imaging. *Radiology* 2006; **239**: 784-792
- 5 **Li H**, Sugimura K, Kaji Y, Kitamura Y, Fujii M, Hara I, Tachibana M. Conventional MRI capabilities in the diagnosis of prostate cancer in the transition zone. *AJR Am J Roentgenol* 2006; **186**: 729-742
- 6 **Yoshizako T**, Wada A, Hayashi T, Uchida K, Sumura M, Uchida N, Kitagaki H, Igawa M. Usefulness of diffusion-weighted imaging and dynamic contrast-enhanced magnetic resonance imaging in the diagnosis of prostate transition-zone cancer. *Acta Radiol* 2008; **49**: 1207-1213
- 7 **Zakian KL**, Eberhardt S, Hricak H, Shukla-Dave A, Kleinman S, Muruganandham M, Sircar K, Kattan MW, Reuter

- VE, Scardino PT, Koutcher JA. Transition zone prostate cancer: metabolic characteristics at 1H MR spectroscopic imaging--initial results. *Radiology* 2003; **229**: 241-247
- 8 **Stamey TA**, McNeal JE. Adenocarcinoma of the prostate. In: Walsh PC, Retik AB, Stamey TA, Vaughan ED, editors. *Campbell's Urology*. 6th ed. Philadelphia: WB Saunders, 1992: 643-658
- 9 **Older RA**, Watson LR. Ultrasound anatomy of the normal male reproductive tract. *J Clin Ultrasound* 1996; **24**: 389-404
- 10 **De Marzo AM**, Coffey DS, Nelson WG. New concepts in tissue specificity for prostate cancer and benign prostatic hyperplasia. *Urology* 1999; **53**: 29-39; discussion 39-42
- 11 **Hricak H**. The prostate gland. In: Hricak H, Carrington B, editors. *MRI of the pelvis*. London: Martin Dunitz, 1991: 249-311
- 12 **McNeal JE**. The prostate gland: morphology and pathology. *Monogr Urol* 1983; **4**: 5-13
- 13 **Engelbrecht MR**, Jager GJ, Laheij RJ, Verbeek AL, van Lier HJ, Barentsz JO. Local staging of prostate cancer using magnetic resonance imaging: a meta-analysis. *Eur Radiol* 2002; **12**: 2294-2302
- 14 **Jager GJ**, Ruijter ET, van de Kaa CA, de la Rosette JJ, Oosterhof GO, Thornbury JR, Barentsz JO. Local staging of prostate cancer with endorectal MR imaging: correlation with histopathology. *AJR Am J Roentgenol* 1996; **166**: 845-852
- 15 **Cornud F**, Hamida K, Flam T, H el enon O, Chr etien Y, Thiounn N, Correas JM, Casanova JM, Moreau JF. Endorectal color doppler sonography and endorectal MR imaging features of nonpalpable prostate cancer: correlation with radical prostatectomy findings. *AJR Am J Roentgenol* 2000; **175**: 1161-1168
- 16 **Cornud F**, Flam T, Chauveinc L, Hamida K, Chr etien Y, Vieillefond A, H el enon O, Moreau JF. Extraprostatic spread of clinically localized prostate cancer: factors predictive of pT3 tumor and of positive endorectal MR imaging examination results. *Radiology* 2002; **224**: 203-210
- 17 **Souli  M**, Aziza R, Escourrou G, Seguin P, Tollon C, Molinier L, Bachaud J, Joffre F, Plante P. Assessment of the risk of positive surgical margins with pelvic phased-array magnetic resonance imaging in patients with clinically localized prostate cancer: a prospective study. *Urology* 2001; **58**: 228-232
- 18 **Cruz M**, Tsuda K, Narumi Y, Kuroiwa Y, Nose T, Kojima Y, Okuyama A, Takahashi S, Aozasa K, Barentsz JO, Nakamura H. Characterization of low-intensity lesions in the peripheral zone of prostate on pre-biopsy endorectal coil MR imaging. *Eur Radiol* 2002; **12**: 357-365
- 19 **Hricak H**, Williams RD, Spring DB, Moon KL Jr, Hedgcock MW, Watson RA, Crooks LE. Anatomy and pathology of the male pelvis by magnetic resonance imaging. *AJR Am J Roentgenol* 1983; **141**: 1101-1110
- 20 **Shimizu T**, Nishie A, Ro T, Tajima T, Yamaguchi A, Kono S, Honda H. Prostate cancer detection: the value of performing an MRI before a biopsy. *Acta Radiol* 2009; **50**: 1080-1088
- 21 **Claus FG**, Hricak H, Hattery RR. Pretreatment evaluation of prostate cancer: role of MR imaging and 1H MR spectroscopy. *Radiographics* 2004; **24** Suppl 1: S167-S180
- 22 **Schiebler ML**, Tomaszewski JE, Bezzi M, Pollack HM, Kressel HY, Cohen EK, Altman HG, Geftter WB, Wein AJ, Axel L. Prostatic carcinoma and benign prostatic hyperplasia: correlation of high-resolution MR and histopathologic findings. *Radiology* 1989; **172**: 131-137
- 23 **Muramoto S**, Uematsu H, Kimura H, Ishimori Y, Sadato N, Oyama N, Matsuda T, Kawamura Y, Yonekura Y, Okada K, Itoh H. Differentiation of prostate cancer from benign prostate hypertrophy using dual-echo dynamic contrast MR imaging. *Eur J Radiol* 2002; **44**: 52-58
- 24 **McNeal JE**, Bostwick DG, Kindrachuk RA, Redwine EA, Freiha FS, Stamey TA. Patterns of progression in prostate cancer. *Lancet* 1986; **1**: 60-63
- 25 **Stamey TA**, Donaldson AN, Yemoto CE, McNeal JE, S ozen S, Gill H. Histological and clinical findings in 896 consecutive prostates treated only with radical retropubic prostatec-

- tomy: epidemiologic significance of annual changes. *J Urol* 1998; **160**: 2412-2417
- 26 **Augustin H**, Erbersdobler A, Graefen M, Fernandez S, Palisaar J, Huland H, Hammerer P. Biochemical recurrence following radical prostatectomy: a comparison between prostate cancers located in different anatomical zones. *Prostate* 2003; **55**: 48-54
 - 27 **Pavelić J**, Zeljko Z, Bosnar MH. Molecular genetic aspects of prostate transition zone lesions. *Urology* 2003; **62**: 607-613
 - 28 **Liu IJ**, Macy M, Lai YH, Terris MK. Critical evaluation of the current indications for transition zone biopsies. *Urology* 2001; **57**: 1117-1120
 - 29 **Pollack HM**. Imaging of the prostate gland. *Eur Urol* 1991; **20** Suppl 1: 50-58
 - 30 **Grossfeld GD**, Coakley FV. Benign prostatic hyperplasia: clinical overview and value of diagnostic imaging. *Radiol Clin North Am* 2000; **38**: 31-47
 - 31 **Ling D**, Lee JK, Heiken JP, Balfe DM, Glazer HS, McClellan BL. Prostatic carcinoma and benign prostatic hyperplasia: inability of MR imaging to distinguish between the two diseases. *Radiology* 1986; **158**: 103-107
 - 32 **Poon PY**, McCallum RW, Henkelman MM, Bronskill MJ, Sutcliffe SB, Jewett MA, Rider WD, Bruce AW. Magnetic resonance imaging of the prostate. *Radiology* 1985; **154**: 143-149
 - 33 **Ellis JH**, Tempany C, Sarin MS, Gatsonis C, Rifkin MD, McNeil BJ. MR imaging and sonography of early prostatic cancer: pathologic and imaging features that influence identification and diagnosis. *AJR Am J Roentgenol* 1994; **162**: 865-872
 - 34 **Sciara A**, Panebianco V, Ciccariello M, Salciccia S, Cattarino S, Lisi D, Gentilucci A, Alfaroni A, Bernardo S, Passariello R, Gentile V. Value of magnetic resonance spectroscopy imaging and dynamic contrast-enhanced imaging for detecting prostate cancer foci in men with prior negative biopsy. *Clin Cancer Res* 2010; **16**: 1875-1883
 - 35 **Bammer R**. Basic principles of diffusion-weighted imaging. *Eur J Radiol* 2003; **45**: 169-184
 - 36 **Chenevert TL**, Stegman LD, Taylor JM, Robertson PL, Greenberg HS, Rehemtulla A, Ross BD. Diffusion magnetic resonance imaging: an early surrogate marker of therapeutic efficacy in brain tumors. *J Natl Cancer Inst* 2000; **92**: 2029-2036
 - 37 **Sato C**, Naganawa S, Nakamura T, Kumada H, Miura S, Takizawa O, Ishigaki T. Differentiation of noncancerous tissue and cancer lesions by apparent diffusion coefficient values in transition and peripheral zones of the prostate. *J Magn Reson Imaging* 2005; **21**: 258-262
 - 38 **Kozlowski P**, Chang SD, Jones EC, Berean KW, Chen H, Goldenberg SL. Combined diffusion-weighted and dynamic contrast-enhanced MRI for prostate cancer diagnosis--correlation with biopsy and histopathology. *J Magn Reson Imaging* 2006; **24**: 108-113
 - 39 **Tanimoto A**, Nakashima J, Kohno H, Shinmoto H, Kuribayashi S. Prostate cancer screening: the clinical value of diffusion-weighted imaging and dynamic MR imaging in combination with T2-weighted imaging. *J Magn Reson Imaging* 2007; **25**: 146-152
 - 40 **desouza NM**, Reinsberg SA, Scurr ED, Brewster JM, Payne GS. Magnetic resonance imaging in prostate cancer: the value of apparent diffusion coefficients for identifying malignant nodules. *Br J Radiol* 2007; **80**: 90-95
 - 41 **Noworolski SM**, Vigneron DB, Chen AP, Kurhanewicz J. Dynamic contrast-enhanced MRI and MR diffusion imaging to distinguish between glandular and stromal prostatic tissues. *Magn Reson Imaging* 2008; **26**: 1071-1080
 - 42 **Kim JH**, Kim JK, Park BW, Kim N, Cho KS. Apparent diffusion coefficient: prostate cancer versus noncancerous tissue according to anatomical region. *J Magn Reson Imaging* 2008; **28**: 1173-1179
 - 43 **Reinsberg SA**, Payne GS, Riches SF, Ashley S, Brewster JM, Morgan VA, deSouza NM. Combined use of diffusion-weighted MRI and 1H MR spectroscopy to increase accuracy in prostate cancer detection. *AJR Am J Roentgenol* 2007; **188**: 91-98
 - 44 **Yoshimitsu K**, Kiyoshima K, Irie H, Tajima T, Asayama Y, Hirakawa M, Ishigami K, Naito S, Honda H. Usefulness of apparent diffusion coefficient map in diagnosing prostate carcinoma: correlation with stepwise histopathology. *J Magn Reson Imaging* 2008; **27**: 132-139
 - 45 **Namiki T**, Koyama K, Tanaka H, Ohmura M, Harada J, Fukuda K. Effect of diffusion-weighted imaging with very high b-factors for detection of prostate cancer. In: Proceedings of the Radiological Society of North America annual meeting. Chicago, 2005: 649
 - 46 **Oto A**, Kayhan A, Tretiakova M, Yang C, Jiang Y, Stadler WM. Role of DWI and DCE-MRI to Distinguish Transitional Zone Prostate Cancer from Benign Prostatic Hyperplasia. In: Proceedings of the Radiologic Society of North America annual meeting. Chicago, 2009
 - 47 **Tamada T**, Sone T, Jo Y, Tshimitsu S, Yamashita T, Yamamoto A, Tanimoto D, Ito K. Apparent diffusion coefficient values in peripheral and transition zones of the prostate: comparison between normal and malignant prostatic tissues and correlation with histologic grade. *J Magn Reson Imaging* 2008; **28**: 720-726
 - 48 **Ren J**, Huan Y, Wang H, Zhao H, Ge Y, Chang Y, Liu Y. Diffusion-weighted imaging in normal prostate and differential diagnosis of prostate diseases. *Abdom Imaging* 2008; **33**: 724-728
 - 49 **Shinmoto H**, Oshio K, Tanimoto A, Higuchi N, Okuda S, Kuribayashi S, Mulkern RV. Biexponential apparent diffusion coefficients in prostate cancer. *Magn Reson Imaging* 2009; **27**: 355-359
 - 50 **Preziosi P**, Orlacchio A, Di Giambattista G, Di Renzi P, Bortolotti L, Fabiano A, Cruciani E, Pasqualetti P. Enhancement patterns of prostate cancer in dynamic MRI. *Eur Radiol* 2003; **13**: 925-930
 - 51 **Rouvière O**, Raudrant A, Ecochard R, Colin-Pangaud C, Pasquiou C, Bouvier R, Maréchal JM, Lyonnet D. Characterization of time-enhancement curves of benign and malignant prostate tissue at dynamic MR imaging. *Eur Radiol* 2003; **13**: 931-942
 - 52 **Hara N**, Okuizumi M, Koike H, Kawaguchi M, Bilim V. Dynamic contrast-enhanced magnetic resonance imaging (DCE-MRI) is a useful modality for the precise detection and staging of early prostate cancer. *Prostate* 2005; **62**: 140-147
 - 53 **Padhani AR**, Gapinski CJ, Macvicar DA, Parker GJ, Suckling J, Revell PB, Leach MO, Dearnaley DP, Husband JE. Dynamic contrast enhanced MRI of prostate cancer: correlation with morphology and tumour stage, histological grade and PSA. *Clin Radiol* 2000; **55**: 99-109
 - 54 **Jackson AS**, Reinsberg SA, Sohaib SA, Charles-Edwards EM, Jhavar S, Christmas TJ, Thompson AC, Bailey MJ, Corbishley CM, Fisher C, Leach MO, Dearnaley DP. Dynamic contrast-enhanced MRI for prostate cancer localization. *Br J Radiol* 2009; **82**: 148-156
 - 55 **Engelbrecht MR**, Huisman HJ, Laheij RJ, Jager GJ, van Leenders GJ, Hulsbergen-Van De Kaa CA, de la Rosette JJ, Blickman JG, Barentsz JO. Discrimination of prostate cancer from normal peripheral zone and central gland tissue by using dynamic contrast-enhanced MR imaging. *Radiology* 2003; **229**: 248-254
 - 56 **Ogura K**, Maekawa S, Okubo K, Aoki Y, Okada T, Oda K, Watanabe Y, Tsukayama C, Arai Y. Dynamic endorectal magnetic resonance imaging for local staging and detection of neurovascular bundle involvement of prostate cancer: correlation with histopathologic results. *Urology* 2001; **57**: 721-726
 - 57 **Ren J**, Huan Y, Wang H, Chang YJ, Zhao HT, Ge YL, Liu Y, Yang Y. Dynamic contrast-enhanced MRI of benign prostatic hyperplasia and prostatic carcinoma: correlation with angiogenesis. *Clin Radiol* 2008; **63**: 153-159
 - 58 **Kurhanewicz J**, Vigneron DB, Hricak H, Parivar F, Nelson

- SJ, Shinohara K, Carroll PR. Prostate cancer: metabolic response to cryosurgery as detected with 3D H-1 MR spectroscopic imaging. *Radiology* 1996; **200**: 489-496
- 59 **Kurhanewicz J**, Vigneron DB, Nelson SJ. Three-dimensional magnetic resonance spectroscopic imaging of brain and prostate cancer. *Neoplasia* 2000; **2**: 166-189
- 60 **Scheidler J**, Hricak H, Vigneron DB, Yu KK, Sokolov DL, Huang LR, Zaloudek CJ, Nelson SJ, Carroll PR, Kurhanewicz J. Prostate cancer: localization with three-dimensional proton MR spectroscopic imaging--clinicopathologic study. *Radiology* 1999; **213**: 473-480
- 61 **Yacoe ME**, Sommer G, Peehl D. In vitro proton spectroscopy of normal and abnormal prostate. *Magn Reson Med* 1991; **19**: 429-438
- 62 **Schick F**, Bongers H, Kurz S, Jung WI, Pfeffer M, Lutz O. Localized proton MR spectroscopy of citrate in vitro and of the human prostate in vivo at 1.5 T. *Magn Reson Med* 1993; **29**: 38-43
- 63 **Mountford C**, Lean C, Malycha P, Russell P. Proton spectroscopy provides accurate pathology on biopsy and in vivo. *J Magn Reson Imaging* 2006; **24**: 459-477
- 64 **Schulte RF**, Trabesinger AH, Boesiger P. Chemical-shift-selective filter for the in vivo detection of J-coupled metabolites at 3T. *Magn Reson Med* 2005; **53**: 275-281
- 65 **Swindle P**, McCredie S, Russell P, Himmelreich U, Khadra M, Lean C, Mountford C. Pathologic characterization of human prostate tissue with proton MR spectroscopy. *Radiology* 2003; **228**: 144-151
- 66 **Costello LC**, Franklin RB. Aconitase activity, citrate oxidation, and zinc inhibition in rat ventral prostate. *Enzyme* 1981; **26**: 281-287
- 67 **Kurhanewicz J**, Dahiya R, Macdonald JM, Chang LH, James TL, Narayan P. Citrate alterations in primary and metastatic human prostatic adenocarcinomas: 1H magnetic resonance spectroscopy and biochemical study. *Magn Reson Med* 1993; **29**: 149-157
- 68 **Mountford CE**, Doran S, Lean CL, Russell P. Proton MRS can determine the pathology of human cancers with a high level of accuracy. *Chem Rev* 2004; **104**: 3677-3704
- 69 **Daly PF**, Lyon RC, Faustino PJ, Cohen JS. Phospholipid metabolism in cancer cells monitored by 31P NMR spectroscopy. *J Biol Chem* 1987; **262**: 14875-14878
- 70 **Fütterer JJ**, Heijmink SW, Scheenen TW, Jager GJ, Hulsbergen-Van de Kaa CA, Witjes JA, Barentsz JO. Prostate cancer: local staging at 3-T endorectal MR imaging--early experience. *Radiology* 2006; **238**: 184-191
- 71 **Morakkabati-Spitz N**, Bastian PJ, Gieseke J, Träber F, Kuhl CK, Wattjes MP, Müller SC, Schild HH. MR imaging of the prostate at 3.0T with external phased array coil - preliminary results. *Eur J Med Res* 2008; **13**: 287-291
- 72 **Turkbey B**, Pinto PA, Mani H, Bernardo M, Pang Y, McKinney YL, Khurana K, Ravizzini GC, Albert PS, Merino MJ, Choyke PL. Prostate cancer: value of multiparametric MR imaging at 3 T for detection--histopathologic correlation. *Radiology* 2010; **255**: 89-99
- 73 **Kim CK**, Park BK, Han JJ, Kang TW, Lee HM. Diffusion-weighted imaging of the prostate at 3 T for differentiation of malignant and benign tissue in transition and peripheral zones: preliminary results. *J Comput Assist Tomogr* 2007; **31**: 449-454
- 74 **Kim CK**, Park BK, Park W, Kim SS. Prostate MR imaging at 3T using a phased-arrayed coil in predicting locally recurrent prostate cancer after radiation therapy: preliminary experience. *Abdom Imaging* 2010; **35**: 246-252

S- Editor Cheng JX L- Editor Webster JR E- Editor Zheng XM

A review on dural tail sign

Houman Sotoudeh, Hadi Rokni Yazdi

Houman Sotoudeh, Department of Radiology, Vali Asr Hospital, Arak University of Medical Sciences, Vali Asr Sq, 38137, Arak, Iran

Hadi Rokni Yazdi, Department of Radiology, Imam Khomeini Hospital, Tehran University of Medical Sciences, Keshavarz Blvd, 1419733141 Tehran, Iran

Author contributions: Sotoudeh H wrote the article; Rokni HR got supervision on the manuscript.

Correspondence to: Hadi Rokni Yazdi, Associated Professor, Department of Radiology, Imam Khomeini Hospital, Tehran University of Medical Sciences, Keshavarz Blvd, 1419733141 Tehran, Iran. hadirokni@yahoo.com

Telephone: +98-21-88953001 **Fax:** +98-21-66404377

Received: March 17, 2010 **Revised:** May 3, 2010

Accepted: May 10, 2010

Published online: May 28, 2010

Sotoudeh H, Yazdi HR. A review on dural tail sign. *World J Radiol* 2010; 2(5): 188-192 Available from: URL: <http://www.wjgnet.com/1949-8470/full/v2/i5/188.htm> DOI: <http://dx.doi.org/10.4329/wjr.v2.i5.188>

HISTORY AND DEFINITION

“Dural tail sign” (DTS), “dural thickening”, “flare sign”, “meningeal sign” are similar terms describing thickening of the dura adjacent to an intracranial neoplasm on contrast-enhanced T1 MR images (Figures 1 and 2). Although this sign has been used in spinal meningioma in the literature, we only use it for intracranial lesions^[1]. Nowadays the term DTS is frequently used as in this article. The above-mentioned terms were first described in meningioma by Wilms *et al*^[2] in 1989. In 1990 the triple criteria for DTS were established by Goldsher *et al*^[3] as: (1) Presence of at least two consecutive sections through the tumor at the same site in more than one imaging plane; (2) Greatest thickness adjacent to the tumor and tapering away from it; and (3) Enhancement more intense than that of the tumor itself.

The criteria established by Goldsher *et al*^[3] are still the most useful in describing DTS. Nowadays, as imaging slices tend to be less than 5 mm, there should always be at least three sections showing the dural tail, depending on the slice thickness^[4].

No equivalent sign has been described in post-contrast CT scans. Post-contrast CT can show dural thickening in 8% of MR proven DTS^[3,5].

Takeguchi *et al*^[6] evaluated the “dural tail” associated with 48 intracranial meningiomas on fluid-attenuated inversion-recovery (FLAIR) and contrast-enhanced T1-weighted images. They noted that the DTS, which was identified on contrast-enhanced magnetic resonance imaging (MRI), was also observed in all the cases of DTS on FLAIR images, and concluded that FLAIR imaging is useful for showing dural abnormalities associated with meningiomas without the need for contrast medium.

Abstract

“Dural tail sign” (DTS) which is a thickening of the dura adjacent to an intracranial pathology on contrast-enhanced T1 MR Images, was first thought to be pathognomonic of meningioma, however, many subsequent studies demonstrated this sign adjacent to various intra- and extra-cranial pathologies and in spinal lesions. In this paper we outline the history, accompanying pathologies and the differentiation and probable pathophysiology of DTS. We also discuss whether we can predict tumoral involvement of the dural tail before surgery and whether the dural tail adjacent to a tumor should be resected.

© 2010 Baishideng. All rights reserved.

Key words: Dural tail sign; Histopathology; Magnetic resonance imaging; Meningioma

Peer reviewers: Mohamed Abou El-Ghar, MD, Department of Radiology, Urology and Nephrology Center-Mansoura University, 72 El-gomhoria St, Mansoura, 35516, Egypt; Feng Chen, MD, PhD, Professor, Department of Radiology, Zhong Da Hospital, Southeast University, 87 Ding Jiaqiao, Nanjing 210009, Jiangsu Province, China

DTS PATHOLOGIES AND THEIR DIFFERENTIAL DIAGNOSIS

At the time of DTS description and criteria formation, DTS was thought to be pathognomonic of meningioma, however, many subsequent studies also demonstrated this sign adjacent to various intra- and extra-cranial pathologies as well as spinal lesions.

So far, DTS has been reported in primary and secondary central nervous system (CNS) lymphoma, chloroma, metastasis (extra- and intra-axial), multiple myeloma, glioblastoma multiforme (GBM), aspergillosis, chordoma, schwannoma, pleomorphic xanthoastrocytoma (PMX), hemangiopericytoma, Wegener's granulomatosis, sarcoidosis, medulloblastoma, eosinophilic granuloma, pituitary adenoma, pituitary apoplexy, and Erdheim-Chester disease^[7-24]. DTS can be seen in all locations of the dura adjacent to meningioma in the falx, tentorium and cerebral convexities^[3,25]. DTS is less frequently seen in posterior fossa and cystic meningioma^[5]. Meningioma in the cerebellopontine (CPA) can show DTS extending to the internal auditory canal and can be mistaken for an acoustic neuroma^[26]. CPA meningiomas sometimes show the DTS but with less enhancement than the primary tumor itself. Previous studies indicated that the DTS has a sensitivity of 58.6% and a specificity of 94.02% for the diagnosis of meningioma^[5]. Primary CNS lymphoma is most frequently caused by B cell lymphoma and can be dural-based and can be mistaken for meningioma because of homogenous enhancement and typical DTS. Hodgkin lymphoma is a very rare tumor and can mimic meningioma in T1 enhanced MRI because of a dural-based lesion and DTS^[6,8,27,28]. Dural-based metastasis and cortical intraparenchymal metastasis can show DTS. DTS is most often seen in prostate and neuroblastoma metastasis but has been reported in papillary adenocarcinoma, bronchogenic tumors and nasopharynx neoplasms^[8,29].

GBM as one of the most frequent intraparenchymal tumors, can extend to the dura and rarely shows dural thickening and DTS. So far no case with tumoral involvement of DTS has been reported in patients suffering from GBM with DTS^[8,30].

Adenoid cystic carcinoma, a neoplasm arising from the salivary glands can involve intracranial structures by perineural spread. Dural involvement and DTS have also been reported in this neoplasm^[4,10].

Chloroma can mimic meningioma because of dural mass and typical DTS^[31]. Hemangiopericytoma can mimic meningioma with positive DTS on imaging but its aggressive behavior, loss of calcification and heterogenous enhancement can differentiate it from meningioma^[11].

Intracranial chordoma is seen more often in sphenoidal and occipital regions. DTS has been rarely reported in intracranial chordoma^[13].

An acoustic neuroma arises from the vestibular portion of the 8th cranial nerve and can locate in the acoustic canal, CP angle or both. CPA acoustic neuroma can mimic meningioma as an extra-axial mass lesion with positive



Figure 1 A 65-year-old woman with meningioma and adjacent hyperostosis. Arrows indicates "dural tail sign".

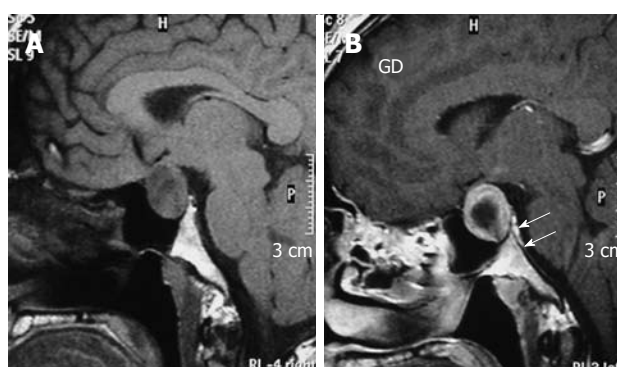


Figure 2 Imaging findings of pituitary macroadenoma. A: T1W sagittal MRI of brain shows a Pituitary macro-adenoma with extension to the suprasellar cistern; B: After gadolinium injection enhancement is noted in periphery of tumour and dura of dorsum sella (arrows), enhancement is greater than that of the tumour itself. Biopsy proved prolactinoma.

DTS, but its hypersignal intensity in T2 sequence and narrower dural attachment can differentiate this tumor from meningioma^[14,32,33].

Intraparenchymal schwannoma is a relatively uncommon neoplasm and DTS has been reported in one case of intraparenchymal schwannoma^[34].

PMX, which is more often seen in cortical regions, typically contains a prominent cystic component and a mural nodule, and sometimes involves the adjacent dura and shows positive DTS but its cystic component, mural nodule and T2 signal should differentiate it from meningioma^[15,35].

Wegener's granulomatosis can involve the dura and intracranial structures and presents with positive DTS adjacent to the PNS sinuses^[17,36].

Erdheim-Chester disease, a histiocytic granulomatosis with both intra- and extra-axial structures involvement, has been reported to show positive DTS in post-contrast T1. DTS has also been reported in other granulomatosis diseases (eosinophilic granulomatosis and sarcoidosis)^[18,24,37].

Although most authors believe that the DTS adjacent to a sellar mass suggests meningioma, dural thickenings and positive DTS can be seen adjacent to pituitary ad-

enomas in 30% of cases. This sign mostly extends into the planum sphenoidale and carotid sulcus. DTS can also be detected adjacent to pituitary apoplexy^[13,19,21,38]. The pituitary gland can be involved in an inflammatory process (hypophysitis). Hypophysitis is rarely reported to present with positive DTS^[20].

Gumma, an inflammatory involvement of CNS structures in tertiary syphilis, is seen as an intra-axial peripherally located mass lesion, however, extra-axial mass lesions have been reported and can show DTS mimicking meningioma in these lesions^[7,39].

Cavernous hemangioma rarely arises from the dura mater, causing adjacent dural thickening and DTS. Dural cavernous hemangioma mostly involves the sinus cavernous dura^[25].

DTS has also been reported adjacent to a posterior cerebral artery aneurysm and in one case of post-operative cerebral aspergillosis^[10,22].

Positive DTS has been reported in three cases of medulloblastoma^[40,41], two cases of multiple myeloma presenting with extra-axial dural tumors^[42,43], one case of primary rhabdomyosarcoma^[44], one case of solitary fibrous tumor^[45] and one case of papillary middle ear tumor with dural invasion^[7].

PATHOPHYSIOLOGY

In contrast to the worldwide accepted diagnostic criteria of DTS, its pathophysiology has not been uniformly established.

It should be noted that DTS is not always due to enhancement of the dura adjacent to tumors. Kuroiwa *et al.*^[46] reported a glioma extending into the subarachnoid space, and a meningioma extending to the subdural space and their MRI appearances mimicked the DTS^[46].

Wilms *et al.*^[2] first reported that thickening of the dura mater represented neoplastic infiltration in or on the surface of the dura in three cases of meningioma with DTS, and described the DTS as indicating tumor invasion. On the other hand, Tokumaru *et al.*^[47] found only increased loose connective tissue, hypervascularity and dilated vessels on histologic examination of the enhanced meninges adjacent to four meningiomas. Although two patients showed tumor cell infiltration of the dura mater in this study, tumor cell infiltration was restricted to within 1 mm of the junction of the dura with the meningioma, therefore it was suggested that the dural tail mainly represented reactive changes to the meningioma and not necessarily neoplastic involvement. Subsequently several other histologic studies of the dural tail were described as reactive changes^[8,25,26]. Kawahara *et al.*^[48] examined the point of attachment of the tumor and the adjacent dura mater in seven patients with DTS and suggested the pathophysiology of the DTS as follow; “initially tumour cells invade vessels and pack them at the point of tumour attachment; then, vessel congestion is induced in the adjacent dura mater, as a result of which it enhances markedly, giving rise to the DTS”. In a histological study on 17 patients with DTS, Rokni-Yazdi *et al.*^[49] reported

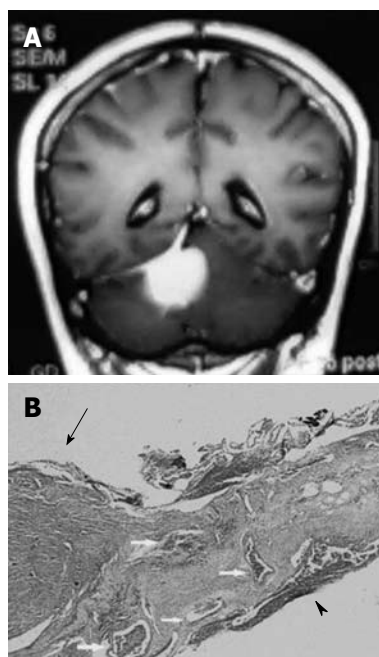


Figure 3 Pathological finding of dural tail sign. A: A 58-year-old female with a tentorial meningioma and dural tail sign; B: Pathology specimen in this case showed a meningioma (arrow) and the attached dura. The dural tail is noted on the right side of the figure (arrowhead). Both the dura beneath the tumor and dural tail contain dilated blood vessels (arrow). There is no dural invasion. HE 30 ×.

that vascular dilatation was seen in all dural tails which is similar to that of Kawahara *et al.*^[48]; however, unlike Kawahara’s study, tumoral invasion of the dura at its point of attachment to the tumor was only reported in 34.1% of cases, so 65.9% of cases did not have invasion and packing of vessels at the point of dural attachment (Figure 3). This was against the Kawahara *et al.*^[48] hypothesis regarding the etiology of DTS in all cases; although it may explain the etiology of DTS in those cases with invasion of the dura beneath the tumor. We suggest that invasion of dural vessels by tumor cells and packing at the point of tumor attachment, reactive hypervascularity and tumoral invasion of the dura are three different pathophysiologies of the DTS. Since its description in 1989, only about 80 DTS have been pathologically evaluated and of this relatively small number of pathologic exams, the DTS has been involved with tumoral cells in more than 50% of published examinations and the rest of the pathologic examinations have described vascular congestion and inflammation^[2,3,5,25,26,47-51].

IMAGE PREDICTION OF TUMORAL INVOLVEMENT IN DTS

Takeguchi *et al.*^[6] in their study on “dural tail” associated with 48 intracranial meningiomas on FLAIR and contrast-enhanced T1-weighted images, evaluated the histology of five cases with abnormal dura mater.

The dural tail was resected, and infiltration of tumor cells and the changes in reactivity were assessed pathologically and compared to the MRI findings.

The results suggested that in the patient without tumor infiltration, the signal of the dural tail was very high on contrast-enhanced T1-weighted and FLAIR images^[6]. Rokni-Yazdi *et al*^[49] in their study on 129 patients with intracranial lesions in which the histology of 17 cases with DTS was evaluated and compared with contrast-enhanced T1 weighted MRI findings, found that pre-operative clinical and imaging criteria did not predict the tumoral involvement of DTS.

Age, sex of patient, pattern of enhancement after contrast injection, size of primary neoplasm and the size of the DTS itself could not predict tumoral invasion into the DTS^[49]. It is controversial as to whether the dura mater showing the tail sign should be resected to prevent recurrence. Kawahara *et al*^[48] suggested that removal of the DTS is not a significant factor in recurrence of meningioma. Rokni-Yazdi *et al*^[49] in their study on a limited number of patients with extra-axial tumor and DTS showed that if the dura below the tumor showed tumoral cells involvement, the dural tail was also involved and if the dura below the primary tumor was free of tumoral cells, the dural tail was also spared. Because of this strong correlation, the authors suggested that in the case of extra-axial tumoral resection without dural tail resection, if the dura below the tumor has tumoral cells involvement then the risk of recurrence may increase. However, further studies are needed to confirm this.

CONCLUSION

DTS is not pathognomonic of meningioma, and various intra- and extra-cranial as well as spinal pathologies can present with this sign on contrast-enhanced T1 MR Images. DTS can also be found on FLAIR images in nearly all cases of DTS proven by contrast-enhanced T1-weighted images. However, post-contrast CT can only show dural thickening in a minority of MR proven DTS.

DTS is not always due to enhancement of the dura adjacent to tumors. There are reports of tumors extending into the subarachnoid and subdural spaces which can mimic the DTS on contrast-enhanced T1 MR Images. DTS has been involved with tumoral cells in more than 50% of published examinations and the remaining pathologic examinations have described vascular congestion and inflammation. There is still controversy as to whether pre-operative criteria can predict tumoral involvement of DTS and whether surgical resection of DTS is mandatory.

REFERENCES

- Liu WC, Choi G, Lee SH, Han H, Lee JY, Jeon YH, Park HS, Park JY, Paeng SS. Radiological findings of spinal schwannomas and meningiomas: focus on discrimination of two disease entities. *Eur Radiol* 2009; **19**: 2707-2715
- Wilms G, Lammens M, Marchal G, Van Calenbergh F, Plets C, Van Fraeyenhoven L, Baert AL. Thickening of dura surrounding meningiomas: MR features. *J Comput Assist Tomogr* 1989; **13**: 763-768
- Goldsher D, Litt AW, Pinto RS, Bannon KR, Kricheff II. Dural "tail" associated with meningiomas on Gd-DTPA-enhanced MR images: characteristics, differential diagnostic value, and possible implications for treatment. *Radiology* 1990; **176**: 447-450
- Guermazi A, Lafitte F, Miaux Y, Adem C, Bonneville JF, Chiras J. The dural tail sign--beyond meningioma. *Clin Radiol* 2005; **60**: 171-188
- Rokni-Yazdi H, Sotoudeh H. Prevalence of "dural tail sign" in patients with different intracranial pathologies. *Eur J Radiol* 2006; **60**: 42-45
- Takeguchi T, Miki H, Shimizu T, Kikuchi K, Mochizuki T, Ohue S, Ohnishi T. The dural tail of intracranial meningiomas on fluid-attenuated inversion-recovery images. *Neuro-radiology* 2004; **46**: 130-135
- Bourekas EC, Wildenhain P, Lewin JS, Tarr RW, Dastur KJ, Raji MR, Lanzieri CF. The dural tail sign revisited. *AJNR Am J Neuroradiol* 1995; **16**: 1514-1516
- Wilms G, Lammens M, Marchal G, Demaerel P, Verplancke J, Van Calenbergh F, Goffin J, Plets C, Baert AL. Prominent dural enhancement adjacent to nonmeningiomatic malignant lesions on contrast-enhanced MR images. *AJNR Am J Neuroradiol* 1991; **12**: 761-764
- Tien RD, Yang PJ, Chu PK. "Dural tail sign": a specific MR sign for meningioma? *J Comput Assist Tomogr* 1991; **15**: 64-66
- Morioka T, Matsushima T, Ikezaki K, Nagata S, Ohta M, Hasuo K, Fukui M. Intracranial adenoid cystic carcinoma mimicking meningioma: report of two cases. *Neuroradiology* 1993; **35**: 462-465
- Chiechi MV, Smirniotopoulos JG, Mena H. Intracranial hemangiopericytomas: MR and CT features. *AJNR Am J Neuroradiol* 1996; **17**: 1365-1371
- Meltzer CC, Fukui MB, Kanal E, Smirniotopoulos JG. MR imaging of the meninges. Part I. Normal anatomic features and nonneoplastic disease. *Radiology* 1996; **201**: 297-308
- Nakasu Y, Nakasu S, Ito R, Mitsuya K, Fujimoto O, Saito A. Tentorial enhancement on MR images is a sign of cavernous sinus involvement in patients with sellar tumors. *AJNR Am J Neuroradiol* 2001; **22**: 1528-1533
- Kutcher TJ, Brown DC, Maurer PK, Ghaed VN. Dural tail adjacent to acoustic neuroma: MR features. *J Comput Assist Tomogr* 1991; **15**: 669-670
- Pierallini A, Bonamini M, Di Stefano D, Siciliano P, Bozzao L. Pleomorphic xanthoastrocytoma with CT and MRI appearance of meningioma. *Neuroradiology* 1999; **41**: 30-34
- Sandhu FA, Schellinger D, Martuza RL. A vascular sarcoïd mass mimicking a convexity meningioma. *Neuroradiology* 2000; **42**: 195-198
- Weinberger LM, Cohen ML, Remler BF, Naheedy MH, Leigh RJ. Intracranial Wegener's granulomatosis. *Neurology* 1993; **43**: 1831-1834
- Okamoto K, Ito J, Furusawa T, Sakai K, Tokiguchi S. Imaging of calvarial eosinophil granuloma. *Neuroradiology* 1999; **41**: 723-728
- Celli P, Cervoni L, Cantore G. Dural tail in pituitary adenoma. *J Neuroradiol* 1997; **24**: 68-69
- Ahmadi J, Meyers GS, Segall HD, Sharma OP, Hinton DR. Lymphocytic adenohypophysitis: contrast-enhanced MR imaging in five cases. *Radiology* 1995; **195**: 30-34
- Koenigsberg RA, Patil K. Pituitary apoplexy associated with dural (tail) enhancement. *AJR Am J Roentgenol* 1994; **163**: 227-228
- Good CD, Kingsley DP, Taylor WJ, Harkness WF. "Dural tail" adjacent to a giant posterior cerebral artery aneurysm: case report and review of the literature. *Neuroradiology* 1997; **39**: 577-580
- Shen WC, Chenn CA, Hsue CT, Lin TY. Dural cavernous angioma mimicking a meningioma and causing facial pain. *J Neuroimaging* 2000; **10**: 183-185
- Tien RD, Brasch RC, Jackson DE, Dillon WP. Cerebral Erdheim-Chester disease: persistent enhancement with Gd-DTPA on MR images. *Radiology* 1989; **172**: 791-792

- 25 **Nägele T**, Petersen D, Klose U, Grodd W, Opitz H, Voigt K. The "dural tail" adjacent to meningiomas studied by dynamic contrast-enhanced MRI: a comparison with histopathology. *Neuroradiology* 1994; **36**: 303-307
- 26 **Aoki S**, Sasaki Y, Machida T, Tanioka H. Contrast-enhanced MR images in patients with meningioma: importance of enhancement of the dura adjacent to the tumor. *AJNR Am J Neuroradiol* 1990; **11**: 935-938
- 27 **Lee JH**, Lee HK, Choi CT, Huh J. Mucosa-associated lymphoid tissue lymphoma of the pituitary gland: MR imaging features. *AJNR Am J Neuroradiol* 2002; **23**: 838-840
- 28 **Johnson MD**, Kinney MC, Scheithauer BW, Briley RJ, Hamilton K, McPherson WF, Barton JH Jr. Primary intracerebral Hodgkin's disease mimicking meningioma: case report. *Neurosurgery* 2000; **47**: 454-456; discussion 456-457
- 29 **Bendszus M**, Warmuth-Metz M, Burger R, Klein R, Tonn JC, Solymosi L. Diagnosing dural metastases: the value of 1H magnetic resonance spectroscopy. *Neuroradiology* 2001; **43**: 285-289
- 30 **Gupta S**, Gupta RK, Banerjee D, Gujral RB. Problems with the "dural tail" sign. *Neuroradiology* 1993; **35**: 541-542
- 31 **Fitoz S**, Atasoy C, Yavuz K, Gozdasoglu S, Erden I, Akyar S. Granulocytic sarcoma. Cranial and breast involvement. *Clin Imaging* 2002; **26**: 166-169
- 32 **Lunardi P**, Mastronardi L, Nardacci B, Acqui M, Fortuna A. "Dural tail" adjacent to acoustic neuroma on MRI: a case report. *Neuroradiology* 1993; **35**: 270-271
- 33 **Noguchi Y**, Komatsuzaki A, Yamada I, Okuno H, Haraguchi H. Vestibular schwannoma showing a dural tail on contrast-enhanced magnetic resonance images. *J Laryngol Otol* 1997; **111**: 877-879
- 34 **Oikawa A**, Takeda N, Aoki N, Takizawa T, Sakoma T. Schwannoma arising from the tentorium at an unusual location: case report. *Neurosurgery* 2002; **50**: 1352-1355
- 35 **Tien RD**, Cardenas CA, Rajagopalan S. Pleomorphic xanthoastrocytoma of the brain: MR findings in six patients. *AJR Am J Roentgenol* 1992; **159**: 1287-1290
- 36 **Murphy JM**, Gomez-Anson B, Gillard JH, Antoun NM, Cross J, Elliott JD, Lockwood M. Wegener granulomatosis: MR imaging findings in brain and meninges. *Radiology* 1999; **213**: 794-799
- 37 **Roberti F**, Lee HH, Caputy AJ, Katz B. "Shave" biopsy of the optic nerve in isolated neurosarcoidosis. *J Neurosurg Sci* 2005; **49**: 59-63; discussion 63
- 38 **Cattin F**, Bonneville F, Andréa I, Barrali E, Bonneville JF. Dural enhancement in pituitary macroadenomas. *Neuroradiology* 2000; **42**: 505-508
- 39 **Takeshima H**, Kaku T, Ushio Y. Cerebral gumma showing spontaneous regression on magnetic resonance imaging study--case report. *Neurol Med Chir (Tokyo)* 1999; **39**: 242-245
- 40 **Detwiler PW**, Henn JS, Porter RW, Lawton MT, White WL, Spetzler RF. Medulloblastoma presenting with tentorial "dural-tail" sign: is the "dural-tail" sign specific for meningioma? *Skull Base Surg* 1998; **8**: 233-236
- 41 **Furtado SV**, Venkatesh PK, Dadlani R, Reddy K, Hegde AS. Adult medulloblastoma and the "dural-tail" sign: rare mimic of a posterior petrous meningioma. *Clin Neurol Neurosurg* 2009; **111**: 540-543
- 42 **Ohta H**, Kawano S, Yokota A. [Multiple myeloma presenting with multiple subcutaneous masses] *No To Shinkei* 2004; **56**: 957-960
- 43 **Nakai Y**, Yanaka K, Iguchi M, Fujita K, Narushima K, Meguro K, Doi M, Nose T. [A case of multiple myeloma presenting with a subcutaneous mass: significance of "dural tail sign" in the differential diagnosis of the meningeal tumors] *No Shinkei Geka* 1999; **27**: 67-71
- 44 **Mitsuhashi T**, Mori K, Wada R, Maeda M. Primary rhabdomyosarcoma associated with tumoral hemorrhage--case report. *Neurol Med Chir (Tokyo)* 2002; **42**: 73-77
- 45 **Hakan T**, Türk CC, Aker FV. Tentorial solitary fibrous tumour: case report and review of the literature. *Neurol Neurochir Pol* 2009; **43**: 77-82
- 46 **Kuroiwa T**, Ohta T. MRI appearances mimicking the dural tail sign: a report of two cases. *Neuroradiology* 2000; **42**: 199-202
- 47 **Tokumaru A**, O'uchi T, Eguchi T, Kawamoto S, Kokubo T, Suzuki M, Kameda T. Prominent meningeal enhancement adjacent to meningioma on Gd-DTPA-enhanced MR images: histopathologic correlation. *Radiology* 1990; **175**: 431-433
- 48 **Kawahara Y**, Niino M, Yokoyama S, Kuratsu J. Dural congestion accompanying meningioma invasion into vessels: the dural tail sign. *Neuroradiology* 2001; **43**: 462-465
- 49 **Rokni-Yazdi H**, Azmoudeh Ardalan F, Asadzandi Z, Sotoudeh H, Shakiba M, Adibi A, Ayatollahi H, Rahmani M. Pathologic significance of the "dural tail sign". *Eur J Radiol* 2009; **70**: 10-16
- 50 **Sekiya T**, Manabe H, Iwabuchi T, Narita T. [The dura mater adjacent to the attachment of meningiomas: its enhanced MR imaging and histological findings] *No Shinkei Geka* 1992; **20**: 1063-1068
- 51 **Hutzelmann A**, Palmié S, Buhl R, Freund M, Heller M. Dural invasion of meningiomas adjacent to the tumor margin on Gd-DTPA-enhanced MR images: histopathologic correlation. *Eur Radiol* 1998; **8**: 746-748

S- Editor Cheng JX L- Editor Webster JR E- Editor Zheng XM

Systemic air embolism after transthoracic lung biopsy: A case report and review of literature

Wessam Bou-Assaly, Perry Pernicano, Ellen Hoeffner

Wessam Bou-Assaly, Department of Radiology, Neuroradiology Division, University of Michigan Health System, Ann Arbor VA Health system, MI 48103, United States

Perry Pernicano, A. Alfred Taubman Health Care Center, 1500 East Medical Center Drive, Room B1-132, Ann Arbor, MI 48109-5030, United States

Ellen Hoeffner, Department of Radiology, University Hospital, 1500 East Medical Center Drive, Room B2A209G, Ann Arbor, MI 48109-5030, United States

Author contributions: Bou-Assaly W reviewed the literature and wrote the case report; Pernicano P and Hoeffner E reviewed the case report.

Correspondence to: Wessam Bou-Assaly, MD, Clinical Lecturer II, Department of Radiology, Neuroradiology Division, University of Michigan Health System, Ann Arbor VA Health system, 2215 Fuller Road, MI 48103, United States. wessam@med.umich.edu

Telephone: +1-734-7697100 Fax: +1-734-8453293

Received: February 1, 2010 Revised: April 14, 2010

Accepted: April 21, 2010

Published online: May 28, 2010

Abstract

Computed tomography (CT)-guided lung biopsy is a common diagnostic procedure that is associated with various complications, including pneumothorax, hemoptysis and parenchymal hemorrhage. Systemic air embolism is a very rare (0.07%) but potentially life-threatening complication. We report a fatal case of air embolism to the cerebral and coronary arteries confirmed by head and chest CT, followed by a review of the literature.

© 2010 Baishideng. All rights reserved.

Key words: Systemic air embolism; Transthoracic lung biopsy; Air embolus; Lung mass; Needle biopsy; Stroke; Complications

Peer reviewers: Filippo Cademartiri, MD, PhD, Department of Radiology - c/o Piastra Tecnica - Piano 0, Azienda Ospedaliero-

Universitaria di Parma, Via Gramsci, 14 - 43100 Parma, Italy; Haiquan Yang, PhD, Research Section, Uni-Hite System Corporation, Shimotsuruma 505-1, Yamato, Kanagawa 242-0001, Japan; Hadi Rokni Yazdi, MD, Associate Professor, Department of radiology, Central Radiology, Imam Khomeini Hospital, Tehran University of Medical Sciences, Keshavarz Blvd, Tehran, 1419733141, Iran; Mario Mascacchi, MD, PhD, Professor, Radiodiagnostic Section, Department of Clinical Physiopathology, University of Florence, Viale Morgagni 50134, Florence, Italy

Bou-Assaly W, Pernicano P, Hoeffner E. Systemic air embolism after transthoracic lung biopsy: A case report and review of literature. *World J Radiol* 2010; 2(5): 193-196 Available from: URL: <http://www.wjgnet.com/1949-8470/full/v2/i5/193.htm> DOI: <http://dx.doi.org/10.4329/wjr.v2.i5.193>

INTRODUCTION

Percutaneous computer tomography scan guided thoracic needle biopsy is a widely accepted and frequently performed procedure for pulmonary lesions. Its rare complications such as pneumothorax, intraparenchymal hemorrhage and hemoptysis are usually conservatively treated with minimal intervention. Systemic air embolus is an extremely rare complication that is potentially fatal, reported to be around 0.02% to 0.07%^[1-7], with a probably higher incidence since it can be undiagnosed in asymptomatic patients. We present a case of a fatal systemic air embolus complicating a percutaneous computed tomography (CT) scan-guided trans-thoracic needle biopsy, performed for a suspicious lung lesion.

CASE REPORT

Our patient is a 76-year-old veteran with known diabetes mellitus, hyperlipidemia and a history of chronic obstructive pulmonary disease and pulmonary fibrosis. A recent CT showed a 3.5 cm round mass in the anterior aspect of the left upper lobe, with few enlarged mediastinal lymph

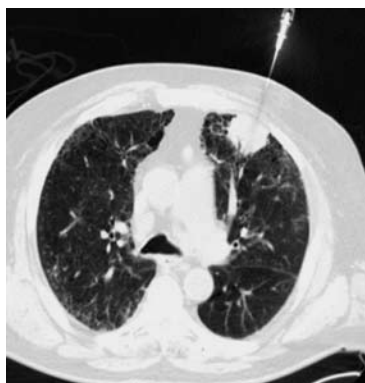


Figure 1 Chest computed tomography (CT) demonstrates the left upper lobe mass during the biopsy. The mass abuts the chest wall with mild adjacent emphysematous changes without large bullae.

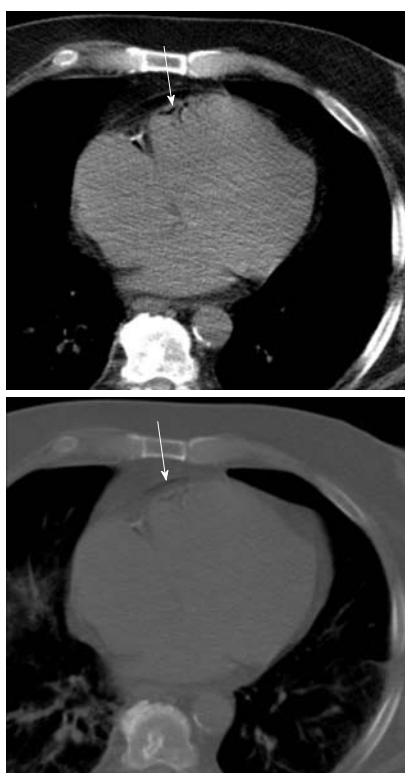


Figure 2 Axial images in soft tissue and lung window through the lower mediastinum, display a small amount of air in the epicardium (arrows), thought to be along the peripheral coronary vessels.

nodes. A positron emission tomography CT was obtained and demonstrated strong increased radiotracer uptake within the mass, highly suspicious for primary lung malignancy, without evidence for loco- regional or distant metastases. A CT guided biopsy of the lesion was requested.

The patient requested to be sedated. The anesthesiology team was consulted to monitor the patient during the biopsy. The procedure was performed by an experienced radiologist; the instrument used was a coaxial 17 gauge introducer with an 18 gauge core biopsy needle (Temno, Cardinal Health system, McGaw Park, IL). The patient was placed in a decubitus position, and was instructed not

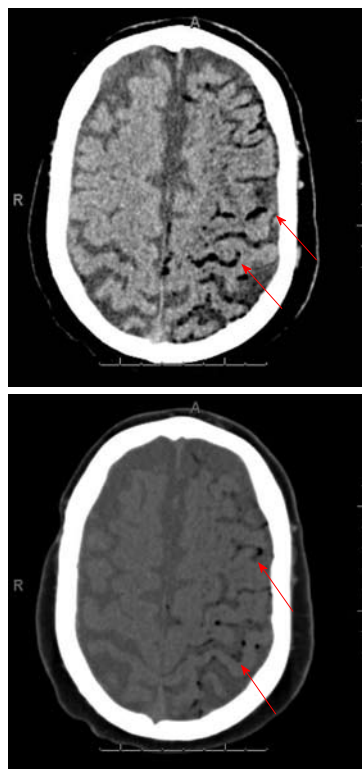


Figure 3 Head CT in brain and soft tissue windows demonstrates abnormal air along the left vertex subarachnoid spaces and cortical vessels (arrows), suggesting air embolus.

to breathe during the introduction and advancement of the needle, during exchanging stylet with the core biopsy needle, during obtaining specimen by pressing the plunger and during removal of the needle and then replacement of the stylet. After a sample was obtained, the core needle biopsy was removed and the stylet was immediately re-inserted (Figure 1). As the sample was being transferred into formalin, the anesthesiologist noted that the patient was bradycardic and he became unresponsive. He was immediately placed on increased oxygen and bag ventilated and the anesthesiologist started reversing his sedation.

A chest and head CT were immediately obtained. The chest CT images demonstrated a small amount of air in the epicardium, probably in the peripheral coronary vessels (Figure 2) without evidence of pneumothorax. The head CT showed a large amount of air along the subarachnoid spaces and peripheral vessels over the left cerebral convexity, in the frontal, parietal and temporal occipital lobes, which were interpreted as gas emboli (Figure 3).

The patient was stabilized and then transferred to a regional hospital for hyperbaric oxygen therapy, where he received treatment for 4 h. A repeat post-treatment head CT showed resolution of the air emboli but demonstrated subtle hypodensities in the left cerebral hemisphere involving the frontal and parietal lobes with slight sulcal effacement suggesting subacute ischemic changes. Magnetic resonance imaging could not be performed given the instability of the patient. The patient was readmitted to our hospital with residual right-sided deficit and agita-

tion. His stay was complicated by diffuse alveolar hemorrhage. The patient who had already signed a Do Not Resuscitate order, died 16 d after the biopsy.

DISCUSSION

Percutaneous needle biopsies of lung lesions are commonly used and are usually regarded as safe procedures with limited morbidity and extremely rare mortality. Most frequent complications are pneumothorax (27%), pulmonary bleeding (11%) and hemoptysis (7%)^[1-3]. These are usually conservatively treated and self-resolving. Other rare complications include systemic air embolus, tumor implantation and empyema. Systemic air emboli are extremely rare with a published incidence of 0.02% from a lung biopsy survey in the United Kingdom to 0.07% in the literature^[2-6], but are serious and can be fatal. To our knowledge, 19 cases have been published in the last 30 years.

Air in the pulmonary venous system embolizes mainly to coronary and cerebral arteries. Only 2 mL of air injected into cerebral circulation can be fatal, and 0.5 to 1.0 mL injected into pulmonary veins can cause cardiac arrest from coronary embolism^[4].

There are three possible ways air can be introduced into the pulmonary venous system during percutaneous needle biopsy of the lung. First, air may directly enter the pulmonary system through the needle, if the needle is placed into a pulmonary vein while the base is exposed to the atmosphere when the stylet is removed, and the atmospheric pressure exceeds the pulmonary veins pressure, as may occur during deep inspiration. Second, air may be introduced into the pulmonary arterial circulation and then reach the pulmonary veins by traversing the pulmonary microvasculature. Third, a needle may penetrate simultaneously at an air-containing space, such as a nearby pulmonary alveolar space, bronchus, cavity or air cyst, and a nearby pulmonary vein, which can create a communicating fistula. Then cough, straining or valsalva maneuvers can increase the pressure in the air-containing space, resulting in air embolus^[2-11]. Some factors are thought to be contributors: coughing during the procedure, positive-pressure ventilation, a needle tip placed within pulmonary veins and procedures performed for a cystic or cavitory lesion and in patients with vasculitis^[8].

Some authors postulated an increased probability of gas embolus related to the size of the needle and the coaxial techniques, since larger needles have an increase risk of involvement a pulmonary vein and the coaxial method increases the risk of contact with the atmosphere after removal of the internal stylet. However, a number of reported cases have described systemic air embolus with smaller needles and without the use of coaxial method, questioning any relationship between the two factors^[6].

Diagnosis of a systemic air embolus is difficult. It is mainly clinically suspected, based on the deterioration of the patient's neurologic and cardiovascular status. Brain and chest CT scan can provide a definitive diagnosis by

showing air bubbles in cerebral vessels, aorta, left atrium and ventricle or pulmonary veins. Coronary embolism may cause myocardial ischemia, decreased myocardial function, and sudden death. Cerebral air embolus may cause focal defects, seizure, and coma. An ophthalmoscopy examination may demonstrate air bubbles in the retinal vessels^[4]. Some authors reported that systemic air embolus is underestimated since it is undiagnosed in asymptomatic patients^[6,12]. The initial treatment consists of immediate administration of 100% oxygen, and placing the patient in the left lateral decubitus position with lowering of the head^[4-6,11,12].

Hyperbaric oxygen therapy is considered the first line therapy for systemic air embolism, by reducing bubble volume and improving tissue oxygenation. The size of a gas bubble is inversely proportional to ambient pressure at constant temperature^[13]. Breathing 100% oxygen at a pressure above that of the atmosphere decreases the size of gas bubbles by raising ambient pressure and also causes systemic hyperoxia^[6,8,14,15]. Hyperoxia produces diffusion of oxygen into the bubble and nitrogen out, and also allows a large quantity of oxygen to dissolve in the plasma and increases oxygen diffusion in tissues. Furthermore, it prevents cerebral edema by reducing the permeability of blood vessels while supporting integrity of blood-brain barrier^[6,9,14].

With cerebral embolism, immediate hyperbaric therapy was reported to decrease the mortality rate to 7%^[4,7]. Although immediate treatment is recommended, delayed hyperbaric oxygen therapy may also increase survival and decrease the neurologic deficit, even many hours after the incidence, because air bubbles have been demonstrated at 48 h after initial events^[4]. In our case, the follow-up CT scan after hyperbaric oxygen treatment showed complete resolution of the cerebral air embolus and the patient started to regain some of his neurological function. His death is thought to be related to his pulmonary hemorrhage, rather than to his cerebral air embolus.

Several considerations have been recommended to reduce the risk of air embolus, such as avoiding biopsy through a cystic or cavitory lesion or bullous lung parenchyma, using a stylet and keeping an occluded hollow at all times, requesting the patient to stop breathing when manipulating the biopsy kit and to restrain from coughing and straining, and penetrating the least amount of parenchyma to reach the lesion^[7].

In our case, the patient did not cough and was instructed to stop breathing during a critical part of the procedure yet this complication still occurred. CT-guided lung biopsy is routinely performed in our institution by an experienced radiologist and such complications never occurred before, which leads us to believe that this dangerous complication can happen in spite of long experience and meticulous care.

Despite the rarity of this dangerous and eventually fatal complication, radiologists should be aware of the possibility of systemic air embolus after lung biopsy and should be ready to provide emergent management for the

treatment of the patient. Although several recommendations and precautions have been proposed to reduce the risk of this complication, it may be inevitable and can occur despite long experience and meticulous care.

REFERENCES

- 1 **Sinner WN.** Complications of percutaneous transthoracic needle aspiration biopsy. *Acta Radiol Diagn (Stockh)* 1976; **17**: 813-828
- 2 **Richardson CM,** Pointon KS, Manhire AR, Macfarlane JT. Percutaneous lung biopsies: a survey of UK practice based on 5444 biopsies. *Br J Radiol* 2002; **75**: 731-735
- 3 **Tomiyama N,** Yasuhara Y, Nakajima Y, Adachi S, Arai Y, Kusumoto M, Eguchi K, Kuriyama K, Sakai F, Noguchi M, Murata K, Murayama S, Mochizuki T, Mori K, Yamada K. CT-guided needle biopsy of lung lesions: a survey of severe complication based on 9783 biopsies in Japan. *Eur J Radiol* 2006; **59**: 60-64
- 4 **Ohashi S,** Endoh H, Honda T, Komura N, Satoh K. Cerebral air embolism complicating percutaneous thin-needle biopsy of the lung: complete neurological recovery after hyperbaric oxygen therapy. *J Anesth* 2001; **15**: 233-236
- 5 **Hiraki T,** Fujiwara H, Sakurai J, Iguchi T, Gobara H, Tajiri N, Mimura H, Kanazawa S. Nonfatal systemic air embolism complicating percutaneous CT-guided transthoracic needle biopsy: four cases from a single institution. *Chest* 2007; **132**: 684-690
- 6 **Ghafoori M,** Varedi P. Systemic air embolism after percutaneous transthoracic needle biopsy of the lung. *Emerg Radiol* 2008; **15**: 353-356
- 7 **Lattin G Jr,** O'Brien W Sr, McCrary B, Kearney P, Gover D. Massive systemic air embolism treated with hyperbaric oxygen therapy following CT-guided transthoracic needle biopsy of a pulmonary nodule. *J Vasc Interv Radiol* 2006; **17**: 1355-1358
- 8 **Wong RS,** Ketai L, Temes RT, Follis FM, Ashby R. Air embolus complicating transthoracic percutaneous needle biopsy. *Ann Thorac Surg* 1995; **59**: 1010-1011
- 9 **Tomabechi M,** Kato K, Sone M, Ehara S, Sekimura K, Kizawa T, Kin M. Cerebral air embolism treated with hyperbaric oxygen therapy following percutaneous transthoracic computed tomography-guided needle biopsy of the lung. *Radiat Med* 2008; **26**: 379-383
- 10 **Kodama F,** Ogawa T, Hashimoto M, Tanabe Y, Suto Y, Kato T. Fatal air embolism as a complication of CT-guided needle biopsy of the lung. *J Comput Assist Tomogr* 1999; **23**: 949-951
- 11 **Kau T,** Rabitsch E, Celedin S, Habernig SM, Weber JR, Hausegger KA. When coughing can cause stroke--a case-based update on cerebral air embolism complicating biopsy of the lung. *Cardiovasc Intervent Radiol* 2008; **31**: 848-853
- 12 **Tolly TL,** Feldmeier JE, Czarnecki D. Air embolism complicating percutaneous lung biopsy. *AJR Am J Roentgenol* 1988; **150**: 555-556
- 13 **Shetty PG,** Fatterpekar GM, Manohar S, Sujit V, Varsha J, Zarir U. Fatal cerebral air embolism as a complication of transbronchoscopic lung biopsy: a case report. *Australas Radiol* 2001; **45**: 215-217
- 14 **Scruggs JE,** Joffe A, Wood KE. Paradoxical air embolism successfully treated with hyperbaric oxygen. *J Intensive Care Med* 2008; **23**: 204-209
- 15 **Arnold BW,** Zwiebel WJ. Percutaneous transthoracic needle biopsy complicated by air embolism. *AJR Am J Roentgenol* 2002; **178**: 1400-1402

S- Editor Cheng JX L- Editor Lalor PF E- Editor Zheng XM

Acknowledgments to reviewers of World Journal of Radiology

Many reviewers have contributed their expertise and time to the peer review, a critical process to ensure the quality of *World Journal of Radiology*. The editors and authors of the articles submitted to the journal are grateful to the following reviewers for evaluating the articles (including those published in this issue and those rejected for this issue) during the last editing time period.

Filippo Cademartiri, MD, PhD, Department of Radiology - c/o Piastra Tecnica - Piano 0, Azienda Ospedaliero-Universitaria di Parma, Via Gramsci, 14 - 43100 Parma, Italy

Herwig R Cerwenka, Professor, MD, Department of Surgery, Medical University of Graz, Auenbruggerplatz 29, A-8036 Graz, Austria

Feng Chen, MD, PhD, Professor, Department of Radiology, Zhong Da Hospital, Southeast University, 87 Ding Jiaqiao, Nanjing 210009, Jiangsu Province, China

James Chow, PhD, Radiation Physicist, Radiation Medicine Program, Princess Margaret Hospital, 610 University Avenue, Toronto, ON, M5G 2M9, Canada

Rivka R Colen, MD, Department of Radiology, Brigham and Women's Hospital, 75 Francis St, Boston, MA 02115, United States

Mohamed Abou El-Ghar, MD, Department of Radiology, Urology and Nephrology Center-Mansoura University, 72 El-gomhoria St, Mansoura, 35516, Egypt

Juebin Huang, MD, PhD, Assistant Professor, Department of Neurology, The University of Mississippi Medical Center, 2500 N. State Street, Jackson, MS 39216, United States

Chan Kyo Kim, MD, Assistant Professor, Department of Radiology, Samsung Medical Center, Sungkyunkwan University School of Medicine, 50 Ilwon-dong, Kangnam-gu, Seoul 135-710, South Korea

Meng Law, MD, MBBS, FRACR, Professor of Radiology and Neurological Surgery, Director of Neuroradiology, Keck School of Medicine, University of Southern California, 1500 San Pablo St, Lost Angeles, CA 90033, United States

Mario Mascalchi, MD, PhD, Professor, Radiodiagnostic Section, Department of Clinical Physiopathology, University of Florence, Viale Morgagni 50134, Florence, Italy

Cem Onal, MD, Department of Radiation Oncology, Adana Research and Treatment Centre, Baskent University Medical Faculty, 01120 Yuregir, Adana, Turkey

Ender Uysal, MD, Sisli Etfal Training and Research Hospital. Clinic of Radiology, Sisli Etfal Eğitim ve Araştırma Hastanesi Radyoloji Kliniği, Etfal sok. Sisli, Istanbul 34377, Turkey

Haiquan Yang, PhD, Research Section, Uni-Hite System Corporation, Shimotsuruma 505-1, Yamato, Kanagawa 242-0001, Japan

Hadi Rokni Yazdi, MD, Associate Professor, Department of radiology, Central Radiology, Imam Khomeini Hospital, Tehran University of Medical Sciences, Keshavarz Blvd, Tehran, 1419733141, Iran

Meetings

Events Calendar 2010

January 4-8

Beaver Creek, Colorado, United States
 18th Annual Winter Diagnostic Imaging Update

January 7-9

Leuven, Belgium
 4th Leuven Course on Ear Imaging

January 16-17

Hollywood, Florida, United States
 The Symposium on Clinical Interventional Oncology

January 17-21

Hollywood, Florida, United States
 The International Symposium on Endovascular Therapy

January 21-22

Cairo, Egypt
 BGICC Breast Gyne International Cancer Conference

January 21-24

Phoenix, AZ, United States
 13th Society for Cardiovascular Magnetic Resonance (SCMR) Annual Scientific Sessions

January 23-23

Atlanta, GA, United States
 Emory Winship Cancer Institute: Breast Cancer 2010: Advances in Science, Emerging Data, and Novel Therapeutics

January 25-29

Maui, HI, United States
 Musculoskeletal & Neuroradiology MR Imaging Update in Maui

January 27-February 2

Albuquerque, NM, United States
 2010 SNM Conjoint Mid-Winter Meetings

January 29-30

Barcelona, Spain
 7th European Congress: Perspectives in Gynecologic Oncology

February 7-12

Vail, CO, United States
 15th Annual Vail 2010: Multislice CT in Clinical Practice

February 11-13

Las Vegas, NV, United States
 5th Annual Symposium on PET/CT and Molecular Imaging

February 16-19

Park City, UT, United States
 6th Interventional/Neurointerventional Conference

February 18-19

London, United Kingdom
 Diagnostic and Interventional Radiology

February 18-21

Las Vegas, NV, United States
 American Society of Spine Radiology Annual Symposium

February 20-20

Jacksonville, Florida, United States
 Mayo Clinic Molecular Markers and Management of Breast Cancer

February 20-21

Bethesda, Maryland, United States
 25th Anniversary Washington Neuroradiology Review

February 21-26

Orlando, FL, United States
 The Abdominal Radiology Course

February 21-27

Snowmass, CO, United States
 16th Annual Snowmass 2010: Clinical Ultrasound

February 22-26

Bethesda, MD, United States
 48th Annual Dr. Kenneth M. Earle Memorial Neuropathology Review

February 24-27

Lake Buena Vista, FL, United States
 ACRO 2010 American College of Radiation Oncology Symposium: Clinical Radiation Oncology Challenges

February 25-27

Chandler, AZ, United States
 Multidisciplinary Head and Neck Cancer Symposium

February 26-27

Brussels, Belgium
 10èmes Mises au Point en Imagerie Ostéo-Articulaire

February 27-March 1

Cairo, Egypt
 7th Gastroenterology Hepatology & Endoscopy Symposium

February 28-March 4

Scottsdale, AZ, United States
 International Congress XXIII on Endovascular Interventions

February 28-March 5

Breckenridge, CO, United States
 5th Annual Breckenridge 2010: Musculoskeletal MRI

March 3-6

Las Vegas, Nevada, United States
 11th Annual Advances in Breast Imaging and Interventions

March 4-8

Vienna, Austria
 European Congress of Radiology (ECR 2010) Annual Meeting

March 5-7

Mt Tremblant, QC, Canada
 Neuroimaging and Head & Neck Radiology Update in Mt Tremblant

March 7-11

San Diego, CA, United States
 SCBT-MR Masters in Body Imaging: "What's New, What's Hot, What You May Not Have Known"

March 10-13

San Antonio, Texas, United States
 Clinical Osteoporosis 2010: An ISCD-NOF Symposium

March 11-13

Barcelona, Spain
 EORTC Group Meeting: EORTC Radiation Oncology Group

March 11-13

Hannover, Germany
 40. Kongress der Deutschen Gesellschaft für Endoskopie und Bildgebende Verfahren e.V.

March 13-18

Tampa, FL, United states
 Society of interventional radiology 35th Annual Scientific Meeting

March 14-17

Park City, UT, United States
 14th Annual Park City 2010: MRI in Clinical Practice

March 22-26

Beaver Creek, CO, United States
 NYU Radiology Spring Skiing Symposium in Beaver Creek

March 22-26

Maui, HI, United States
 18th Annual Spring Diagnostic Imaging Update

March 24-27

San Diego, California, United States
 2010 American institute of ultrasound in Medicine Annual Convention Preliminary Program

March 24-27

Barcelona, Spain
 7th European Breast Cancer Conference

April 8-12

Shanghai, China
 The 26th International Congress of Radiology

September 8-12

Guangzhou, China
 Chinese Society of Interventional Radiology, 2010 CSIR

November 28-December 03

Chicago, United States
 Radiological Society of North America: 2010 Annual Meeting

Instructions to authors

GENERAL INFORMATION

World Journal of Radiology (*World J Radiol*, *WJR*, online ISSN 1949-8470, DOI: 10.4329), is a monthly, open-access (OA), peer-reviewed journal supported by an editorial board of 308 experts in Radiology from 39 countries.

The biggest advantage of the OA model is that it provides free, full-text articles in PDF and other formats for experts and the public without registration, which eliminates the obstacle that traditional journals possess and usually delays the speed of the propagation and communication of scientific research results. The open access model has been proven to be a true approach that may achieve the ultimate goal of the journals, i.e. the maximization of the value to the readers, authors and society.

The role of academic journals is to exhibit the scientific levels of a country, a university, a center, a department, and even a scientist, and build an important bridge for communication between scientists and the public. As we all know, the significance of the publication of scientific articles lies not only in disseminating and communicating innovative scientific achievements and academic views, as well as promoting the application of scientific achievements, but also in formally recognizing the "priority" and "copyright" of innovative achievements published, as well as evaluating research performance and academic levels. So, to realize these desired attributes of *WJR* and create a well-recognized journal, the following four types of personal benefits should be maximized. The maximization of personal benefits refers to the pursuit of the maximum personal benefits in a well-considered optimal manner without violation of the laws, ethical rules and the benefits of others. (1) Maximization of the benefits of editorial board members: The primary task of editorial board members is to give a peer review of an unpublished scientific article *via* online office system to evaluate its innovativeness, scientific and practical values and determine whether it should be published or not. During peer review, editorial board members can also obtain cutting-edge information in that field at first hand. As leaders in their field, they have priority to be invited to write articles and publish commentary articles. We will put peer reviewers' names and affiliations along with the article they reviewed in the journal to acknowledge their contribution; (2) Maximization of the benefits of authors: Since *WJR* is an open-access journal, readers around the world can immediately download and read, free of charge, high-quality, peer-reviewed articles from *WJR* official website, thereby realizing the goals and significance of the communication between authors and peers as well as public reading; (3) Maximization of the benefits of readers: Readers can read or use, free of charge, high-quality peer-reviewed articles without any limits, and cite the arguments, viewpoints, concepts, theories, methods, results, conclusion or facts and data of pertinent literature so as to validate the innovativeness, scientific and practical values of their own research achievements, thus ensuring that their

articles have novel arguments or viewpoints, solid evidence and correct conclusion; and (4) Maximization of the benefits of employees: It is an iron law that a first-class journal is unable to exist without first-class editors, and only first-class editors can create a first-class academic journal. We insist on strengthening our team cultivation and construction so that every employee, in an open, fair and transparent environment, could contribute their wisdom to edit and publish high-quality articles, thereby realizing the maximization of the personal benefits of editorial board members, authors and readers, and yielding the greatest social and economic benefits.

The major task of *WJR* is to rapidly report the most recent improvement in the research of medical imaging and radiation therapy by the radiologists. *WJR* accepts papers on the following aspects related to radiology: Abdominal radiology, women health radiology, cardiovascular radiology, chest radiology, genitourinary radiology, neuroradiology, head and neck radiology, interventional radiology, musculoskeletal radiology, molecular imaging, pediatric radiology, experimental radiology, radiological technology, nuclear medicine, PACS and radiology informatics, and ultrasound. We also encourage papers that cover all other areas of radiology as well as basic research.

The columns in the issues of *WJR* will include: (1) Editorial: To introduce and comment on major advances and developments in the field; (2) Frontier: To review representative achievements, comment on the state of current research, and propose directions for future research; (3) Topic Highlight: This column consists of three formats, including (A) 10 invited review articles on a hot topic, (B) a commentary on common issues of this hot topic, and (C) a commentary on the 10 individual articles; (4) Observation: To update the development of old and new questions, highlight unsolved problems, and provide strategies on how to solve the questions; (5) Guidelines for Basic Research: To provide guidelines for basic research; (6) Guidelines for Clinical Practice: To provide guidelines for clinical diagnosis and treatment; (7) Review: To review systemically progress and unresolved problems in the field, comment on the state of current research, and make suggestions for future work; (8) Original Articles: To report innovative and original findings in radiology; (9) Brief Articles: To briefly report the novel and innovative findings in radiology; (10) Case Report: To report a rare or typical case; (11) Letters to the Editor: To discuss and make reply to the contributions published in *WJR*, or to introduce and comment on a controversial issue of general interest; (12) Book Reviews: To introduce and comment on quality monographs of radiology; and (13) Guidelines: To introduce consensus and guidelines reached by international and national academic authorities worldwide on the research in radiology.

CSSN

ISSN 1949-8470 (online)

Published by

Beijing Baishideng BioMed Scientific Co., Ltd.

SUBMISSION OF MANUSCRIPTS

Manuscripts should be typed in 1.5 line spacing and 12 pt. Book Antiqua with ample margins. Number all pages consecutively, and start each of the following sections on a new page: Title Page, Abstract, Introduction, Materials and Methods, Results, Discussion, Acknowledgements, References, Tables, Figures, and Figure Legends. Neither the editors nor the publisher are responsible for the opinions expressed by contributors. Manuscripts formally accepted for publication become the permanent property of Beijing Baishideng BioMed Scientific Co., Ltd., and may not be reproduced by any means, in whole or in part, without the written permission of both the authors and the publisher. We reserve the right to copy-edit and put onto our website accepted manuscripts. Authors should follow the relevant guidelines for the care and use of laboratory animals of their institution or national animal welfare committee. For the sake of transparency in regard to the performance and reporting of clinical trials, we endorse the policy of the International Committee of Medical Journal Editors to refuse to publish papers on clinical trial results if the trial was not recorded in a publicly-accessible registry at its outset. The only register now available, to our knowledge, is <http://www.clinicaltrials.gov> sponsored by the United States National Library of Medicine and we encourage all potential contributors to register with it. However, in the case that other registers become available you will be duly notified. A letter of recommendation from each author's organization should be provided with the contributed article to ensure the privacy and secrecy of research is protected.

Authors should retain one copy of the text, tables, photographs and illustrations because rejected manuscripts will not be returned to the author(s) and the editors will not be responsible for loss or damage to photographs and illustrations sustained during mailing.

Online submissions

Manuscripts should be submitted through the Online Submission System at: <http://www.wjgnet.com/1949-8470office>. Authors are highly recommended to consult the ONLINE INSTRUCTIONS TO AUTHORS (http://www.wjgnet.com/1949-8470/g_info_20100316162358.htm) before attempting to submit online. For assistance, authors encountering problems with the Online Submission System may send an email describing the problem to wjr@wjgnet.com, or by telephone: +86-10-59080036. If you submit your manuscript online, do not make a postal contribution. Repeated online submission for the same manuscript is strictly prohibited.

MANUSCRIPT PREPARATION

All contributions should be written in English. All articles must be submitted using word-processing software. All submissions must be typed in 1.5 line spacing and 12 pt. Book Antiqua with ample margins. Style should conform to our house format. Required information for each of the manuscript sections is as follows:

Title page

Title: Title should be less than 12 words.

Running title: A short running title of less than 6 words should be provided.

Authorship: Authorship credit should be in accordance with

the standard proposed by International Committee of Medical Journal Editors, based on (1) substantial contributions to conception and design, acquisition of data, or analysis and interpretation of data; (2) drafting the article or revising it critically for important intellectual content; and (3) final approval of the version to be published. Authors should meet conditions 1, 2, and 3.

Institution: Author names should be given first, then the complete name of institution, city, province and postcode. For example, Xu-Chen Zhang, Li-Xin Mei, Department of Pathology, Chengde Medical College, Chengde 067000, Hebei Province, China. One author may be represented from two institutions, for example, George Sgourakis, Department of General, Visceral, and Transplantation Surgery, Essen 45122, Germany; George Sgourakis, 2nd Surgical Department, Korgialenio-Benakio Red Cross Hospital, Athens 15451, Greece

Author contributions: The format of this section should be: Author contributions: Wang CL and Liang L contributed equally to this work; Wang CL, Liang L, Fu JF, Zou CC, Hong F and Wu XM designed the research; Wang CL, Zou CC, Hong F and Wu XM performed the research; Xue JZ and Lu JR contributed new reagents/analytic tools; Wang CL, Liang L and Fu JF analyzed the data; and Wang CL, Liang L and Fu JF wrote the paper.

Supportive foundations: The complete name and number of supportive foundations should be provided, e.g., Supported by National Natural Science Foundation of China, No. 30224801

Correspondence to: Only one corresponding address should be provided. Author names should be given first, then author title, affiliation, the complete name of institution, city, postcode, province, country, and email. All the letters in the email should be in lower case. A space interval should be inserted between country name and email address. For example, Montgomery Bissell, MD, Professor of Medicine, Chief, Liver Center, Gastroenterology Division, University of California, Box 0538, San Francisco, CA 94143, United States. montgomerybissell@ucsf.edu

Telephone and fax: Telephone and fax should consist of +, country number, district number and telephone or fax number, e.g., Telephone: +86-10-59080039 Fax: +86-10-85381893

Peer reviewers: All articles received are subject to peer review. Normally, three experts are invited for each article. Decision for acceptance is made only when at least two experts recommend an article for publication. Reviewers for accepted manuscripts are acknowledged in each manuscript, and reviewers of articles which were not accepted will be acknowledged at the end of each issue. To ensure the quality of the articles published in *WJR*, reviewers of accepted manuscripts will be announced by publishing the name, title/position and institution of the reviewer in the footnote accompanying the printed article. For example, reviewers: Professor Jing-Yuan Fang, Shanghai Institute of Digestive Disease, Shanghai, Affiliated Renji Hospital, Medical Faculty, Shanghai Jiaotong University, Shanghai, China; Professor Xin-Wei Han, Department of Radiology, The First Affiliated Hospital, Zhengzhou University, Zhengzhou, Henan Province, China; and Professor Anren Kuang, Department of Nuclear Medicine, Huaxi Hospital, Sichuan University, Chengdu, Sichuan Province, China.

Abstract

There are unstructured abstracts (no more than 256 words) and structured abstracts (no more than 480). The specific requirements for structured abstracts are as follows:

An informative, structured abstracts of no more than 480 words should accompany each manuscript. Abstracts for original contributions should be structured into the following sections. AIM (no more than 20 words): Only the purpose should be included. Please write the aim as the form of "To investigate/study/...; MATERIALS AND METHODS (no more than 140 words); RESULTS (no more than 294 words): You should present *P* values where appropriate and must provide relevant data to illustrate how they were obtained, e.g. 6.92 ± 3.86 vs 3.61 ± 1.67 , $P < 0.001$; CONCLUSION (no more than 26 words).

Key words

Please list 5-10 key words, selected mainly from *Index Medicus*, which reflect the content of the study.

Text

For articles of these sections, original articles, rapid communication and case reports, the main text should be structured into the following sections: INTRODUCTION, MATERIALS AND METHODS, RESULTS and DISCUSSION, and should include appropriate Figures and Tables. Data should be presented in the main text or in Figures and Tables, but not in both. The main text format of these sections, editorial, topic highlight, case report, letters to the editors, can be found at: http://www.wjgnet.com/1949-8470/g_info_20100313183720.htm.

Illustrations

Figures should be numbered as 1, 2, 3, *etc.*, and mentioned clearly in the main text. Provide a brief title for each figure on a separate page. Detailed legends should not be provided under the figures. This part should be added into the text where the figures are applicable. Figures should be either Photoshop or Illustrator files (in tiff, eps, jpeg formats) at high-resolution. Examples can be found at: <http://www.wjgnet.com/1007-9327/13/4520.pdf>; <http://www.wjgnet.com/1007-9327/13/4554.pdf>; <http://www.wjgnet.com/1007-9327/13/4891.pdf>; <http://www.wjgnet.com/1007-9327/13/4986.pdf>; <http://www.wjgnet.com/1007-9327/13/4498.pdf>. Keeping all elements compiled is necessary in line-art image. Scale bars should be used rather than magnification factors, with the length of the bar defined in the legend rather than on the bar itself. File names should identify the figure and panel. Avoid layering type directly over shaded or textured areas. Please use uniform legends for the same subjects. For example: Figure 1 Pathological changes in atrophic gastritis after treatment. A: ...; B: ...; C: ...; D: ...; E: ...; F: ...; G: ...*etc.* It is our principle to publish high resolution-figures for the printed and E-versions.

Tables

Three-line tables should be numbered 1, 2, 3, *etc.*, and mentioned clearly in the main text. Provide a brief title for each table. Detailed legends should not be included under tables, but rather added into the text where applicable. The information should complement, but not duplicate the text. Use one horizontal line under the title, a second under column heads, and a third below the Table, above any footnotes. Vertical and italic lines should be omitted.

Notes in tables and illustrations

Data that are not statistically significant should not be noted. ^a $P < 0.05$, ^b $P < 0.01$ should be noted ($P > 0.05$ should not be noted). If there are other series of *P* values, ^c $P < 0.05$ and ^d $P < 0.01$ are used. A third series of *P* values can be expressed as ^e $P < 0.05$ and ^f $P < 0.01$. Other notes in tables or under illustrations should be expressed as ¹F, ²F, ³F; or sometimes as other symbols with a superscript (Arabic numerals) in the upper left corner. In a multi-curve illustration, each curve should be labeled with ●, ○, ■, □, ▲, △, *etc.*, in a certain sequence.

Acknowledgments

Brief acknowledgments of persons who have made genuine contributions to the manuscript and who endorse the data and conclusions should be included. Authors are responsible for obtaining written permission to use any copyrighted text and/or illustrations.

REFERENCES**Coding system**

The author should number the references in Arabic numerals according to the citation order in the text. Put reference numbers in square brackets in superscript at the end of citation content or after the cited author's name. For citation content which is part of the narration, the coding number and square brackets should be typeset normally. For example, "Crohn's disease (CD) is associated with increased intestinal permeability^[1,2]". If references are cited directly in the text, they should be put together within the text, for example, "From references^[19,22-24], we know that..."

When the authors write the references, please ensure that the order in text is the same as in the references section, and also ensure the spelling accuracy of the first author's name. Do not list the same citation twice.

PMID and DOI

Pleased provide PubMed citation numbers to the reference list, e.g. PMID and DOI, which can be found at <http://www.ncbi.nlm.nih.gov/sites/entrez?db=pubmed> and <http://www.crossref.org/SimpleTextQuery/>, respectively. The numbers will be used in E-version of this journal.

Style for journal references

Authors: the name of the first author should be typed in bold-faced letters. The family name of all authors should be typed with the initial letter capitalized, followed by their abbreviated first and middle initials. (For example, Lian-Sheng Ma is abbreviated as Ma LS, Bo-Rong Pan as Pan BR). The title of the cited article and italicized journal title (journal title should be in its abbreviated form as shown in PubMed), publication date, volume number (in black), start page, and end page [PMID: 11819634 DOI: 10.3748/wjg.13.5396].

Style for book references

Authors: the name of the first author should be typed in bold-faced letters. The surname of all authors should be typed with the initial letter capitalized, followed by their abbreviated middle and first initials. (For example, Lian-Sheng Ma is abbreviated as Ma LS, Bo-Rong Pan as Pan BR) Book title. Publication number. Publication place: Publication press, Year: start page and end page.

Instructions to authors

Format

Journals

English journal article (list all authors and include the PMID where applicable)

- 1 **Jung EM**, Clevert DA, Schreyer AG, Schmitt S, Rennert J, Kubale R, Feuerbach S, Jung F. Evaluation of quantitative contrast harmonic imaging to assess malignancy of liver tumors: A prospective controlled two-center study. *World J Gastroenterol* 2007; **13**: 6356-6364 [PMID: 18081224 DOI: 10.3748/wjg.13.6356]

Chinese journal article (list all authors and include the PMID where applicable)

- 2 **Lin GZ**, Wang XZ, Wang P, Lin J, Yang FD. Immunologic effect of Jianpi Yishen decoction in treatment of Pixu-diarrhoea. *Shijie Huaren Xiaobua Zazhi* 1999; **7**: 285-287

In press

- 3 **Tian D**, Araki H, Stahl E, Bergelson J, Kreitman M. Signature of balancing selection in Arabidopsis. *Proc Natl Acad Sci USA* 2006; In press

Organization as author

- 4 **Diabetes Prevention Program Research Group**. Hypertension, insulin, and proinsulin in participants with impaired glucose tolerance. *Hypertension* 2002; **40**: 679-686 [PMID: 12411462 PMCID:2516377 DOI:10.1161/01.HYP.0000035706.28494.09]

Both personal authors and an organization as author

- 5 **Vallancien G**, Emberton M, Harving N, van Moorselaar RJ; Alf-One Study Group. Sexual dysfunction in 1, 274 European men suffering from lower urinary tract symptoms. *J Urol* 2003; **169**: 2257-2261 [PMID: 12771764 DOI:10.1097/01.ju.0000067940.76090.73]

No author given

- 6 21st century heart solution may have a sting in the tail. *BMJ* 2002; **325**: 184 [PMID: 12142303 DOI:10.1136/bmj.325.7357.184]

Volume with supplement

- 7 **Geraud G**, Spierings EL, Keywood C. Tolerability and safety of frovatriptan with short- and long-term use for treatment of migraine and in comparison with sumatriptan. *Headache* 2002; **42** Suppl 2: S93-99 [PMID: 12028325 DOI:10.1046/j.1526-4610.42.s2.7.x]

Issue with no volume

- 8 **Banit DM**, Kaufer H, Hartford JM. Intraoperative frozen section analysis in revision total joint arthroplasty. *Clin Orthop Relat Res* 2002; **(401)**: 230-238 [PMID: 12151900 DOI:10.1097/00003086-200208000-00026]

No volume or issue

- 9 Outreach: Bringing HIV-positive individuals into care. *HRSA Careaction* 2002; 1-6 [PMID: 12154804]

Books

Personal author(s)

- 10 **Sherlock S**, Dooley J. Diseases of the liver and biliary system. 9th ed. Oxford: Blackwell Sci Pub, 1993: 258-296

Chapter in a book (list all authors)

- 11 **Lam SK**. Academic investigator's perspectives of medical treatment for peptic ulcer. In: Swabb EA, Azabo S. Ulcer disease: investigation and basis for therapy. New York: Marcel Dekker, 1991: 431-450

Author(s) and editor(s)

- 12 **Breedlove GK**, Schorfheide AM. Adolescent pregnancy. 2nd ed. Wiczorek RR, editor. White Plains (NY): March of Dimes Education Services, 2001: 20-34

Conference proceedings

- 13 **Harnden P**, Joffe JK, Jones WG, editors. Germ cell tumours V. Proceedings of the 5th Germ cell tumours Conference; 2001 Sep 13-15; Leeds, UK. New York: Springer, 2002: 30-56

Conference paper

- 14 **Christensen S**, Oppacher F. An analysis of Koza's computational effort statistic for genetic programming. In: Foster JA, Lutton E, Miller J, Ryan C, Tettamanzi AG, editors. Genetic programming. EuroGP 2002: Proceedings of the 5th European Conference on Genetic Programming; 2002 Apr 3-5; Kinsdale, Ireland. Berlin: Springer, 2002: 182-191

Electronic journal (list all authors)

- 15 Morse SS. Factors in the emergence of infectious diseases. *Emerg Infect Dis* serial online, 1995-01-03, cited 1996-06-05; 1(1): 24 screens. Available from: URL: <http://www.cdc.gov/ncidod/EID/eid.htm>

Patent (list all authors)

- 16 **Pagedas AC**, inventor; Ancel Surgical R&D Inc., assignee. Flexible endoscopic grasping and cutting device and positioning tool assembly. United States patent US 20020103498. 2002 Aug 1

Statistical data

Write as mean \pm SD or mean \pm SE.

Statistical expression

Express *t* test as *t* (in italics), *F* test as *F* (in italics), chi square test as χ^2 (in Greek), related coefficient as *r* (in italics), degree of freedom as *v* (in Greek), sample number as *n* (in italics), and probability as *P* (in italics).

Units

Use SI units. For example: body mass, *m* (B) = 78 kg; blood pressure, *p* (B) = 16.2/12.3 kPa; incubation time, *t* (incubation) = 96 h, blood glucose concentration, *c* (glucose) 6.4 \pm 2.1 mmol/L; blood CEA mass concentration, *p* (CEA) = 8.6 24.5 μ g/L; CO₂ volume fraction, 50 mL/L CO₂, not 5% CO₂; likewise for 40 g/L formaldehyde, not 10% formalin; and mass fraction, 8 ng/g, etc. Arabic numerals such as 23, 243, 641 should be read 23 243 641.

The format for how to accurately write common units and quantum can be found at: http://www.wjgnet.com/1949-8470/g_info_20100313185816.htm.

Abbreviations

Standard abbreviations should be defined in the abstract and on first mention in the text. In general, terms should not be abbreviated unless they are used repeatedly and the abbreviation is helpful to the reader. Permissible abbreviations are listed in Units, Symbols and Abbreviations: A Guide for Biological and Medical Editors and Authors (Ed. Baron DN, 1988) published by The Royal Society of Medicine, London. Certain commonly used abbreviations, such as DNA, RNA, HIV, LD50, PCR, HBV, ECG, WBC, RBC, CT, ESR, CSF, IgG, ELISA, PBS, ATP, EDTA, mAb, can be used directly without further explanation.

Italics

Quantities: *t* time or temperature, *c* concentration, *A* area, *l* length, *m* mass, *V* volume.

Genotypes: *gyrA*, *arg 1*, *c myc*, *c fos*, etc.

Restriction enzymes: *EcoRI*, *HindI*, *BamHI*, *Kho I*, *Kpn I*, etc.
Biology: *H. pylori*, *E. coli*, etc.

RE-SUBMISSION OF THE REVISED PAPER

Please revise your article according to the revision policies of *WJR*. The revised version including manuscript and high-resolution image figures (if any) should be re-submitted or uploaded online. The author should send copyright transfer letter, and responses to the reviewers and science news to us *via* email.

Editorial Office

World Journal of Radiology

Editorial Department: Room 903, Building D,
Ocean International Center,
No. 62 Dongsihuan Zhonglu,
Chaoyang District, Beijing 100025, China
E-mail: wjr@wjgnet.com
<http://www.wjgnet.com>
Telephone: +86-10-59080036
Fax: +86-10-85381893

Language evaluation

The language of a manuscript will be graded before it is sent for revision. (1) Grade A: priority publishing; (2) Grade B: minor language polishing; (3) Grade C: a great deal of language polishing needed; and (4) Grade D: rejected. Revised articles should reach Grade A or B.

Copyright assignment form

Please download a Copyright assignment form from http://www.wjgnet.com/1949-8470/g_info_20100313185522.htm.

Responses to reviewers

Please revise your article according to the comments/suggestions provided by the reviewers. The format for responses to the reviewers' comments can be found at: http://www.wjgnet.com/1949-8470/g_info_20100313185358.htm.

Proof of financial support

For paper supported by a foundation, authors should provide a copy of the document and serial number of the foundation.

Science news releases

Authors of accepted manuscripts are suggested to write a science news item to promote their articles. The news will be released rapidly at EurekaAlert/AAAS (<http://www.eurekaalert.org>). The title for news items should be less than 90 characters; the summary should be less than 75 words; and main body less than 500 words. Science news items should be lawful, ethical, and strictly based on your original content with an attractive title and interesting pictures.

Publication fee

Authors of accepted articles must pay a publication fee. EDITORIAL, TOPIC HIGHLIGHTS, BOOK REVIEWS and LETTERS TO THE EDITOR are published free of charge.